BAW-2118

November 1991

LOW UPPER-SHELF TOUGHNESS FRACTURE ANALYSIS OF REACTOR VESSELS OF TURKEY POINT UNITS 3 AND 4

FOR LOAD LEVEL A & B CONDITIONS

for

B&W Owners Group Materials Committee
Reactor Vessel Working Group
Commonwealth Edison Company
Duke Power Company
Entergy Operations
Florida Power Corporation
Florida Power & Light Company
GPU Nuclear Corporation
Rochester Gas & Electric Corporation
Toledo Edison Company
Virginia Power Company
Wisconsin Electric Power Company

B&W Document No. 77-2118-01

B&W Nuclear Service Company
Engineering and Plant Services Division
P. O. Box 10935
Lynchburg, Virginia 24506-0935

CONTENTS

		Page
1.	INTRODUCTION	1-1
1.1.	Background	1-1
1.2.	Master Integrated Reactor Vessel Surveillance Program	1-6
1.2.1.	General Description	1-6
1.2.2.	Plant-Specific Surveillance Programs	1-8
2.	REACTOR VESSEL OF TURKEY POINT UNITS 3 AND 4	2-1
2.1.	Turkey Point Unit 3	2-1
2.2.	Turkey Point Unit 4	2-1
2.3.	Surveillance Data Bases	2-2
2.3.1.	Turkey Point Unit 3	2-2
2.3.2.	Turkey Point Unit 4	2-3
2.3.3.	Integrated Surveillance Program	2-3
2.3.4.	Spare Capsules	2-3
2.3.5.	Archive Surveillance Material	2-3
2.3.6.	Overview of Surveillance Data	2-4
2.4.	Evaluation of Reactor Vessel End-of-Life Material Properties	2-3
3.	ELASTIC-PLASTIC FRACTURE MECHANICS METHODOLOGY	3-1
3.1.	Acceptance Criteria for Low Upper Shelf Fracture Toughness Analysis	3-2
3.1.1.	Acceptance Standard for Level A and B Conditions	3-2
3.2.	"J"-based Elastic-Plastic Fracture Mechanics Analysis Method	3-3
3.2.1.	"J" Solution for Reference Flaw	3-3
3.2.2.	"J" Solution for a Circumferential Flaw in a Cylinder	3-5
3.2.3.	Instability Analysis Method	3-7
3.3.	Ramberg-Osgood Parameters	3-9
4.	MATERIAL PROPERTY CHARACTERIZATION	4-1
4.1.	Fracture Toughness Model Development Methods	4-1
4.1.1.	Key Variables and Model Form	4-1
4.1.2.	Model Calibration	4-3
4.2.	Data Analysis	4-4
4.2.1.	B&W Owners Group Data Base Description	4-4

Contents (Cont'd)

Page

4.2.2. J Control Limit 4-5
4.2.3. Data Assembly 4-5
4.2.4. Candidate Variables for J-R Model 4-5
4.2.5. Pattern Recognition and Model Form 4-6
4.2.6. Determination of Optimal Parameters 4-8
4.2.7. Model Verification 4-8
4.3. Power and Test Reactor Toughness Data 4-9
4.4. J-R Model Prediction Trends 4-10
4.5. Comparison Between J-R Model and SA-1101 Specimen Data 4-10

5. FRACTURE MECHANICS ANALYSIS 5-1

5.1. Plant Specific Input Data 5-1
5.2. Applied Loads for Service Levels A and B Condition 5-1
5.3. Lower Bounding J-R Equation for Turkey Point Units 5-2
5.4. J Analysis 5-4
5.5. Stability Analysis 5-5
5.5.1. DPFAD Analysis 5-5
5.5.2. J-Δa Method 5-5

6. CONCLUSIONS 6-1

7. REFERENCES 7-1

8. CERTIFICATION 8-1

List of Tables

Table

2-1. Chemical Composition of Beltline Region Materials for Turkey Point Unit 3 2-7
2-2. Heat Treatment of Beltline Region Materials for Turkey Point Unit 3 2-8
2-3. Unirradiated Mechanical Properties of Beltline Region Materials for Turkey Point Unit 3 2-9
2-4. Chemical Composition of Beltline Region Materials for Turkey Point Unit 4 2-10
2-5. Heat Treatment of Beltline Region Materials for Turkey Point Unit 4 2-11
2-6. Unirradiated Mechanical Properties of Beltline Region Materials for Turkey Point Unit 4 2-12

Tables (Cont'd)

Table — Page

2-7. Turkey Point Unit 3 Description and Properties of Reactor Vessel Surveillance Program Materials 2-13
2-8. Turkey Point Unit 4 Description and Properties of Reactor Vessel Surveillance Program Materials 2-14
2-9. Irradiated Charpy Data for Weld Metals SA-1094 and SA-1101 2-15
2-10. Evaluation of Turkey Point Unit-3 Reactor Vessel End-of-Life (32 EFPY) Upper-Shelf Energy 2-16
2-11. Evaluation of Turkey Point Unit-4 Reactor Vessel End-of-Life (32 EFPY) Upper-Shelf Energy 2-17
2-12. Summary of Evaluation of Effects of Neutron Irradiation on Upper-Shelf Energy of Controlling Weld Metals in Turkey Point 3 and 4 . . 2-18
2-13. Irradiated Charpy Data for Weld Metals SA-1094 and SA-1101 2-19
5-1. Reactor Vessel Design Data 5-6
5-2. Tensile Properties of Irradiated Weld Metal 5-7

List of Figures

Figure

2-1 Identification and Location of Base Materials and Weld Metals in Turkey Point Units 3 and 3 Reactor Vessels 2-20
2-2 Comparison of Irradiated Charpy 30 ft-lb Temperatures for Weld Metals SA-1094 and SA-1101 With Predictions Based on Regulatory Guide 1.99, Revision 2, Position 1 2-21
2-3 Comparison of Irradiated Charpy 30 ft-lb Temperatures for Weld Metals SA-1094 and SA-1101 With Predictions Based on Regulatory Guide 1.99, Revision 2, Position 2 2-22
2-4 Comparison of Irradiated Charpy Upper-Shelf Energy Data for Weld Metals SA-1094 and SA-1101 With Predictions Based on BAW-1803, Revision 1 2-23
3-1 Geometry of Reactor Vessel Beltline With ASME Appendix G Postulated Flaw 3-11
3-2 Cross-Sections of Turkey Point Reactor Vessels 3-12
3-3 Schematic of a Part-Through, Circumferential Surface Flaw in a Cylinder - Elliptical Flaw 3-13
3-4 Schematic of a Part-Through, Circumferential Surface Flaw in a Cylinder - Constant Depth Flaw 3-13
3-5 F Factors and Curve Fit Equation 3-14
3-6 Deformation Plasticity Failure Assessment Diagram 3-15
3-7 J-Δa Analysis 3-16
4-1 K_{IC} Curve 4-17

Figures (Cont'd)

Figure		Page
4-2	J Control Limit Assessment	4-18
4-3	B&WOG Data on Log-Log Scale - J_D-Δa	4-19
4-4	B&WOG Data on Log-Log Scale - J_M-Δa	4-20
4-5	Transformation Analysis Plot (TAP) for ln C_1 - J_D	4-21
4-6	Transformation Analysis Plot (TAP) for ln C_1 - J_M	4-22
4-7	TAP for Cu x Fluence$^{0.1908}$ on J_D	4-23
4-8	TAP for Cu x Fluence$^{0.1908}$ on J_M	4-24
4-9	TAP for Temperature on J_D	4-25
4-10	TAP for Temperature on J_M	4-26
4-11	TAP for Net Thickness on J_D	4-27
4-12	TAP for Net Thickness on J_M	4-28
4-13	Normalized J_D Plot - B&WOG Data	4-29
4-14	Normalized J_M Plot - B&WOG Data	4-30
4-15	Normalized J_D Versus Copper Content	4-31
4-16	Normalized J_D Versus Fluence	4-32
4-17	Normalized J_D Versus Temperature	4-33
4-18	Normalized J_D Versus Specimen Thickness	4-34
4-19	Effect of Fluence and Copper Content on J-B&WOG Data	4-35
4-20	Effect of Temperature and Fluence on J	4-36
4-21	Effect of Net Thickness and Copper Content on J	4-37
4-22	J-R Model and HSST Data Comparison - I	4-38
4-23	J-R Model and HSST Data Comparison - II	4-39
5-1	Reactor Vessels and Weld Metal Orientation	5-8
5-2	Cooldown Ramp and K_{IT}	5-9
5-3	Mean and Lower Bound J-R Curves	5-10
5-4	Comparison of Two Models	5-11
5-5	Applied J As A Function of Pressure	5-12
5-6	Applied J-Δa Against J-R Curve	5-13
5-7	J Versus Δa Plot	5-14
5-8	DPFAD Analysis	5-15

1. INTRODUCTION

This report describes an analysis of Turkey Point Units 3 and 4 reactor pressure vessels to demonstrate adequate fracture toughness after the Charpy V-notch upper-shelf energy (C_vUSE) of materials is estimated to fall below the required 50 ft-lb (67J) energy value.

The ability of the reactor pressure vessel to resist fracture is the primary factor in ensuring the safety of the primary system in light water-cooled reactors. The beltline region of the reactor vessel is the most critical region of the vessel because it is exposed to neutron irradiation. The general effects of fast neutron irradiation on the mechanical properties of such low-alloy ferritic steels as SA508, Class 2, used in the fabrication of the Turkey Point Units 3 and 4 reactor vessels, are well characterized and documented in the literature. The low-alloy ferritic steels used in the beltline region of reactor vessels exhibit an increase in ultimate and yield strength properties with a corresponding decrease in ductility after irradiation. The most significant mechanical property change in reactor pressure vessel steels is the increase in transition from ductile to brittle fracture accompanied by a reduction in the Charpy upper-shelf energy value. The regulations for addressing these changing material properties are found Ref. 1 and 2. These requirements are applied to operating reactor vessels by the procedures described in BAW-10046[3] and BAW-1543[4].

1.1. Background

It became apparent in the late 1950's that neutron embrittlement could seriously degrade the mechanical properties of steels used in reactor vessels. This was a phenomenon that varied significantly from one type of steel to another, from

one heat to another, and from one weld to another. Accordingly, a number of research programs were conducted to evaluate the phenomenon. By the time the first commercial nuclear plants were designed, enough data were accumulated to confirm that the neutron irradiation damage to the reactor vessel materials could significantly degrade the properties. Not all of the first generation reactor vessels were equipped with surveillance capsules to monitor irradiation damage; however, out of this initial period of nuclear development, the guidelines for establishing an RVSP were adopted. ASTM Standard E185-61T,[5] "Tentative Recommended Practice for Surveillance Tests on Structural Materials in Nuclear Reactors" was issued and conveyed the current state-of-the-art technology for designing a surveillance program.

Research on neutron irradiation damage to reactor vessel steels continued in the 1960's. Specifically, the effects of the principal parameters influencing neutron embrittlement sensitivity was studied, including the effects of differing neutron spectra, neutron flux rates, irradiation temperature, and chemical composition on pressure vessel steels. These studies were conducted using both commercial power plants and test reactors with the primary objective of determining the sensitivity of commonly used reactor vessel steels to neutron irradiation.[6-9]

In the late 1960's, a significant discovery was made when the copper and phosphorus contents in reactor vessel materials were identified by the Naval Research Laboratory as principal parameters contributing to mechanical property degradation.[10-13] Further work, in cooperation with Babcock & Wilcox, confirmed the role of these two elements and led to their control in steels and weld metal to be exposed to neutron irradiation.

In 1973, in a concerted effort to improve the quality of reactor pressure vessel integrity and to base the assessment of vessel integrity on a theoretical rather than an empirical basis, the concept of fracture mechanics techniques was implemented through Nuclear Regulatory Commission (NRC) regulation. These requirements are included in 10CFR50, Appendix G, "Fracture Toughness Requirements." Also included was a requirement for monitoring the neutron embrittlement

of the reactor vessel beltline region, which is described in 10CFR50, Appendix H, "Reactor Vessel Material Surveillance Program Requirements." With the issue of Appendix H, a justification was established for a concerted effort to acquire the necessary information by testing irradiated specimens from surveillance capsules and to standardize the existing surveillance program to the extent possible. Also, these Appendices made an RVSP mandatory. Up to this point, the data gathered from an RVSP had received low priority and RVSPs were nonuniform in format and content since the requirements were broadly defined and gave considerable latitude to surveillance program designers. It was not until 1979 that ASTM E185 required that the specific "controlling" weld be included in the surveillance capsules. ASTM E185-73[14] was further revised to support the requirements of 10CFR50, Appendix H through a cooperative effort between the standard development committee and the regulators.

Today, the requirements of 10CFR50, Appendixes G and H, together with ASTM Standard E185-82[15], are recognized throughout the nuclear industry as the standards and procedures for ensuring the integrity of nuclear reactor pressure vessels subject to inservice environmental degradation. These regulations require the Owners of light-water cooled nuclear power plants to monitor the neutron radiation-induced changes in impact toughness and mechanical properties of materials comprising the reactor vessel. Test data obtained from RVSPs allow determination of the conditions under which the reactor vessel may be operated to avoid nonductile failure within a prescribed margin of safety. Fracture mechanics techniques are used to quantitatively define plant operating conditions in terms of pressure-temperature (P-T) limits. The fracture mechanics analyses are performed in accordance with 10CFR50, Appendix G. The input information for these analyses includes material properties, applied stresses, neutron fluence, a reference flaw size, and system operating considerations.

On July 26, 1983, a revision to 10CFR50, Appendixes G and H, became effective. The most significant revisions were to (1) extend the coverage of Appendix G to include steels with specified minimum yield strengths from 50,000 to 90,000 psi, (2) determine the temperature shift at the 30 ft-lb level (this does not change

the 50 ft-lb minimum upper-shelf energy criterion), (3) satisfy predicted end-of-life fracture toughness requirements using radiation conditions at the "critical location on the crack front of the assumed flaw," and (4) extend Appendix H rules to define the basic requirements of an integrated surveillance program.

The unirradiated C_vUSE level of Linde 80 welds was not high enough to accommodate regulatory requirements regarding the effects of neutron irradiation. At the time these early reactor vessels were fabricated, applicable codes and regulations did not specify minimum irradiated and unirradiated C_vUSE levels. Even though these conditions existed before the current requirements for reactor vessel fracture toughness were established, it is now required that all reactor vessel materials, regardless of the date of manufacture, must exhibit adequate toughness to prevent failures. 10CFR50, Appendix G, requires that when significant radiation-induced degradation of material fracture toughness properties occurs, corrective measures must be determined and submitted to the NRC for review three years before the material's C_vUSE is predicted to drop below 50 ft-lbs. If corrective actions are not applied in a timely manner, plant availability may be severely limited.

Imposition of these restrictions is described in 10CFR50, Appendix G, and the ASME Boiler and Pressure Vessel (B&PV) Code, Section III.[16] Paragraph V.B of 10CFR50, Appendix G, in part, states the following requirements:

> Reactor vessels may continue to be operated only for that service period within which the requirements of Section IV of this Appendix are satisfied using the predicted value of the adjusted reference temperature and the predicted value of the upper-shelf energy at the end of the service period to account for the effects of radiation on the fracture toughness of the beltline materials.

In the event that these requirements cannot be satisfied as stated in 10CFR50, Appendix G, or by alternative procedures acceptable to the Nuclear Regulatory Commission (NRC), reactors may continue to operate provided all the following requirements of 10CFR50, Appendix G, paragraph V.C are satisfied:

1. A volumetric examination of 100 percent of the beltline materials that do not satisfy the requirements of Section V.B of this Appendix is made

and any flaws characterized according to Section XI[28] of the ASME B&PV Code and as otherwise specified by the Director, Office of Nuclear Reactor Regulation.

2. Additional evidence of the fracture toughness of the beltline materials after exposure to neutron irradiation is to be obtained from results of supplemental fracture toughness tests.

3. A fracture analysis shall be performed that conservatively demonstrates, making appropriate allowances for all uncertainties, the existence of equivalent margins of safety for continued operations.

Paragraph V.D further states, "If the procedures of Section V.C of this Appendix do not indicate the existence of an equivalent safety margin, the reactor vessel beltline region may, subject to the approval of the Director, Office of Nuclear Reactor Regulation, be given a thermal annealing treatment to recover the fracture toughness of the material." Appendix A provides a detailed discussion on reactor vessel thermal annealing. All nuclear plants, regardless of the fabrication date, must meet the requirements stated above.

Since Appendix G also applies to the early fabrication period reactor vessels, continued operation must be justified by demonstrating that equivalent margins of safety exist for any beltline material suspected to exhibit C_vUSE less than 50 ft-lb. This requires obtaining fracture toughness data for the affected materials and performing a fracture mechanics analysis using these data.

A revision in 1983 to 10CFR50, Appendix H expanded the basic requirements of an integrated surveillance program. The B&W Owners Group integrated RVSP approach was accepted by the NRC and has been in operation by B&W since 1976. For an integrated RVSP to be acceptable to the NRC, a number of criteria, as provided by 10CFR50, Appendix H, must be met. Paragraph II. C of Appendix H states the following:

A. An integrated surveillance program may be considered for a set of reactors that have similar design and operating features.

B. The representative materials chosen for surveillance from each reactor in the set may be irradiated in one or more of the reactors, but there must be an adequate dosimetry program for each reactor.

C. No reduction in the requirements for number of materials to be irradiated, specimen types, or number of specimens per reactor is permitted, but the amount of testing may be reduced if the initial results agree with predictions.

D. Integrated surveillance programs must be approved by the Director, Office of Nuclear Reactor Regulation, on a case-by-case basis. Criteria for approval include the following considerations.

E. The design and operating features of the reactors in the set must be sufficiently similar to permit accurate comparison of the predicted amount of radiation damage as a function of total power output.

F. There must be adequate arrangement for data sharing between plants.

G. There must be a contingency plan to assure that the surveillance program for each reactor will not be jeopardized by operation at reduced power level or by an extended outage of another reactor from which data are expected.

H. There must be substantial advantages to be gained, such as reduced power outages or reduced exposure to radiation, as a direct result of not requiring surveillance capsules in all reactors in the set.

The above criteria and considerations are satisfied by the B&W Owners Group MIRVP approach.

1.2. Master Integrated Reactor Vessel Surveillance Program

1.2.1. General Description

The master integrated reactor vessel surveillance program (MIRVP) combines 17 separate RVSPs and, where appropriate or necessary, provides for sharing of irradiation sites. Additionally, it addresses both the short- and long-term requirements for acquiring irradiation data and the need to improve the quality and quantity of fracture toughness data to support the continued licensability of the participating reactor pressure vessels.

The MIRVP correlates data from both power reactor surveillance monitoring and test reactor research programs. The principal sources of information are the power reactor surveillance programs; this discussion, therefore, is mainly concerned with the power reactor program, which is comprised of three parts. The first part is the continuation of the plant-specific surveillance programs that

monitor the irradiation damage to selected materials, as originally planned for each individual plant. The capsules contain samples of weld metal, plate or forging material, and heat-affected zone (HAZ) material from the vessel beltline and neutron dosimetry and thermal monitors; this part of the program will therefore continue to monitor the long-term effects of neutron irradiation on the reactor vessel materials.

The second part of the program consists of a series of specially designed supplementary surveillance capsules (SUPCAPS) to study the effects of irradiation on a number of weld metals, which are anticipated to be sensitive to irradiation damage because of their chemical composition and low initial Charpy upper-shelf energies. These capsules differ from regular plant-specific RVSP capsules in that they contain the necessary specimens to obtain fracture toughness properties of individual weld metals. The capsules are located in the same irradiation holder tubes as the regular plant-specific surveillance capsules at Crystal River-3 and Davis-Besse.

The third part of the MIRVP consists of higher fluence supplementary weld metal surveillance capsules (HUPCAPS) to obtain irradiated weld metal data (primarily fracture toughness properties) to satisfy the requirements of 10CFR50, Appendixes G and H for the current license and the license renewal of the plants involved in the program. Additional objectives are to (1) provide for a capsule of Westinghouse design for correlation of irradiation data in the Westinghouse neutronic environment with the B&W 177-FA environment; (2) provide irradiation of reconstituted specimens (to accelerate data gathering); and, (3) provide definitive information on the annealing response of this family of materials.

The MIRVP also provides for the comparing of the above capsule data with data obtained on the same material by various test reactor research programs. The high flux available in a test reactor makes it possible to achieve high fluence in specimens in a relatively short time, e.g., EOL fluence in six months irradiation time. However, the neutron damage mechanism in this high flux and particular neutron energy spectrum and temperature can be different than that experienced in PWRs. Data comparisons for fluences up to approximately 1.4 x

10^{19} n/cm^2 have been completed. However, analysis of the high fluence data is not complete and additional test reactor irradiations may be necessary to fully evaluate the effects of flux density and neutron energy spectrum on the irradiation damage to these materials.

The surveillance materials in the capsules of the plant-specific RVSP were not selected in accordance with ASTM E 185-73. Hence, the materials monitored by the RVSP are not always the materials judged in 10CFR50, Appendix H, to most likely be the controlling beltline region materials with regard to radiation embrittlement for the reactor vessel for which the RVSP was designed. Consequently, the applicability of the data to be generated by the plant-specific RVSP becomes limited. However, by combining the data from all the RVSPs, it is practical to develop a data base to determine the probable values and predict the irradiation behavior of those welds for which there are no specific data. This does not preclude a plant-specific materials characterization should sufficient data be available.

1.2.2. Plant-Specific Surveillance Programs

The plant-specific surveillance programs include irradiation (1) in host reactors of surveillance capsules that were removed from the B&W 177-FA reactors, and (2) of capsules from those plants in which the irradiations are being conducted. Each plant participating in the MIRVP has a plant-specific surveillance program that was designed to meet the requirements of the NRC and the ASTM E 185 revision at the time the program was developed. The following sections summarizes the salient features of the B&W 177-FA and Westinghouse-designed plant RVSPs.

1.2.2.1. Babcock and Wilcox-Designed Reactor Vessel Surveillance Programs

There are eight B&W-designed reactor vessels that contain high-copper, Linde 80 ASA weld seams. Irradiation of RVSP capsules for these eight reactors is currently being performed in two "host" reactors, Crystal River-3 and Davis-Besse. Originally, TMI-2 was a host reactor for TMI-1, however, the incident on March 29, 1979 at TMI-2 terminated its use. The capsules in TMI-2 were

requalified[17] for continued irradiation (except for those which were destructively tested for requalification).

Each plant-specific RVSP consists of six surveillance capsules, four of which are the prime data-collecting capsules, and the others are "standby" capsules. The prime capsules are withdrawn at designated time intervals so that the data collected are for irradiation levels ranging from low fluence to that equal to the vessel inner surface (IS) at end of life (EOL). The standby capsules provide any necessary additional data late in the operating life of the plant.

Three basic types of specimens, in varying combinations, are placed in these capsules: Charpy V-notch, tension test, and compact fracture toughness (CT). The Charpy V-notch specimens are 0.394 inch square, 2.165 inches long, and conform to ASTM E 23-72.[18] The tension test specimens are 4.25 inches long and conform to ASTM E 8-69T.[19] The compact fracture toughness specimens are 0.5 inch thick by 1.25 by 1.20 inches, and conform to the basic requirements of ASTM E 399-81[20] and E 813-81.[21] Specimen identity is maintained throughout the program by a die-stamped identification code (a combination of letters and numbers) on the top and bottom of each specimen.

1.2.2.2. Westinghouse-Designed Reactor Vessel Surveillance Programs

There are nine Westinghouse-designed, B&W-fabricated reactor vessels that contain high-copper, Linde 80 ASA weld seams. Each of these plants has an RVSP that consists of either six or eight surveillance capsules. Each capsule contains a combination of specimens that include Charpy V-notch, tension test, and Wedge-Opening Loading (WOL) fracture toughness specimens representative of reactor vessel material. The capsules also contain neutron dosimeters and thermal monitors.

Each plant-specific RVSP was designed to meet the requirements of the NRC and the ASTM E 185 revision in effect at the time the program was developed. For each plant a WCAP (Westinghouse Commercial Atomic Power) report was prepared that describes the fabrication and design of the RVSP capsules. The Westinghouse-

designed Turkey Point Units No. 3 and 4 associated surveillance program reports are as follows.

Turkey Point Unit No. 3

WCAP-7656 Florida Power and Light Company, Turkey Point Unit No. 3 Reactor Vessel Radiation Surveillance Program, Westinghouse Electric Corporation, Pittsburgh, Pennsylvania, May 1971.

Turkey Point Unit No. 4

WCAP-7660 Florida Power and Light Company, Turkey Point Unit No. 4 Reactor Vessel Radiation Surveillance Program, Westinghouse Electric Corporation, Pittsburgh, Pennsylvania, May 1971.

2. REACTOR VESSEL OF TURKEY POINT UNITS 3 AND 4

The establishment of the mechanical and toughness properties of reactor pressure vessels in accordance with applicable regulations and standards is an essential aspect of the licensing process. As these rules are improved it is necessary to ensure that the data used for licensing of the reactor vessels are representative the best information and materials properties available for each specific reactor vessel. The data are also essential in establishing the normal pressure-temperature operating limitations as required by 10CFR50, Appendix G.

2.1. Turkey Point Unit 3

The materials and chemical composition data for the Turkey Point Unit 3 reactor vessel are presented in Tables 2-1 through 2-3. These data represent an accumulation of information from various sources (References 22, 23 and 24) and are complete as to the data available. The current essential data for the weld metals are available. In addition, the initial reference temperature data represents the best available data as defined in Section 2.4.

The location and identification of the forgings and welds within the beltline region of the Turkey Point Unit 3 reactor pressure vessel are shown in Figure 2-1.

2.2. Turkey Point Unit 4

The data for Turkey Point Unit 4 reactor vessel are presented in Tables 2-4 through 2-6. These data represent an accumulation of information from various sources (References 22, 25 and 26) and are complete except for the limited amount of data for the weld metals. The current essential data for the weld metals are available. In addition, the initial reference temperature data represents the best available data as defined in Section 2.4.

The location and identification of the forgings and welds within the beltline region of the Turkey Point Unit 4 reactor pressure vessel are shown in Figure 2-2.

2.3. Surveillance Data Bases

Each reactor vessel has a surveillance program to monitor the neutron radiation damage of the materials in the beltline region. These data for each reactor vessel at the Turkey Point site were tabulated separately from the main data base as a convenience for easy reference.

The design of a reactor vessel materials surveillance program is based on the need to monitor the toughness properties of the controlling radiation sensitive material from which the reactor vessel was fabricated. Of equal importance is the benchmarking, or verification, of the fluence which the reactor vessel experiences.

The extent to which a surveillance program meets these objectives depends on when the reactor vessel was fabricated. This is due to the evolution of surveillance program requirements as more knowledge has been obtained from existing programs. Some of the requirements can be upgraded to meet the current 10CFR50, Appendix H while other reactor vessels will be required to make do with the installed programs. Each of the Turkey Point reactor vessel surveillance programs will be described separately.

2.3.1. Turkey Point Unit 3

The surveillance program was designed in accordance with ASTM E185-66. The controlling materials are contained in the program. In addition, the program contains wedge opening loading (WOL) specimens which at the time were state-of-the-art for evaluating the effects of radiation on the fracture toughness of the reactor vessel materials. The materials contained in the surveillance program and a summary of their chemical composition and mechanical properties are contained in Table 2-7.

2.3.2. Turkey Point Unit 4

The surveillance program was designed in accordance with ASTM E185-66. The controlling materials as defined by ASTM E185-66 are contained in the program. In addition, the program contains wedge opening loading (WOL) specimens which at the time were state-of-the-art for evaluating the effects of radiation on the fracture toughness of the reactor vessel materials. The materials contained in the surveillance program and a summary of their chemical composition and mechanical properties are contained in Table 2-8.

2.3.3. Integrated Surveillance Program

2.3.4. Spare Capsules

Extra surveillance capsules not required to meet the current requirements of ASTM E185-82 will remain in the reactor vessel. These capsules can be used in the future to provide data for the verification of reactor vessel fluence calculations or to provide materials data for support of plant life extension. To ensure that the extra capsules will provide useful data in the future they will be moved to maximum lead factor positions during the appropriate inservice inspection as the positions become available, in order to maximize the total accumulated fluence.

2.3.5. Archive Surveillance Material

The availability of additional surveillance material is important in the event that additional materials properties data is needed for the reactor vessel controlling beltline region materials; or, in the event that licensing requirements change and new data is required which necessitates applying improved testing techniques to the original materials of fabrication. An inventory of the available materials applicable to Turkey Point Units 3 and 4 was made and documented for future reference as needed.

2.3.6. Overview of Surveillance Data

The available surveillance data from Turkey Point Units 3 and 4 are presented in Table 2-9. The summary presented are the critical data needed to evaluate the

controlling weld metals in Turkey Point Units 3 and 4. In addition, the only available test reactor irradiated data for weld metal SA-1101 is included for comparison to the plant specific surveillance program data.

The irradiated Charpy 30 ft-lb temperatures (RT_{NDT}) for weld metals SA-1094 and SA-1101 are compared to the predicted values based on Regulatory Guide 1.99, Revision 2, Position 1, in Figure 2-3. The test reactor data for SA-1101 is included for comparison and support of the behavior of the surveillance data for SA-1101. These data show that the Regulatory Guide 1.99 with margin is a conservative prediction of the expected irradiation behavior of the SA-1101 weld metal. The same relationship is observed for the SA-1094 weld metal based on the chemistry for the weld metal. However, both of these weld metals were fabricated with the same weld wire (Mn-Mo-Ni Wire/Heat No. 71249) but different lots of Linde 80 weld flux and, therefore, it is expected that the two weld metals would behave in a similar manner. Based on the evaluation of the individual weld metals it would indicate that a significant difference existed between the two weld metals. An evaluation of the two weld metals based on Regulatory Guide 1.99, Position 2, and using the SA-1101 weld metal data for the calculation of the mean curve is shown in Figure 2-4. This demonstrates that the SA-1094 weld metal properties are within the two standard deviations of the surveillance data for the SA-1101 weld metal.

The upper-shelf energy data for SA-1094 and SA-1101 weld metals are compared to the correlation developed for Mn-Mo-Ni/Linde 80 submerged-arc weld metals in BAW-1803, Revision 1,[45] and are presented in Figure 2-5. These data also include two test reactor data points for SA-1101. All the data points for SA-1101 group around the 0.30% copper line which indicates a similar response of the weld metals to neutron radiation. It is significant that the data point for the SA-1094 weld metal is displaced about 0.10 percentage points from the similar data for SA-1101. Unlike, the data for the Charpy shift data shown in Figure 2-3, the data in Figure 2-5 is not adjustable but represents the measured values. Based on these observations it is possible that the differences observed in the data is attributable to unidentified parameters which are not readily obvious from the

record for these data. These include, but may not be limited to, parameters such as: 1) error in the Charpy impact test process, 2) deviation in chemical composition for the established composition, and 3) unidentified factors influencing the irradiation environment.

In conclusion, the Charpy 30 ft-lb temperature data is representative of that which would be expected based on fluence and chemical composition. The irradiated upper-shelf energy data exhibits an inconsistency between the data for SA-1101 and SA-1094. It appears that there is an inconsistency in the SA-1094 weld metal data that cannot be identified. The variation is not important because it is estimated that both materials will decrease below 50 ft-lbs prior to end-of-life. Since the controlling material in the actual reactor vessel is SA-1101 weld metal, the analysis of the reactor vessel will be based on SA-1101 weld metal properties.

2.4. Evaluation of Reactor Vessel End-of-Life Material Properties

The reactor vessels end-of-life fracture properties were evaluated to determine the need to implement the appropriate actions as defined in 10CFR50, Appendix G. The weld metals were identified as the most neutron radiation sensitive materials in the reactor vessels. The reactor vessel weld end-of-life (32 EFPY) fracture toughness properties for Turkey Point Units 3 and 4 are presented in Tables 2-10 and 2-11. These data show that the upper-shelf energy of weld metal SA-1101 (controlling weld metal for both reactor vessels) is estimated to decrease to a value less than 50 ft-lbs prior to the end of the reactor vessel design life. This decrease is estimated to occur only when the Regulatory Guide 1.99, Revision 2, formulation is used to make the estimate and not that included in BAW-1803, Revision 1. The data used to develop the correlation in BAW-1803, Revision 1, is based entirely on reactor vessel surveillance program data and thereby is the best correlation currently available.

Reactor vessel surveillance program capsule data from Turkey Point Unit 3 and the available test reactor data for weld metal SA-1101 are presented in Figure 2-5. These data indicate that it is reasonable to expect weld metal SA-1101 upper-

shelf energy to decrease to below 50 ft-lbs at or near to the end of design life of the reactor vessels.

The data from Regulatory Guide 1.99, Revision 2, the upper-shelf correlation data from BAW-1803, Revision 1 and the data obtained from the available surveillance capsules and test reactor research programs are summarized in Table 2-12. The data developed using the Regulatory Guide procedures demonstrates just how outmotive the technique is for estimating irradiated upper-shelf energies. By contrast, the correlation lower bound from BAW-1803, Revision 1 compares very favorably with the limited surveillance program data and the data points obtained from test reactor research programs. These data could be interpreted to justify that the upper-shelf energies will not decrease below the required 50 ft-lb. However, the uncertainty in the data precludes defining the relationship with absolute certainty either to upper-shelf energy level and/or reactor vessel life. Therefore, the prudent approach is to evaluate the reactor vessel as if the 50 ft-lb requirement was violated.

Table 2-1. Chemical Composition of Beltline Region Materials for Turkey Point Unit 3[a]

Material Identification	Chemical Composition, wt %								
	C	Mn	P	S	Si	Ni	Cr	Mo	Cu
123P461 (SA508, Cl.2)	0.20	0.64	0.010	0.010	0.26	0.70	0.40	0.62	0.058
123S266 (SA508, Cl.2)	0.20	0.62	0.010	0.008	0.20	0.67	0.38	0.58	0.079
SA-1484 ASA/Linde 80	0.08	1.52	0.018	0.015	0.42	0.60	0.09	0.39	0.24
SA-1101 ASA/Linde 80	0.07	1.28	0.021	0.014	0.52	0.60	0.16	0.37	0.26
SA-1135 ASA/Linde 80	0.08	1.45	0.011	0.013	0.49	0.54	0.08	0.38	0.25

[a]Per BAW-2150, December 1990.

Table 2-2. Heat Treatment of Beltline Region Materials for Turkey Point Unit 3

Material Identification	Heat Number	Flux Lot Number	Specification	Supplier	Heat Treatment
123P461 (SA508, Cl.2)	123P461VA1	N.A.	SA508 Cl.2	Bethlehem	1550°F for 13 hours; water quench 1210°F for 18 hours; air cooled 1125°F for 10 1/2 hours; furnace cool to 600°F
123S266 (SA508, Cl.2)	123S266VA1	N.A.	SA508 Cl.2	Bethlehem	1550°F for 13 hours; water quench 1210°F for 18 hours; air cooled 1125°F for 10 1/2 hours; furnace cool to 600°F
SA-1484 ASA/Linde 80	72442	8579	Mn-Mo-Ni/Linde 80	Page/Linde	Stress relief: 1125F for 10 1/4 hours, furnace cool to 600°F
SA-1101 ASA/Linde 80	71249	8445	Mn-Mo-Ni/Linde 80	Page/Linde	Stress relief: 1125°F for 10 1/4 hours; furnace cool to 600°F
SA-1135 ASA/Linde 80	61782	8457	Mn-Mo-Ni/Linde 80	Page/Linde	Stress relief: 1125°F for 10 1/4 hours; furnace cool to 600°F

Note: All data per Certified Material Test Reports unless noted otherwise.

Table 2-3. Unirradiated Mechanical Properties of Beltline Region Materials for Turkey Point Unit 3

Material Identification	Heat Treatment	Toughness Properties						Tensile Properties			
		C_v + 10F, ft-lbs	C_v 30, F	C_v 50, F	C_v USE, ft-lbs	T_{NDT}, F	RT_{NDT}, F	YS, ksi	UTS, ksi	El, %	RA, %
123P461 (SA508, C1.2)	See Table 2-2	+82	-32	-19	150	+40	+40	65.8	89.2	25.9	68.5
123S266 (SA508, C1.2)	"	+88	-59	-48	178	+30	+30	59.3	86.0	27.6	71.2
SA-1484 ASA/Linde 80	"	+44	---	---	---	---	---	--	84.0	--	--
SA-1101 ASA/Linde 80	"	+45	---	+10*	+95*	-90*	-50*	68.6	84.2	28.5	--
SA-1135 ASA/Linde 80	"	+52	---	---	---	---	---	68.3	81.8	28.3	--

Note: All data per Certified Material Test Reports unless noted otherwise.

*Tests performed after original Certified Material Test Report.

Table 2-4. Chemical Composition of Beltline Region Materials for Turkey Point Unit 4[a]

Material Identification	Chemical Composition, wt %								
	C	Mn	P	S	Si	Ni	Cr	Mo	Cu
123P481 (SA508, C1.2)	0.20	0.65	0.010	0.010	0.24	0.68	0.32	0.59	0.054
122S180 (SA508, C1.2)	0.22	0.60	0.010	0.009	0.22	0.74	0.35	0.60	0.056
WF-70 (OD) ASA/Linde 80	0.09	1.63	0.018	0.009	0.54	0.59	0.10	0.40	0.35
WF-67 (ID) ASA/Linde 80	0.08	1.55	0.016	0.016	0.58	0.60	0.09	0.39	0.24
SA-1101 ASA/Linde 80	0.07	1.28	0.021	0.014	0.52	0.60	0.16	0.37	0.26
SA-1135 ASA/Linde 80	0.08	1.45	0:011	0.013	0.49	0.54	0.08	0.38	0.25

[a]Per BAW-2150, December 1990.

Table 2-5. Heat Treatment of Beltline Region Materials for Turkey Point Unit 4

Material Identification	Heat Number	Flux Lot Number	Specification	Supplier	Heat Treatment
123P481 (SA508, Cl.2)	123P481	N.A.	SA508, Cl.2	Bethlehem	1550°F for 10 1/4 hours; water quench 1210°F for 18 hours; air cooled 1125°F for 10 1/2 hours; furnace cool to 600°F
122S180 (SA508, Cl.2)	122S180	N.A	SA508, Cl.2	Bethlehem	1550°F for 10 1/2 hours; water quench 1200°F for 18 hours; air cooled 1125°F for 10 1/2 hours; furnace cooled to 600°F
WF-70 (OD 33%) ASA/Linde 80	72105	8669	Mn-Mo-Ni/Linde 80	Page/Linde	Stress relief: 1125F for 10 1/2 hours, furnace cooled to 600°F
WF-67 (ID 67%) ASA/Linde 80	72442	8669	Mn-Mo-Ni/Linde 80	Page/Linde	Stress relief: 1125F for 10 1/2 hours, furnace cooled to 600°F
SA-1101 ASA/Linde 80	71249	8445	Mn-Mo-Ni/Linde 80	Page/Linde	Stress relief: 1125F for 10 1/2 hours, furnace cooled to 600°F
SA-1135 ASA/Linde 80	61782	8457	Mn-Mo-Ni/Linde 80	Page/Linde	Stress relief: 1125F for 10 1/2 hours, furnace cooled to 600°F

Note: All data per Certified Material Test Reports unless noted otherwise.

Table 2-6. Unirradiated Mechanical Properties of Beltline Region Materials for Turkey Point Unit 4

Material Identification	Heat Treatment	Toughness Properties						Tensile Properties			
		C_v + 10F, ft-lbs	C_v 30, F	C_v 50, F	C_v USE, ft-lbs	T_{NDT}, F	RT_{NDT}, F	YS, ksi	UTS, ksi	El, %	RA, %
123P481 (SA508, C1.2)	See Table 2-5	+45	+16	+ 44	>135	+50	+50	69.5	92.1	24.8	66.8
122S180 (SA508, C1.2)	"	+64	-54	- 26	>150	+40	+40	71.1	91.9	24.1	67.4
WF-70 (OD) ASA/Linde 80	"	+39	+65*	+120*	58*	-50*	+74*	69.0	85.5	25.8	64.7
WF-67 (ID) ASA/Linde 80	"	+31	+25*	+ 57*	70*	-20*	- 3*	64.0	81.5	31.3	65.8
SA-1101 ASA/Linde 80	"	+45	---	+10*	+95*	-90*	-50*	68.6	84.2	28.5	--
SA-1135 ASA/Linde 80	"	+52	---	--	---	---	---	68.3	81.8	28.3	--

Note: All data per Certified Material Test Reports unless noted otherwise.

*Tests performed after original Certified Materials Test Report.

Table 2-7. Turkey Point Unit 3 Description and Properties of Reactor Vessel Surveillance Program Materials[a]

Material ID	Chemical Composition, %									Impact Properties				
	C	Mn	P	S	Si	Ni	Cr	Mo	Cu	T_{NDT}, F	RT_{NDT}, F	C_vUSE, ft-lb	UTS, ksi	YS, ksi
Base metal A (123P461 VA-1)	0.20	0.64	0.010	0.010	0.26	0.70	0.40	0.62	0.058	--	--	145	86.2	64.4
Base metal B (123S266 VA-1)	0.20	0.62	0.010	0.008	0.20	0.67	0.38	0.58	0.079	--	--	154	82.6	57.4
Weld metal[c] (SA-1101)	0.08	1.56	0.019	0.008	0.59	0.54	0.16	0.38	0.21	--	--	66	92.8	76.3
Correlation Plate (A0421)	0.24	1.34	0.011	0.023	0.23	0.18	0.11	0.51	0.20	--	--	76	--	--

Material ID	Heat No.	Spec No.	Supplier	Heat Treatment		
				Austenitizing	Tempering	Stress Relief
Base metal A	123P461 VA-1	SA508 Cl.2 CC 1332-2	Beth.	1550F for 13 h, water quenched	1210F for 8 h, air cooled	1125F for 10-1/2 h, furnace-cooled to 600F
Base metal B	123S266 VA-1	SA508 Cl.2 CC 1332-2	Beth.	Same as above	Same as above	Same as above
Weld metal	SA-1101	N/A[b]	N/A	N/A	N/A	1125F for 10-1/4 h, furnace-cooled to 600F
Correlation Plate	A0421	SA302, GR B	U.S.S.	1650 for 4 h	1200F for 6 h	

[a]All data per WCAP-7656 unless designated otherwise.

[b]N/A - Not Applicable.

[c]Per BAW-1803, Revision 1, May 1991.

Table 2-8. Turkey Point Unit 4 Description and Properties of Reactor Vessel Surveillance Program Materials[a]

Material ID	Chemical Composition, %									Impact Properties			UTS, ksi	YS, ksi
	C	Mn	P	S	Si	Ni	Cr	Mo	Cu	T_{NDT}, F	RT_{NDT}, F	C_vUSE, ft-lb		
Base metal A (123P481 VA-1)	0.22	0.67	0.010	0.009	0.20	0.71	0.33	0.56	0.054	--	--	135	90.1	68.6
Base metal B (122S180 VA-1)	0.21	0.67	0.011	0.009	0.23	0.70	0.31	0.56	0.056	--	--	132	91.5	70.8
Weld metal[b] (SA-1094)	0.10	1.44	0.014	0.011	0.50	0.60	0.14	0.36	0.30	--	--	68	90.8	70.2
Correlation Plate (HSST 02)	0.22	1.48	0.012	0.018	0.25	0.68	--	0.52	0.14	--	--	122	--	--

Material ID	Heat No.	Spec No.	Supplier	Heat Treatment[b]		
				Austenitizing	Tempering	Stress Relief
Base metal A	123P481 VA-1	SA508 C1.2 CC 1332-2	Beth.	1550F for 10-1/2 h, water quenched	1200F for 18 h, air cooled	1125F for 10-1/2 h, furnace-cooled to 600F
Base metal B	122S180 VA-1	SA508 C1.2 CC 1332-2	Beth.	1550F for 10-1/4 h, water quenched	1210F for 18 h, air cooled	Same as above
Weld metal A	SA-1094	N/A[c]	N/A	N/A	N/A	1125F for 10-1/4 h, furnace-cooled to 600F
Correlation Plate	A-1195-1	SA533 Gr B C1.1	Luken	1600F for 4 h, water quenched	1225F for 4 h, furnaced-cooled	1150 for 40 h, furnace-cooled to 600F

[a]All data per WCAP-7660 unless designated otherwise.

[b]Per BAW-1803, Revision 1, May 1991.

[c]N/A - Not Applicable.

Table 2-9. Irradiated Charpy Data for Weld Metals SA-1094 and SA-1101

Data Source		Fluence n/cm^2	Charpy 30 ft-lb Temperature Initial F	Charpy 30 ft-lb Temperature Irradiated F	Charpy 30 ft-lb Temperature Change F	Charpy Upper-Shelf Energy Initial ft-lbs	Charpy Upper-Shelf Energy Irradiated ft-lbs	Charpy Upper-Shelf Energy Change ft-lbs	Reference
Surveillance Data									
Weld Metal Capsule									
Turkey Point Unit 3									
SA-1101	T	7.01E+18	+12	+176	164	66	62	4	46
SA-1101	V	1.23E+19	+12	+190	178	66	48	18	47
Turkey Point Unit 4									
SA-1094	T	7.54E+18	0	+224	224	68	43	25	48
Test Reactor Data									
Weld Metal	Source								
SA-1101	HSST/Tk3	8.75E+18	-34	+120	154	68	52	16	49
SA-1101	HSST/Tk3	1.16E+19	-34	+145	179	68	51	17	49

Table 2-10. Evaluation of Turkey Point Unit-3 Reactor Vessel End-of-Life (32 EFPY) Upper-Shelf Energy

Material Description			Material Chemical Composition		Estimated EOL Fluence		Initial USE	Estimated EOL-USE per RG 1.99/2[a]		Estimated EOL-USE per BAW-1803/1[b]		Estimated EFPY to 50 ft-lbs at T/4 Location	
Reactor Vessel Beltline Region Location	Heat Number	Type	Copper w/o	Nickel w/o	Inside Surface n/cm^2	T/4 Wall Location n/cm^2	ft-lbs	Inside Surface	T/4 Wall Location	Inside Surface	T/4 Wall Location	RG 1.99/2	BAW-1803/1
Upper shell	123P461	SA508, C12	0.058	0.70	2.8E+19	1.8E+19	150[c]	122	124	N.A.	N.A.	>32	N.A.
Lower shell	123S266	SA508, C12	0.079	0.67	2.8E+19	1.8E+19	178[c]	140	144	N.A.	N.A.	>32	N.A.
Upper circum. weld (100%)	SA-1484	Weld	0.24	0.60	4.2E+18	2.7E+18	(70)[b]	48	50	54	55	>32	>32
Mid. circum. weld (100%)	SA-1101	Weld	0.26	0.60	2.8E+19	1.8E+19	65[c]	33	35	49	50	~1.5	>32
Lower circum. weld (100%)	SA-1135	Weld	0.25	0.54	<1.0E+16	<1.0E+16	(70)[b]	Neg.	Neg.	Neg.	Neg.	>32	>32

[a]Per Regulatory Guide 1.99, Revision 2, dated May 1988.

[b]Estimated per BAW-1803, Revision 1, dated March 1991.

[c]Per Certified Materials Test Reports.

Table 2-11. Evaluation of Turkey Point Unit-4 Reactor Vessel End-of-Life (32 EFPY) Upper-Shelf Energy

Material Description: Reactor Vessel Beltline Region Location	Heat Number	Type	Material Chemical Composition: Copper w/o	Material Chemical Composition: Nickel w/o	Estimated EOL Fluence: Inside Surface n/cm²	Estimated EOL Fluence: T/4 Wall Location n/cm²	Initial USE ft-lbs	Estimated EOL-USE per RG 1.99/2[a]: Inside Surface	Estimated EOL-USE per RG 1.99/2[a]: T/4 Wall Location	Estimated EOL-USE per BAW-1803/1[b]: Inside Surface	Estimated EOL-USE per BAW-1803/1[b]: T/4 Wall Location	Estimated EFPY to 50 ft-lbs at T/4 Location: RG 1.99/2	Estimated EFPY to 50 ft-lbs at T/4 Location: BAW-1803/1
Upper shell	123P481	SA508, C12	0.054	0.71	2.7E+19	1.7E+19	135[c]	108	112	N.A.	N.A.	>32	N.A.
Lower shell	122S180	SA508, C12	0.056	0.70	2.7E+19	1.7E+19	150[c]	122	124	N.A.	N.A.	>32	N.A.
Upper circum weld (OD 33%)	WF-70	Weld	0.35	0.59	N.A.	N.A.	(70)[b]	--	--	--	--	--	>32
Upper circum weld (ID 67%)	WF-67	Weld	0.24	0.60	4.1E+18	2.6E+18	(70)[b]	48	50	54	55	>32	>32
Mid. circum. weld (100%)	SA-1101	Weld	0.26	0.60	2.7E+19	1.7E+19	65[c]	32	36	49	50	-2.0	>32
Lower circum. weld (100%)	SA-1135	Weld	0.25	0.54	<1.0E+16	<1.0E+16	66[c]	Neg.	Neg.	Neg.	Neg.	>32	>32

[a] Per Regulatory Guide 1.99, Revision 2, dated May 1988.

[b] Estimated per BAW-1803, Revision 1, dated March 1991.

[c] Per Certified Materials Test Reports.

Table 2-12. Summary of Evaluation of Effects of Neutron Irradiation on Upper-Shelf Energy of Controlling Weld Metals in Turkey Point 3 and 4

Material Identification	Fluence 32 EFPY T/4 Wall	RG 1.99/R2[a]		BAW-1803/R1[b]		Surveillance Data[c]	
		T/4 Wall Location	50 ft-lb EFPY	T/4 Wall Location	50 ft-lb EFPY	T/4 Wall Location	50 ft-lb EFPY
Turkey Point-3							
Mid. Circ. Weld (SA-1101)	1.8E+19	35	~1.5	50	>32	49.9	~31.5
Turkey Point-4							
Mid. Circ. Weld (SA-1101)	1.7E+19	36	~2.0	50	>32	50.0	~32

[a]Per Regulatory Guide 1.99, Revision 2, dated May 1988.

[b]Estimated per BAW-1803, Revision 1, dated May 1991.

[c]Per Regulatory Guide 1.99, Revision 2, Regulatory Position 2 and related surveillance capsule reports.

Figure 2-1 Identification and Location of Base Materials and Weld Metals in Turkey Point Unit 3 Reactor Vessel

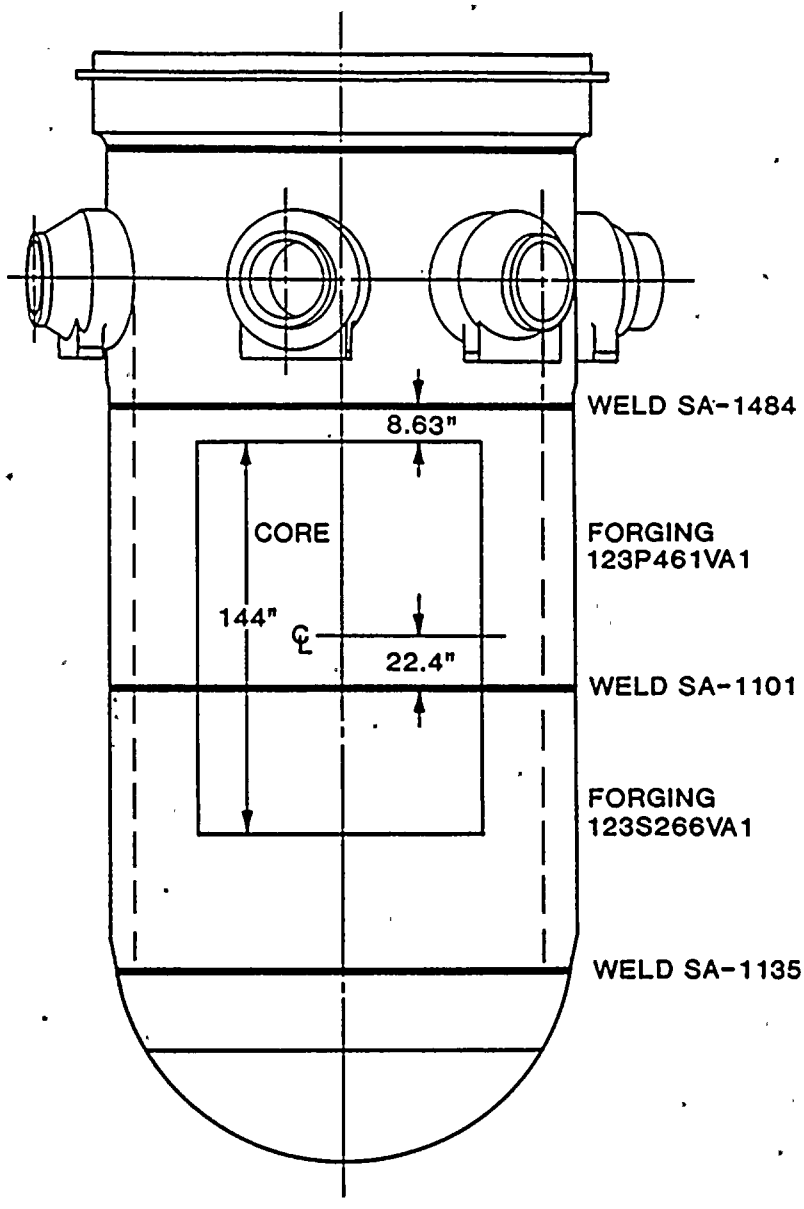

Figure 2-2 Identification and Location of Base Materials and Weld Metals in Turkey Point Unit 4 Reactor Vessel

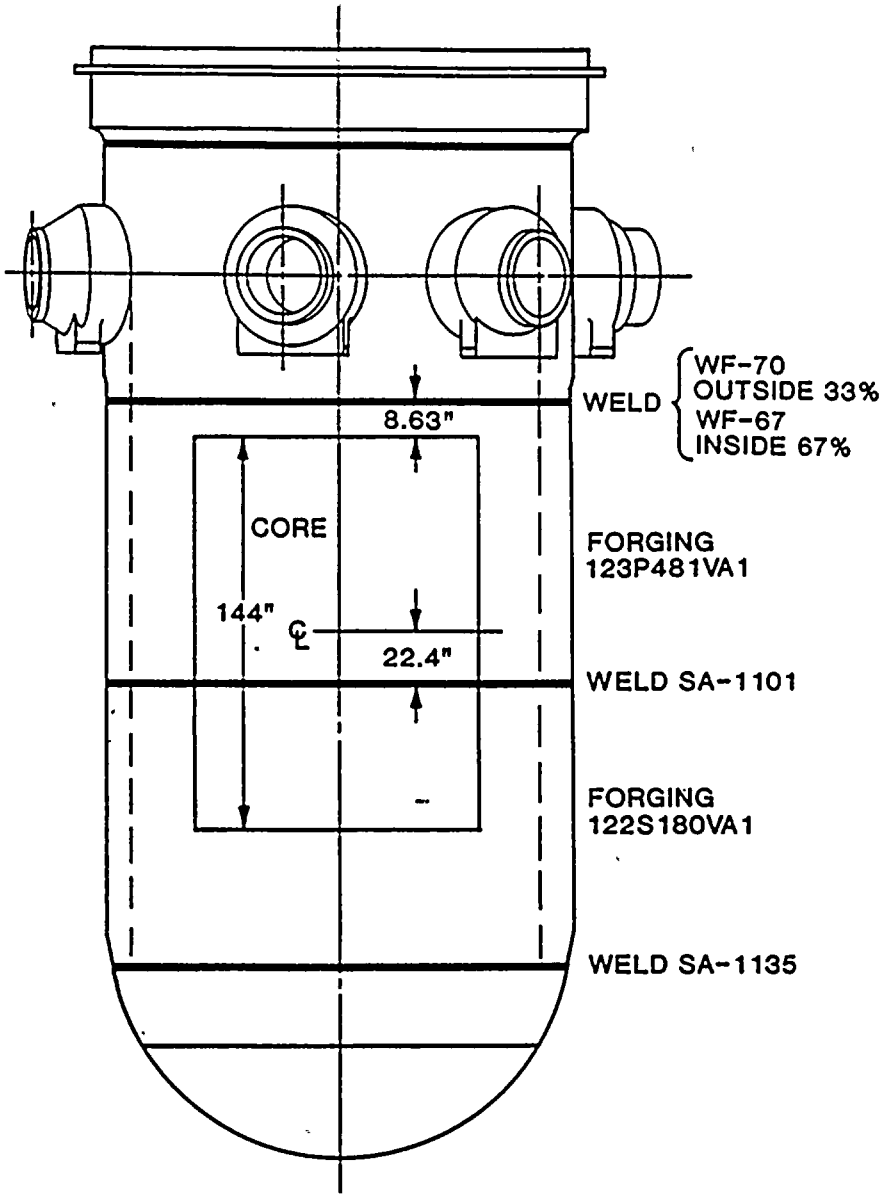

Figure 2-3 Comparison of Irradiated Charpy 30 ft-lb Temperatures for Weld Metals SA-1094 and SA-1101 With Predictions Based on Regulatory Guide 1.99, Revision 2, Position 1

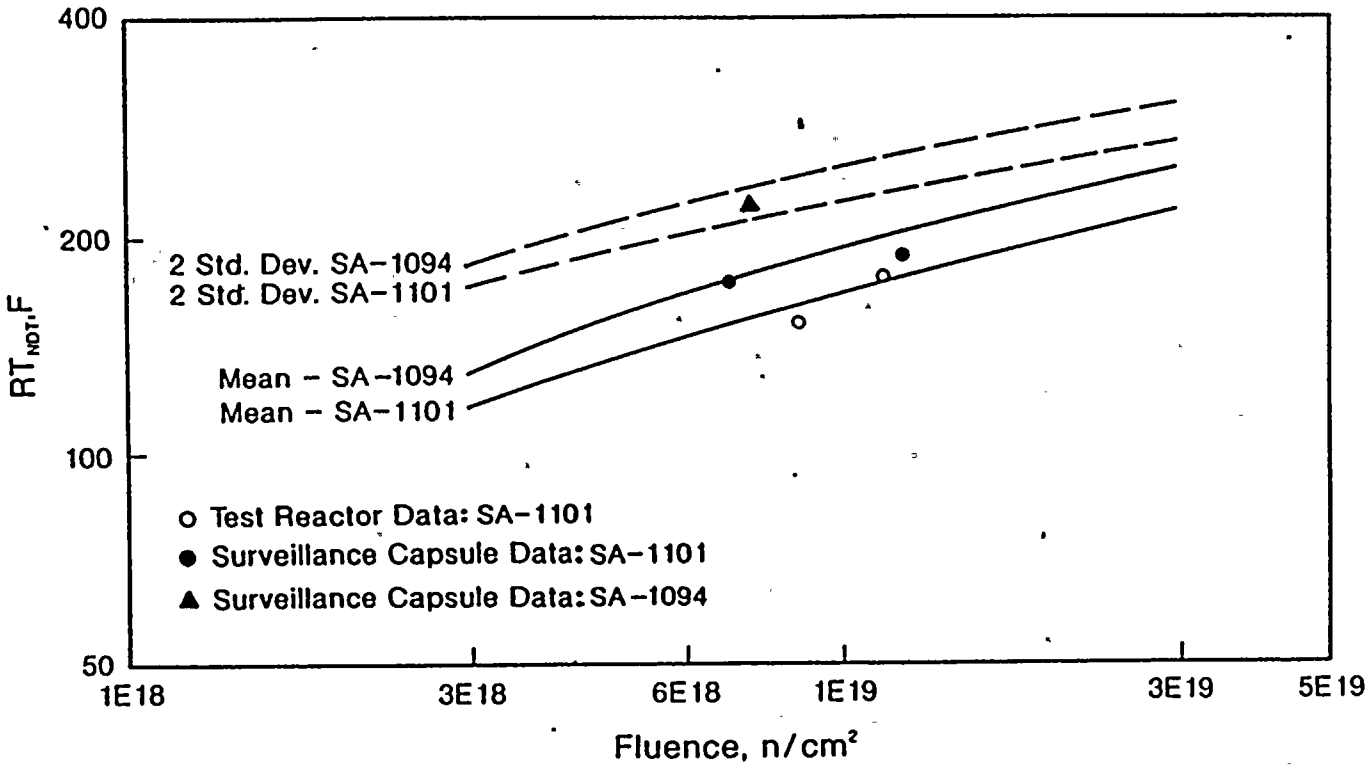

Figure 2-4 Comparison of Irradiated Charpy 30 ft-lb Temperatures for Weld Metals SA-1094 and SA-1101 With Predictions Based on Regulatory Guide 1.99, Revision 2, Position 2

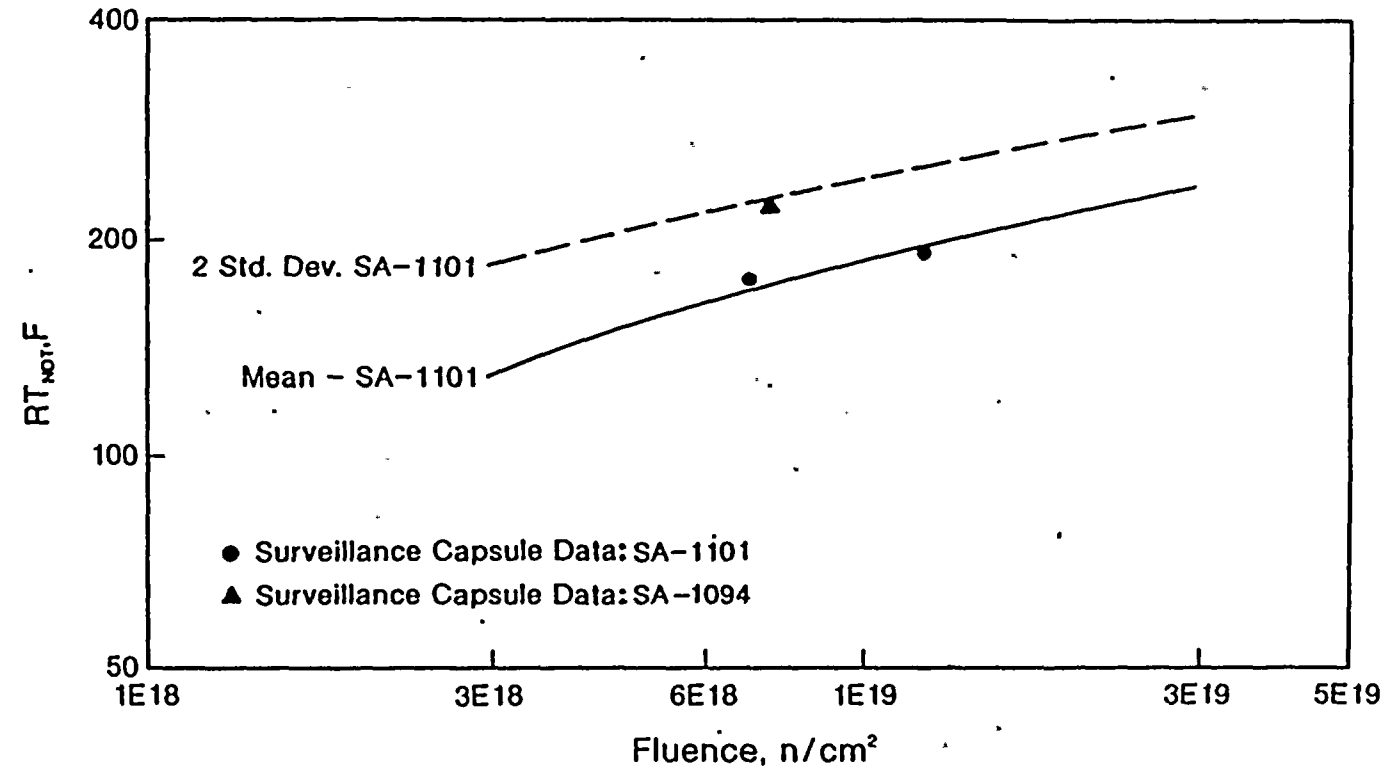

Figure 2-5 Comparison of Irradiated Charpy Upper-Shelf Energy Data for Weld Metals SA-1094 and SA-1101 With Predictions Based on BAW-1803, Revision 1

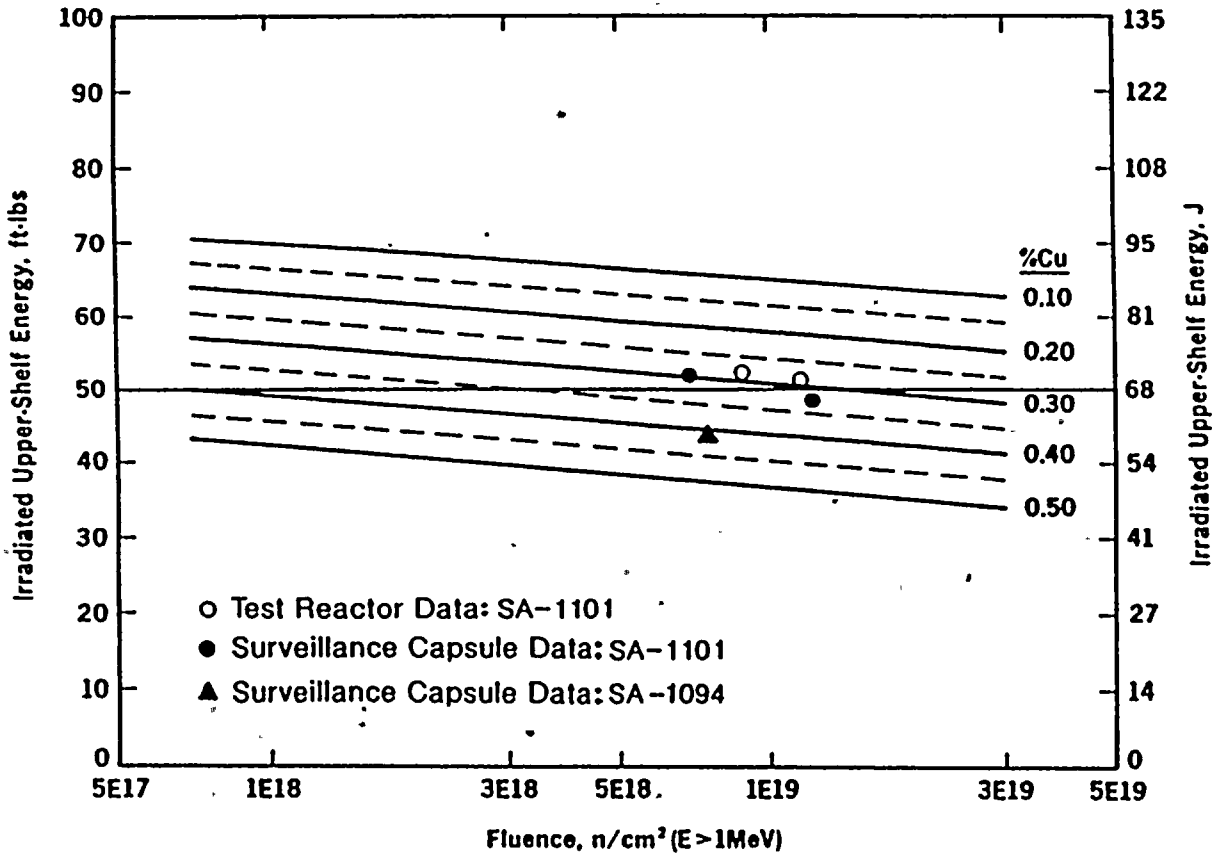

3. ELASTIC-PLASTIC FRACTURE MECHANICS METHODOLOGY

The analytical procedures given in Section III Appendix G of ASME Boiler & Pressure Vessel Code are applicable for the areas of the pressure boundary which must comply with the material upper-shelf toughness restrictions as required by 10CFR50 Appendix G, (i.e. a Charpy upper-shelf energy no less than 50 ft-lbs). If the material does not comply with these requirements then a supplemental fracture mechanics analysis is required to assure the reactor coolant pressure boundary integrity. If a material exhibits less than 50 ft-lbs absorbed energy but greater than 30 ft-lbs, the adjusted shift in RT_{NDT} can be determined in accordance with Regulatory Guide 1.99[27]. 10 CFR 50, Appendix G, specifies that a Charpy upper-shelf energy below 50 ft-lbs is permitted only if the component is verified to have a sufficient margin of safety. The only area of the reactor coolant boundary which is predicted to potentially fall below the 50 ft-lbs level is the reactor vessel beltline region. The evaluation described in this report will be restricted to the beltline region but similar evaluations could be performed on other areas of the system.

Section XI, Appendix G, of the ASME Code[28] contains the operating guidelines for the prevention of non-ductile failure. The general philosophy is to index the fracture toughness to temperature and require that the component be operated at a sufficiently low pressure as to preclude non-ductile failure. However, in the high operating temperature regime ductile tearing is the predicted fracture mode for the ferritic reactor vessel materials. The current specifications in ASME Appendix G do not provide any guidance in preventing ductile failures, implying that the non-ductile failure limit would conservatively cover the ductile failure mode. Recently, the Working Group on Flaw Evaluation of Section XI of ASME Boiler and Pressure Vessel Code recognized the fact that at the upper shelf

temperature range there is no longer concern over cleavage type failures and established a new and separate set of acceptance criteria solely for the upper shelf temperature region. Evaluation for ductile fracture is allowed by a J-integral based elastic-plastic fracture mechanics method.

3.1. Acceptance Criteria for Lower Upper Shelf Fracture Toughness Analysis

ASME Boiler and Pressure Vessel Code Section XI developed a set of acceptance criteria for low upper-shelf fracture toughness analysis by an industry consensus group. This new standard was transmitted to the NRC[29].

3.1.1. Acceptance Standard for Level A and B Conditions

Level A and B Conditions

For a postulated semi-elliptical surface flaw with an a/t = 0.25 and with an aspect ratio of 6 to 1 (i.e. surface length to flaw depth), and oriented along the weld, two criteria must be satisfied as described below. If the base metal is governing, the postulated flaw must be longitudinally oriented. Smaller flaw sizes may be used on an individual case basis if a smaller size of the above postulated flaw can be justified. The expected accumulation pressure to be discussed below is the maximum pressure defined in the Overpressure Protection Report which satisfies the requirement of ASME Section III, NB-7311(b).

1. The crack driving force must be shown to be less than the material toughness as given below:

$$J_{applied} < J_{0.1} \qquad (1)$$

where $J_{applied}$ is the J-integral value calculated for the postulated flaw under pressure and thermal loading where the assumed pressure is 1.15 times expected accumulation pressure, with thermal loading using the plant specified heatup and cooldown conditions. The parameter $J_{0.1}$ is the J-integral characteristic of the material resistance to ductile tearing ($J_{material}$), as usually denoted by a J-R curve test, at a crack extension of 0.1 inch.

2. The flaw must be stable under ductile crack growth as given below:

$$\frac{dJ_{applied}}{da} < \frac{dJ_{material}}{da} \qquad (2)$$

at

$$J_{applied} = J_{material}$$

where $J_{applied}$ is calculated for the postulated flaw under pressure and thermal loading for all service level A and B conditions where the assumed pressure is 1.25 times expected accumulation pressure, with thermal loading, as is defined above.

The J-integral resistance versus crack growth curve shall reflect a conservative bound to J-Δa data representative of the vessel material under evaluation.

3.2. "J"-based Elastic-Plastic Fracture Mechanics Analysis Method

3.2.1. "J" Solution for Reference Flaw

For reactor vessel materials which can be modeled by deformation plasticity and whose stress-strain behavior can be represented by a power law strain-hardening equation, the $J_{applied}$ can be evaluated for the reference flaw[16] shown in Figure 3-1 using the expression

$$J = J^E(a_{eff},P) + J^P(a,P,n) \qquad (3\text{-}1)$$

where J^E is the elastic contribution based on Irwin's effective crack depth, a_{eff}, and J^P is the deformation plasticity contribution from ref. 3. P is the applied pressure and n is the strain-hardening exponent. For the beltline area of the reactor vessel, assuming a semi-elliptical axial flaw on the inside of the vessel (Figure 3-1), the stress intensity factor for pressure loading[30] is

$$K_I = \frac{PR_i}{t}\sqrt{\frac{\pi a}{Q}}\ F(a/\ell,a/t) \qquad (3\text{-}2)$$

where: P = applied pressure

R_i = inside radius

t = thickness

$$F = 0.97[M_1 + M_2(a/t)^2 + M_3 (a/t)^4]f_c$$

$$M_1 = 1.13 - 0.18\ a/\ell$$

$$M_2 = -0.54 + 0.445/(0.1 + a/\ell)$$

$$M_3 = 0.5 - 1/(0.65 + 2a/\ell) + 14(1-2a/\ell)^{24}$$

$$f_c = \frac{R_o^2 + R_i^2}{R_o^2 - R_i^2} + 1 - 0.5 \frac{a}{t} \frac{t}{R_i}.$$

$$Q = 1 + 4.595(a/\ell)^{1.65}$$

ℓ = length of flaw

a = flaw depth

R_o = outside radius of vessel

$E' = E/(1 - \nu^2)$,

E = Young's modulus

ν = Poisson's ratio

then

$$J^E(a_e) = \frac{P^2R_i^2}{t^2} \frac{\pi a_e}{Q} \frac{F^2}{E'}. \qquad (3\text{-}3)$$

The effective crack size (a_e) is given by

$$a_e = a + \frac{1}{6\pi} \frac{(n-1)}{(n+1)} \frac{K_I^2}{\sigma_o^2[1+(P/P_L)^2]}$$

where: n = strain hardening exponent (Ramberg-Osgood)

σ_o = engineering yield stress

$$P_L = \frac{2}{\sqrt{3}} \sigma_o \frac{(t - a^*)}{(R_i + a^*)} \qquad (3\text{-}4)$$

The basic expression for the limit pressure, P_L, is for a continuous axial flaw. To obtain the limit pressure expression for a part-through wall flaw, the flaw size a is replaced by a* which is given as

$$a^* = \frac{a(1 - s)}{1 - (a/t)s} \tag{3-5}$$

where: $s = (1 + \ell^2/2t^2)^{-0.5}$

The plastic part of J is given by the following expression

$$J^P = \alpha \frac{\sigma_o^2}{E} a(1 - a/t)h_1(P/P_L)^{n+1} \tag{3-6}$$

where α and n are obtained from the Ramberg-Osgood stress-strain relation and h_1 is a dimensionless term which is a function of a/t, a/ℓ , n and t/R_i. This latter constant is evaluated from finite element results[31].

3.2.2. "J" Solution for a Circumferential Flaw in a Cylinder

The acceptance criteria allow a reference flaw in the circumferential direction (Figure 3-2) only in the case where there are only circumferential welds in the reactor vessel beltline region. The reactor vessels of Turkey Point Units 3 and 4 have welds only in the circumferential direction as shown in Figure 2-1.

The K_I solution for a cicumferential flaw shown in Fig. 3-3 is from Kumar et al.[32]

$$K_I = \sigma\sqrt{\frac{\pi a}{Q}}\, F(a/\ell, a/t, R/t) \tag{3-7}$$

where: σ = applied stress

$$\sigma = P\left[\frac{R_i^2}{R_o^2 - R_i^2} + 1\right]$$

$$F = 1.026 + 0.27(a/t) + 0.40\,(a/t)^2 \tag{3-8}$$

Eq. 3-8 is a curve fit equation to the F factors tabulated in Ref. 32 as shown in Fig. 3-4.

Then,

$$J^E(a) = \frac{K_I^2}{E'} \tag{3-9}$$

The effective crack size is given by

$$a_e = a + \frac{1}{6\pi}\,\frac{(n-1)}{(n+1)}\,\frac{K_I^2}{\sigma_o^2[1+(P/P_L)^2]} \tag{3-10}$$

where: n = strain hardening exponent (Ramberg-Osgood)

σ_o = engineering yield stress

$$P_L = \sigma_o \Gamma \frac{(R_o^2 - R_i^2)}{R_i^2} \tag{3-11}$$

$$\Gamma = [R_o^2 - R_c^2 + (1 - \gamma/\pi)(R_c^2 - R_i^2)]/(R_o^2 - R_i^2)$$

$$R_c = R_i + a_o + \Delta a$$

$$R_o = R_i + t$$

and

$\gamma = 3a/R_i$, flaw angle defined in Figure 3-5

The plastic part of J, J^P, for a constant depth and a finite length arc, part through flaw (Fig. 3-5) solution is available from Ref. 33.

$$J^P = \alpha \frac{\sigma_o^2}{E}\, a\left(1 - \frac{a}{t}\right) h_1 \left(\frac{P}{P_L}\right)^{n+1}$$

where h_i can be conservatively set at a constant value of 20.

Now total J is

$$J = J^E(a_o) + J^P(a)$$

3.2.3. Instability Analysis Method

Once an applied J solution for the reference flaw, J_{app}, is selected as given in Section 3.2.1 or 3.2.2, an instability load point can be determined by any one of the following methods using a material J-resistance curve:

1. Failure Assessment Diagram Method
2. J/T Diagram Method
3. J-Δa Analysis Method

The Deformation Plasticity Failure Assessment Diagram (DPFAD) and J-Δa analysis methods were selected for this report. However, all three methods will produce approximately the same results. Further details of the DPFAD method are found in references 3 and 4. An application of this method is illustrated in reference 35. The process is summarized here only for the beltline flaw evaluation.

3.2.3.1. Deformation Plasticity Failure Assessment Diagram Method

DPFAD Curve Generation

The DPFAD curve expression is obtained by normalizing the sum of the elastic and plastic response by the "elastic" J-integral of the flawed reactor vessel in terms of "a,"

$$K_r = \left[\frac{J^E(a)}{J^E(a_o) + J^P(a)} \right]^{1/2} = f(S_r) \qquad (3\text{-}12)$$

where $S_r = P/P_L(a)$.

P is the applied pressure and P_L is the reference plastic collapse pressure or limit pressure, a function of "a" and the material yield strength, σ_o.

Equation 3-7 defines a DPFAD curve which is a function of the flaw geometry, structural configuration, and stress-strain behavior of the material of interest. This curve shown in Fig. 3-6, in terms of K_r, S_r is independent of the magnitude of the applied loading.

Assessment Point Evaluation

Having defined the DPFAD curve, the beltline of the vessel can be evaluated for a given set of material properties. Assessment points are denoted by K_r', S_r' and are defined as follow:

$$K_r'(a_o + \Delta a) = \left[\frac{J^E(a_o + \Delta a)}{J_R(\Delta a)}\right]^{1/2} \quad (3\text{-}13)$$

$$S_r'(a_o + \Delta a) = \frac{P}{P_L\ (a_o + \Delta a)} \quad (3\text{-}14)$$

where terms are as defined in section 3.1 and $J_R(\Delta a)$ is the material J-R property and a_o is the initial postulated flaw size. Some typical assessment points are added to Fig. 3-6 as an illustration.

Instability Pressure Prediction

To evaluate the structure, the applied pressure is held constant and successive assessment points are calculated incrementing the crack size. Among those assessment points the one which is the minimum distance from the origin represents the maximum crack growth which the structure can sustain before becoming unstable when corresponding instability pressure P_{inst} is applied. The P_{inst} is determined by extending a line from the origin through the maximum crack extension point to the DPFAD curve. The pressure is scalable in the K_r-S_r plane.

3.2.3.2. J-Δa Analysis Method

For a given flaw size with appropriate crack extensions, applied J values may be calculated at a number of Δa values forming an applied J-Δa curve. Two of applied J-Δa curves, one for the accumulation pressure times safety factor of 1.15 plus the thermal gradient load case and another with the accumulation pressure times 1.25 and the thermal load are plotted against an appropriate lower bounding J-R curve as shown in Fig. 3-7.

To check the first criterion, one must determine whether the applied J at crack size of a quarter of the vessel thickness plus 0.1 inch (a = t/4 + 0.1 inch) is

less than the material J-R curve at $\Delta a = 0.1$ inch. And also the slope of the applied J curve should be less than the slope of the J-R curve at $\Delta a = 0.1$ inch point. By calculating several J applied values near 0.1 inch one can determine the slope of the applied J curve as indicated in Fig. 3-7.

The second criterion in Section 3.1.1 is an instability check. To satisfy this criterion, an instability point load (or instability pressure) can be shown to be greater than the applied load with appropriate margin. Alternately, it is sufficient to demonstrate that the vessel under a combined load of 1.25 times of accumulation pressure, P_{acc}, and thermal gradient stress is "stable," as shown in Figure 3-8.

By examining this plot one can establish that

$$J_{appl} = J_R \text{ at point A}$$

and

$$\frac{dJ}{da} < \frac{dJ_R}{da} \text{ at point A}$$

The flaw will not propagate beyond $\Delta a = \Delta a_A$ unless there is a further increase in the applied load. Therefore this structure with this flaw is stable under this prescribed loading condition.

3.3. Ramberg-Osgood Parameters

Ramberg-Osgood parameters are obtained by fitting the following equation to a true stress-strain curve.

$$\epsilon/\epsilon_o = \sigma/\sigma_o + \alpha\,(\sigma/\sigma_o)^n$$

Alternately, these parameters can be calculated by the following equations[34] using only yield and ultimate strength values of the material. This approach is used in this analysis.

$$\alpha = \frac{n\,(1.002 + \sigma_y/E)}{\sigma_y/E \times (1.002 + \sigma_y/E)^n} \qquad (3\text{-}15)$$

$$\left[\frac{1/n}{\ell n\ (1.002 + \sigma_u/E)}\right]^{1/n} - \frac{\sigma_u\ e^{1/n}}{\sigma_y\ (1.002 + \sigma_y/E)} = 0 \qquad (3\text{-}16)$$

where

σ_y = yield stress

σ_u = ultimate strength

E = Young's modulus

Figure 3-1 Geometry of Reactor Vessel Beltline With ASME Appendix G Postulated Flaw

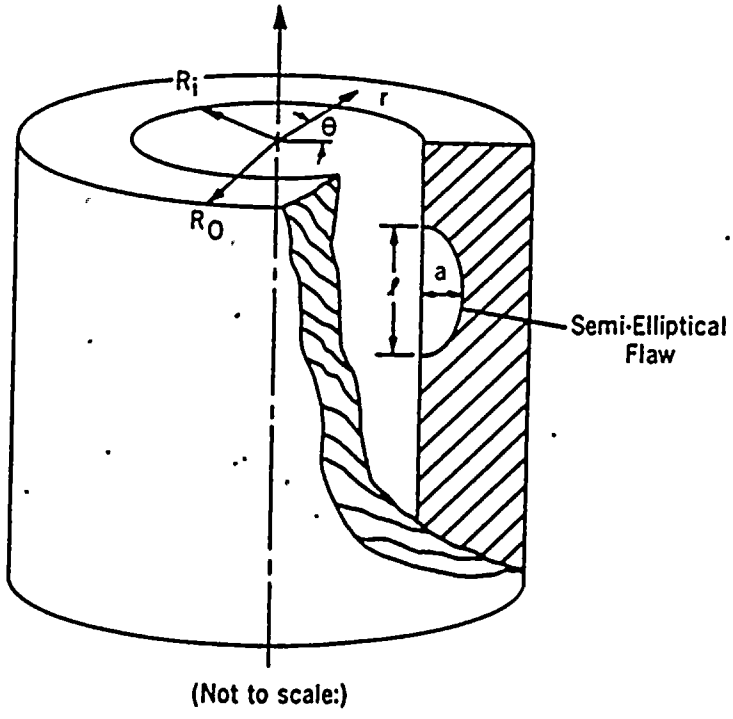

Figure 3-2 Cross-Sections of Turkey Point Reactor Vessels

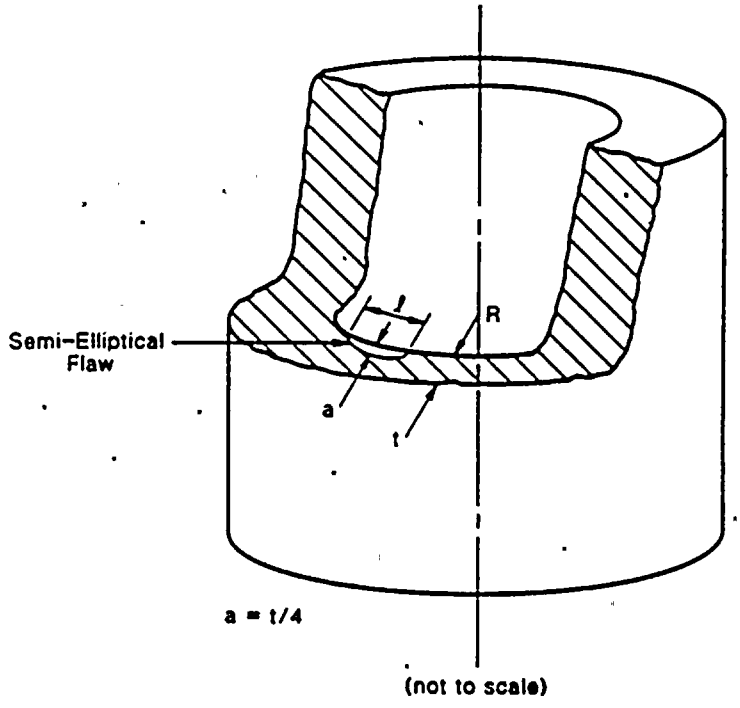

Figure 3-3 Schematic of a Part-Through, Circumferential Surface Flaw in a Cylinder - Elliptical Flaw

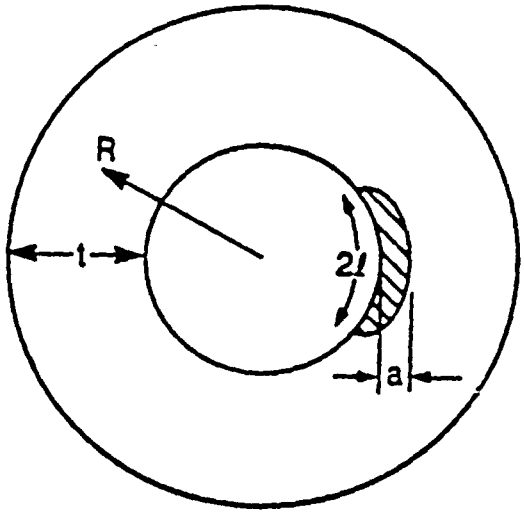

Figure 3-4 Schematic of a Part-Through, Circumferential Surface Flaw in a Cylinder - Constant Depth Flaw

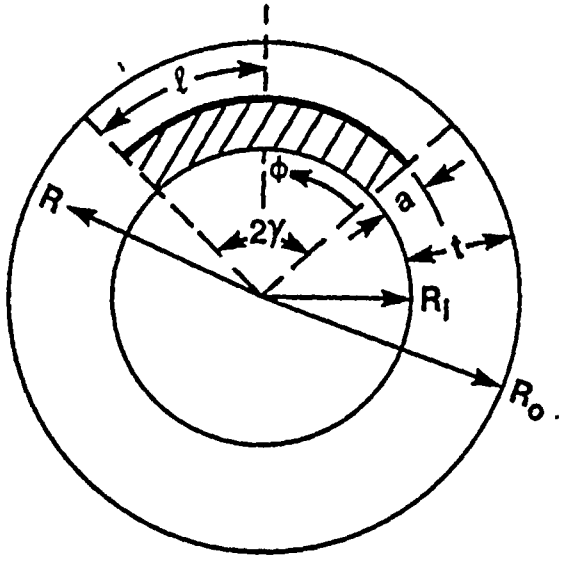

Figure 3-5 F Factors and Curve Fit Equation

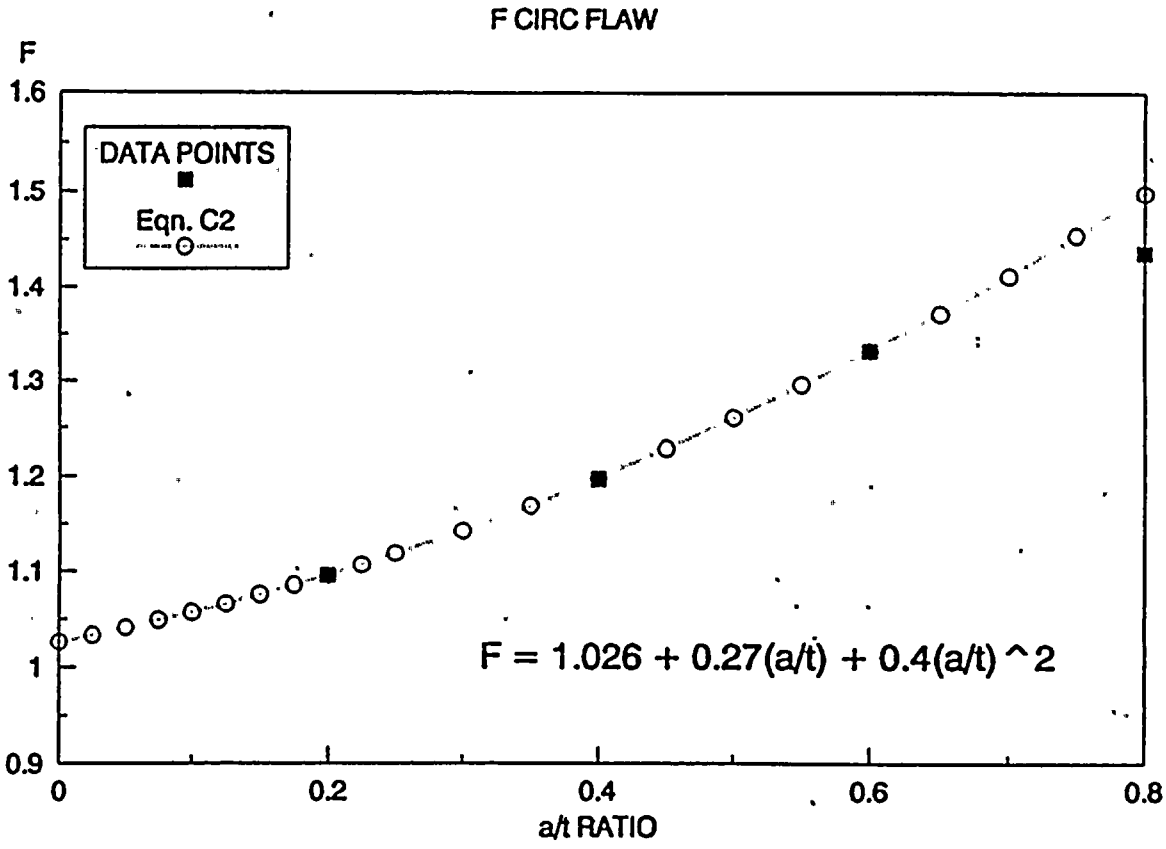

Figure 3-6 Deformation Plasticity Failure Assessment Diagram

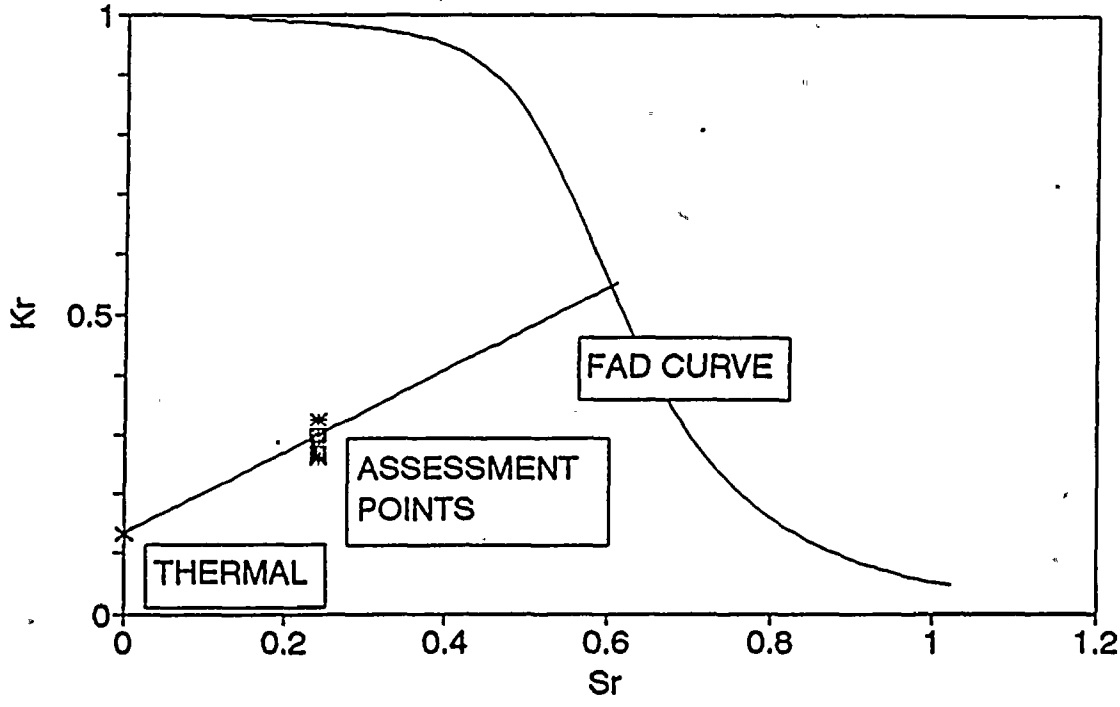

Figure 3-7 J-Δa Analysis

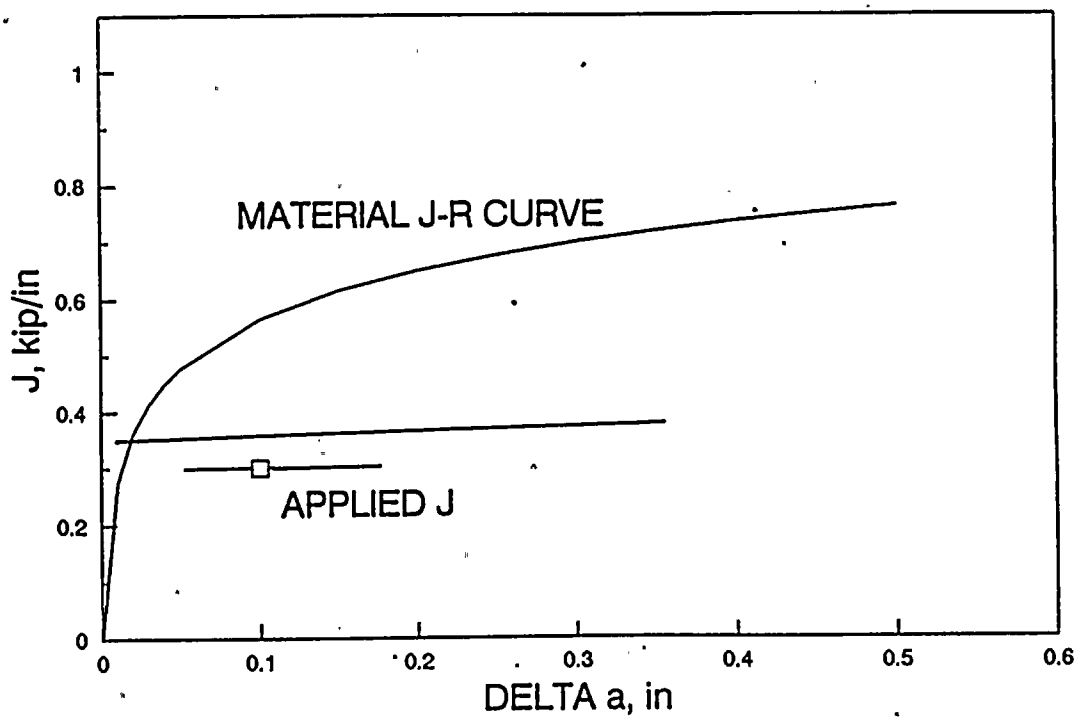

Figure 3-8 Stability Assessment - J-Δa Method

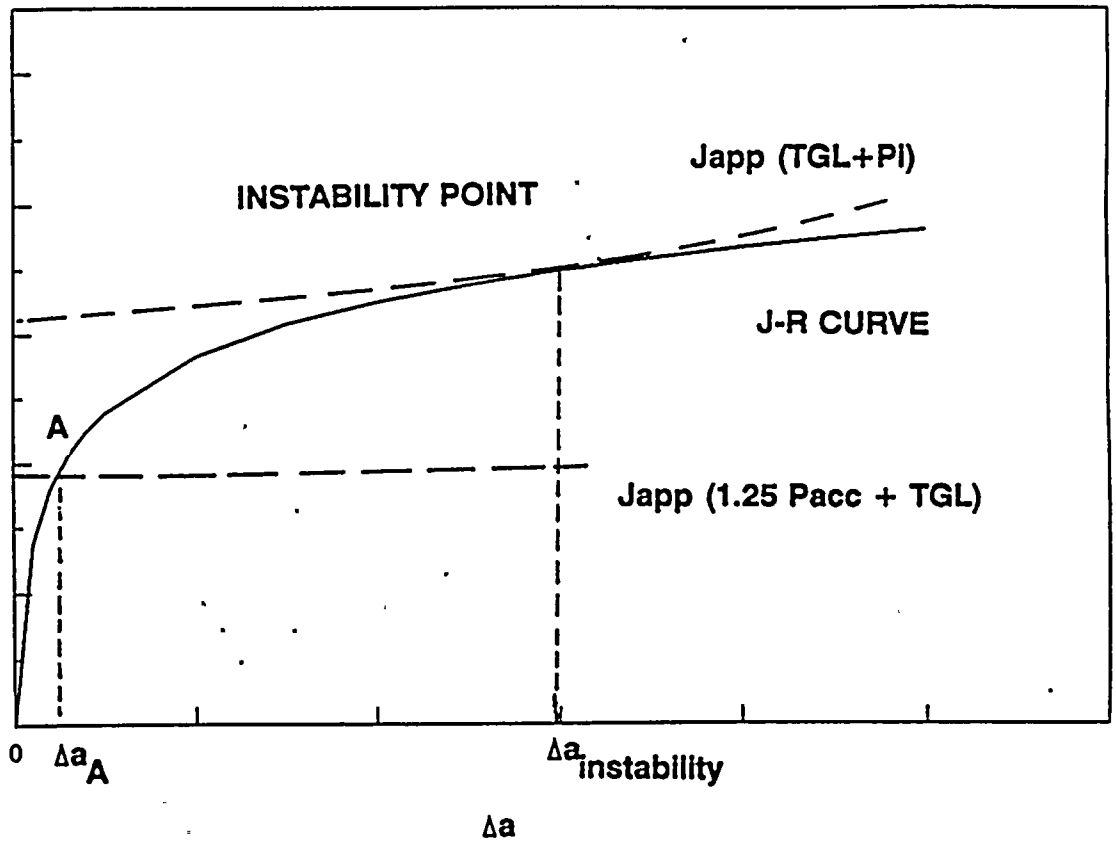

PI - instability pressure

TGL - thermal gradient load

4. MATERIAL PROPERTY CHARACTERIZATION

4.1. Fracture Toughness Model Development Methods

The objective of the fracture toughness model development is, in the absence of a physical model describing the irradiated J-resistance (J-R) behavior of the Linde 80 material, to empirically extract all variables affecting the behavior of J-R properties of Mn-Mo-Ni/Linde 80 welds and the inter-relationship among these key variables. The resulting mathematical model facilitates two very important necessary functions. The model enables any interpolation or extrapolation of the variables selected in the model and also provides a means to define a lower bounding limit to satisfy the regulatory requirement of the material J-R curve.

Recent developments in pattern recognition techniques provided a new method to obtain mathematical models of materials data behavior. In 1989, it was demonstrated through a pilot program under the NRC's sponsorship[36] that J-R data can be analyzed by this approach. Additional work was performed to model the HSST J-R data[37]; the software that was used in those programs were applied to the current B&W Owners Group data analysis in this report.

The primary data analysis methods are the ACE and SURFIT computer programs developed by Modeling and Computing Services. Data analysis and model construction using these two programs are discussed below.

4.1.1. Key Variables and Model Form

Advanced methods of data analysis have recently been developed to allow simultaneous consideration of the effects of many variables and to allow the data and/or physical considerations to establish the best model form.

In usual statistical approaches, modeling forms (usually linear) are assumed and then compared to the data. The advanced methods use the data directly to show the analyst the form of model to use.

The ACE computer code identifies key variables and the optimal form of function to use for multivariable surface-fitting, going directly from the data without restrictive assumptions about the form of the model. ACE identifies the numerically defined transformations $\theta(y)$ and $\phi_j(x_j)$ such that

$$\theta(y) = \sum_{j=1}^{n} \phi_j(x_j) \tag{4-1}$$

The transformations are not chosen in advance, instead they are the unknowns that are calculated by ACE and are displayed graphically. The form specified by Eq. 4-1 is very general, capable of representing any function of a sum of arbitrary functions, products of arbitrary functions.

ACE does not actually use mathematical forms for the transformations; it numerically smooths the raw data. ACE alternately estimates pointwise values of $\theta(y)$ given all $\phi_j(x_j)$, then each $\phi_j(x_j)$ given $\theta(y)$, and iteratively refines these estimates until the error in satisfying Eq. 4-1 is minimized in a least squares sense. The mathematical algorithm and an elegant proof of convergence and optimality were presented in Ref. 38. The method can be proven to converge to unique, optimal transformations under certain conditions, and it works well in practice on multivariable nonlinear problems. ACE was first applied to engineering materials problems in Reference .

ACE requires as input the raw data in a matrix format

$$\begin{array}{llllll} y_1 & x_{11} & x_{12} & x_{13} & x_{14} & \cdots x_{1n} \\ y_2 & x_{21} & x_{22} & x_{23} & x_{24} & \cdots x_{2n} \\ \cdot & & & & & \\ \cdot & & & & & \\ \cdot & & & & & \\ y_m & x_{m1} & x_{m2} & x_{m3} & x_{m4} & \cdots x_{mn} \end{array} \tag{4-2}$$

where the independent variables x_{ii} can be either continuous or categorical. Typical categorical variables might be material form, i.e. plate or forging or weld, or different laboratories or investigators when correlating any type of data from multiple sources. ACE is very useful for identifying laboratories or investigators that produce outlier results.

The output from ACE is in graphical form, including plots of each transformed variable. The plots are presented in standard deviation coordinates so that it is easy to identify the variables that account for most of the apparent scatter in response values. This is important since a variable that accounts for three standard deviations of "scatter" in response values is a more important variable for modeling than one that only accounts for one standard deviation. The plots also indicate by their shape the mathematical forms that should be used for modeling the data. After viewing the plot, the analyst can choose a functional form and confirm the choice by introducing transformed variables $\theta(y)$ and $\phi_j(x_j)$ in place of the original variables y, x_j in Eq. 4-2 and reapplying ACE. Theoretically-based mechanistic models can be introduced in the same way, if desired. If the appropriate functional form is chosen, the ACE plots will be nearly linear on the second try. Note that the <u>data</u> establish the form of the transformations; the analyst only checks potential mathematical forms <u>after</u> looking at the results. This is a fundamental advance over previous ways of doing modeling and data analysis.

<u>4.1.2. Model Calibration</u>

Once the important variables have been identified and the shapes of the functional relationships for each term have been determined, the remaining task is to develop a working model and estimate its parameters. The data are then normalized to a common set of conditions using the model. The normalizing step is essential for correlating multivariable data since only when the data are normalized by a fitted model can the trends in each variable be clearly seen.

SURFIT is a nonlinear least squares surface fitting code that allows complete freedom in specification of the fitting functions. Whatever functions that

appear useful, based on ACE analysis and theoretical considerations, can be conveniently introduced to SURFIT. Constraints and weighting can be imposed to give greater emphasis to higher quality data or known asymptotic values. The analyst can also control the form of the residuals, allowing fits that minimize absolute residuals, log residuals, relative error, and residuals perpendicular to the model. The input to SURFIT is the same form as Eq. 4-2, plus a user-defined fitting function. Minimization of the sum of squares of the residuals is performed numerically, using a modification of the Powell nonlinear least squares algorithm[39].

Use of ACE and SURFIT is an iterative process, since the results of ACE provide insight to SURFIT model forms and vice versa. The first successful application of this approach to J-R model was made for the NRC and followed by an expanded program in 1990[37].

4.2. Data Analysis

4.2.1. B&W Owners Group Data Base Description

In the elastic-plastic fracture mechanics analysis as proposed in this report, toughness is in terms of the J-resistance (J-R) curve and strength properties are in the form of Ramberg-Osgood parameters which need a true stress-strain curve. The B&W Owners Group data base has both J-R and stress-strain data. The Integrated Reactor Vessel Surveillance Program (IRVSP) conducted over the last 15 years has accumulated a large body of J-R data including irradiated and unirradiated specimen test results. Table 4-1 shows the extent of the B&W Owners Group data base for J-R curves and additional J-R data are available from the NRC HSST program.

Since this report deals specifically with the low upper shelf issue, these J data were further screened to obtain those J-R data relevant to the upper shelf temperature range. Data below 390 F was excluded based on the following reasoning. The K_{Ic} curve found in Section XI of the ASME Boiler and Pressure Vessel Code (Fig. 4-1) shows that K_{Ic} reaches 200 ksi $\sqrt{in.}$, the upper shelf toughness, when the T minus RT_{NDT} value is above approximately 105 F. Assuming

that for the greatest irradiation-damaged weld metal RT_{NDT} is the same as the PTS screening criteria[40], 270 F, the choice of 390 deg F assures that all J-R data above this temperature is at the upper shelf level.

4.2.2. J Control Limit

ASTM Standard E1152-87[41] allows ten percent of the initial ligament to be the validity limit for crack extension in compact specimen testing. However, many researchers found that ductile tearing data behave nicely far beyond the ASTM recommended limit. In particular, Mn-Mo-Ni/Linde 80 J-R data show valid data range from 35 to 50 percent of the initial ligament. Joyce[42] proposed a method to define an engineering J control limit based on a relationship between plastic displacement and crack extension. Ref. 42 suggests that the point where the deviation from the linear slope is 5 percent may be taken as the J control limit. A sample plot in Fig. 4-2 shows that the deviation from the linearity starts at a crack extension equivalent to 36 and 44 percent of the initial ligament. For this evaluation, a conservative validity limit was selected: 35 percent of the initial ligament. .

4.2.3. Data Assembly

Prior to running pattern recognition, the Mn-Mo-Ni/Linde 80 weld J-R data were assembled. J-Δa points beyond the J control limit were excluded and those data points with test temperature less than 390 F were also excluded to assure a data base for the upper shelf temperature range only. In addition, data points with Δa less than 0.01 were eliminated since J values at small Δa values usually exhibit larger scatter.

4.2.4. Candidate Variables for J-R Model

The following variables were selected for consideration:

Fluence - Fluence strongly affects material degradation and is clearly a candidate variable.

Test Temperature - It was observed as test temperature increases, the J values decrease for Mn-Mo-Ni/Linde 80 weld metal.

Chemical Composition - The effect of chemical composition on irradiation damage is well known (Ref. 27); the nine elements are therefore included in the selection as shown in Tables 4-2 and 4-3.

Specimen Size - As specimen size has been shown to be a variable in J_d sets, therefore, net specimen thickness was selected as a candidate variable.

Data Group - To determine whether "power reactor" and "test reactor" irradiations have distinctly different patterns, data group name was selected as a categorical variable.

Yield and Ultimate Strengths - To investigate the impact of mechanical strength properties to J value, these two are included as candidate variables.

Uniform Elongation - This property is also selected as a candidate variable.

Charpy Energy - This is selected to show whether Charpy energy value can represent the irradiation damage in place of the fluence.

4.2.5. Pattern Recognition and Model Form

The data plots in Figures 4-3 and 4-4 show all the raw J-Δa points assembled for pattern recognition analysis. To determine the pattern of the data behavior, the ACE program was run using trial transformations of the Y variable and the seventeen candidate variables. Based on earlier work performed by the B&W Owners Group, it was learned that the following J equation best describes J-R curves for Mn-Mo-Ni/Linde 80 weld metals.

$$J = C1\ (\Delta a)^{C2} \exp(C3\ \Delta a^{C4}) \qquad (4\text{-}3)$$

Equation 4-3 is a power law expression with a modifier exponential function that better fits the small Δa part of the J-R curve. The power law behavior of J-R data points can be seen in Figures 4-3 through 4-4.

Figures 4-5 and 4-6 are the transformation analysis output from ACE showing that the natural logarithm of C1 from the J equation strongly influences the data set. Relying on the insights gained by early NRC data analysis[36] and a series of power law fit model development work by the B&W Owners Group, application of ACE showed that four variables had major effects on the data set, as shown in Figures

4-7 through 4-12. These variables are fluence, copper content, temperature, and specimen size. The remaining variables from the initial selection of seventeen variables are insignificant. Through numerous trials to find the optimum functional relationships among these variables, it was learned that a product of copper content and fluence is more significant as a key variable than when considered separately. This product was further refined by raising the fluence to the power "a" thus:

$$Cu\ (\phi t)^a$$

where Cu is the copper content in weight percent, ϕt is fluence in units of 10^{18} n/cm^2, and a is a number less than unity.

The current low upper shelf toughness issue regulation is based on Charpy upper-shelf values. Charpy absorbed energy values are taken as an indication of fracture toughness. In this data analysis, the Charpy upper shelf energy (CvUSE) is used as an alternative parameter to account for irradiation damage to fracture toughness; this assumes that irradiation effects are reflected in the Charpy test results of irradiated specimens. Use of CvUSE as a fracture toughness degradation indicator was partly based on the observation that the initial plant surveillance programs had mostly Charpy specimens and very few, if any, CT specimens. There is no definite mechanistic linkage between CvUSE and J-R curves to date. In the present data analysis effort, CvUSE is selected to be an alternate variable in place of the $Cu(\phi t)^a$ term; both terms were used for model development.

The current model form of the J-R equation is obtained as follows:

From $$J = C1\ (\Delta a)^{C2} \exp(C3\ \Delta a^{C4}) \qquad (4\text{-}3)$$

Take natural logarithms:

$$\ell n\ J = \ell n\ C1 + C2\ \ell n(\Delta a) + C3\ (\Delta a)^{C4}$$

A series of combinations of the proposed model were tried. When a form of the model was derived through repeated and improved combinations and transformations, the following final form was obtained:

$$\ell n\ C1 = a1 + a2 \left[\frac{Cu(\phi t)^{a7}}{\ell nCv} \right] + a3\ T + a4\ \ell n\ B_N \qquad (4\text{-}4)$$

$$C2 = d1 + d2\ \ell n\ C1 + d3\ \ell n\ B_N \qquad (4\text{-}5)$$

$$C3 = d4 + d5\ \ell n\ C1 + d6\ \ell n\ B_N \qquad (4\text{-}6)$$

where T is temperature in F, B_N is net specimen thickness in inches and Cv is the Charpy upper shelf engergy in ft-lb. It is noteworthy that J_M takes d3 and d6 as zeroes, indicating that specimen size dependency is not applicable.

4.2.6 Determination of Optimal Parameters

SURFIT was applied to the above model (Paragraph 4.2.5), first against the combined data set of HSST and B&W Owners Group data and second only against the B&W Owners Group set to determine optimal sets of constants in the equation, C1 through C4, by means of constants a's and d's. By applying these constants in Equations 4-4 through 4-6, a specific J-R curve can be generated for a particular application. The results are tabulated in Tables 4-4 and 4-5.

4.2.7. Model Verification

To verify how the above multivariable equation fits all the test data used to develop this equation, a series of verification plots are made on a standard condition. There are more than 1300 data points in the B&W Owners Group data set and more than 3300 points in the combined B&W Owners and HSST data set. Any single data point from this set represents a unique condition, i.e. specific fluence, temperature, specimen thickness, and copper content. Since the model equation represents functional relationships among these variables, this data point can be converted to a standard condition - normalized condition selected based on typical values of all variables. The standard condition selected for the normalization is

fluence, $\phi t = 8.0 \times 10^{18}$ n/cm^2

flaw extension, $\Delta a = 0.1$ in.

temperature, T = 480 deg F

specimen thickness, $B_N = 0.8$ in.

copper content, Cu = 0.30 wt%

Normalization is made based on the following conversion equation,

$$J_{i\ std.\ cond.} = J_{i\ test\ data}\ [J_{calc\ @\ std\ cond.}/J_{calc\ @ith\ cond.}]$$

When all the data points are converted to the normalized condition, these points will form a master J-R curve for the standard condition if the model is reasonable. Such normalization has been performed and the results are shown in Figures 4-13 and 4-14. These are plots of an overall normalized J versus Δa curves. The overall fit is very good considering the range of variables involved in the entire data set, providing a master J-R curve of Mn-Mo-Ni/Linde 80 weld metal for the standard condition.

Further, to determine the effect of individual variables on the data set, normalized variables were shown against the standard deviation of the data set. Figures 4-15 through 4-18 show these effects for the B&W Owners Group data set. Similar trends are true for modified J, J_M.

The final J-R model, equation 4-3 with all the necessary parameters, are defined by a set of equations, 4-4 through 4-6. The constants a's and d's needed to determine the parameters are tabulated in Tables 4-4 and 4-5.

4.3. Power and Test Reactor Toughness Data

The B&W Owners Group IRVSP power reactor irradiations were conducted in Crystal River Unit 3 and Davis Besse Unit 1. Both of these reactors have similar neutron spectrum characteristics and, therefore, the data can be used interchangeably. A nominal fast neutron flux in these commercial power reactors is 7.4×10^{10} n/cm^2/sec. In contrast, the flux in the test reactor where the HSST specimens were irradiated has a nominal flux of 1.5×10^{12} n/cm^2/sec. Since there is no well established mechanistic model for flux effects on the long term irradiation damage in metal structures, only an empirical observation is possible at this point. One such observation can be made through this type of modeling effort. As a categorical variable there are some differences between the power reactor irradiated specimen data and the HSST irradiated specimen data. However, the

magnitude is insignificant in terms of total standard deviation of the combined data set. Further, difference may occur from the fact that the HSST program has more larger-size specimens and irradiated to fluences above 8.5 x 10^{18} n/cm^2. The power reactor specimens were irradiated to fluences of 8.5 x 10^{18} n/cm^2. Therefore, it is concluded that there is no significant difference in two data sets for this class of weld metal irradiated J-R test data.

4.4. J-R Model Prediction Trends

A mathematical model for Linde 80 weld metals is now available and in this section a number of trends exhibited by this model will be studied. Among the key contributing variables, effects of the fluence term can be seen in Figure 4-19, where J at Δa= 0.1 inch is plotted against fluence with four levels of copper content and temperature and specimen size held constant. It is noteworthy that there is an initial drop of J from the unirradiated condition to the first level of fluence calculated, then almost linearly decreasing Js with increasing fluence can be observed.

Figure 4-20 shows a plot of J at 0.1-inch crack extension versus test temperature with varying fluence level and a fixed copper content and a fixed B_N. In Figure 4-21, J at 0.1 inch crack extension is plotted against specimen thickness at various copper content at a fixed value of fluence. Compared to the normalized data plots in the previous sections, these trends support the data behavior as expected.

4.5. Comparison Between J-R Model and SA-1101 Specimen Data

SA-1101 weld material is identified as the controlling welds in Turkey Point Units 3 and 4 reactor vessels. In the current J data bases, very few SA-1101 CT specimen test data are available. Specimens of SA-1101 and weld material of the same weld wire heat but different lot are listed in Table 4-6.

There is only one irradiated CT specimen of SA-1101 available from the HSST data set, i.e. , a 4T CT specimen with fluence of 1.4 x 10^{19} n/cm^2, tested at 350 F. Three selected unirradiated SA-1101 J-R curves and the 4T CT irradiated specimen data J-R curves are shown with a mean and a lower bounding J-R curves

predicted by the model equation for unirradiated material in Figure 4-22. It is obvious that SA-1101 is relatively tougher material in Mn-Mo-Ni/Linde 80 weld metal. The predicted mean curve for unirradiated material is much lower than the irradiated material curve. It is apparent that this model is very conservative for this application. The same J-R data points are plotted against model curves with the same fluence as the 4T CT specimen in Figure 4-23.

Table 4-1. Summary of B&W Owners Group J-R Data Base

Table 4-2. Chemical Composition of Weld Metals in Data Base Used to Develop Correlation Models

Item	Plant	Weld ID	Chemical Composition, w/o								
			C	Mn	P	S	Si	Cr	Ni	Mo	Cu
1	Oconee Unit 1	WF-112	0.08	1.47	0.016	0.015	0.54	0.07	0.59	0.40	0.32
2	Oconee Unit 2	WF-209-1A[a]	0.11	1.55	0.022	0.010	0.65	0.09	0.58	0.39	0.36
3	Oconee Unit 3	WF-209-1B[a]	0.08	1.63	0.017	0.012	0.61	0.10	0.58	0.39	0.30
4	TMI Unit 1	WF-25	0.09	1.62	0.013	0.015	0.46	0.10	0.66	0.40	0.33
5	Crystal River-3	WF-209-1C[b]	0.08	1.65	0.021	0.013	1.00	0.07	0.10	0.45	0.41
6	ANO Unit 1	WF-193A[a]	0.09	1.49	0.016	0.016	0.51	0.06	0.59	0.39	0.28
7	Rancho Seco	WF-193B[a]	0.09	1.49	0.016	0.016	0.51	0.06	0.59	0.39	0.28
8	Davis-Besse	WF-182-1	0.09	1.69	0.014	0.013	0.41	0.15	0.63	0.40	0.21
9	Pt. Beach Unit 1	SA-1263	0.09	1.47	0.019	0.024	0.49	0.13	0.57	0.39	0.22
10	Pt. Beach Unit 2	WF-193C[a]	0.08	1.40	0.014	0.013	0.55	0.07	0.59	0.39	0.25
11	R. E. Ginna	SA-1036	0.08	1.41	0.012	0.016	0.59	0.09	0.56	0.36	0.23
12	Turkey Pt. Unit 3	SA-1101	0.08	1.56	0.019	0.008	0.59	0.16	0.54	0.38	0.21
13	Turkey Pt. Unit 4	SA-1094	0.10	1.44	0.014	0.011	0.50	0.14	0.60	0.36	0.30
14	Zion Unit 1	WF-209-1D[a]	0.09	1.51	0.020	0.013	0.68	0.06	0.57	0.39	0.35
15	Zion Unit 2	WF-209-1E[a]	0.08	1.51	0.017	0.013	0.68	0.06	0.57	0.39	0.30
16	Surry Unit 1	SA-1526	0.09	1.53	0.013	0.017	0.53	0.08	0.68	0.42	0.35
17	Kori Unit 1	WF-233	0.10	1.45	0.021	0.015	0.42	0.08	0.68	0.44	0.27
18	B&W Owners Group	WF-25	0.09	1.58	0.015	0.016	0.54	0.09	0.67	0.42	0.35
19	B&W Owners Group	WF-67	0.08	1.55	0.021	0.016	0.58	0.10	0.60	0.40	0.22
20	B&W Owners Group	SA-1585	0.08	1.45	0.016	0.016	0.51	0.09	0.59	0.38	0.21
21	B&W Owners Group	WF-70	0.09	1.63	0.018	0.009	0.54	0.11	0.59	0.40	0.42
22	B&W Owners Group	WF-112	0.08	1.47	0.016	0.015	0.54	0.07	0.59	0.40	0.32
23	B&W Owners Group	SA-1135	0.08	1.45	0.011	0.013	0.49	0.08	0.59	0.38	0.27

(a) Same weld wire/flux combination used for more than one surveillance weld metal with different processing treatment. Letter following identification signifies that welding parameters, or fabrication variables, may cause differences in properties between weldments with identical wire-flux combinations.

(b) Atypical weld metal.

Table 4-3. Chemical Composition of HSST Submerged-Arc Welds

WELD	Average[a] composition, wt %								
	C	Mn	P	S	Si	Cr	Ni	Mo	Cu
	0.09	1.48	0.020	0.014	0.57	0.16	0.63	0.37	0.28
	0.07	1.45	0.018	0.014	0.55	0.16	0.62	0.36	0.26
	0.10	1.52	0.021	0.015	0.58	0.17	0.64	0.38	0.31
	0.083	1.51	0.016	0.007	0.59	0.120	0.537	0.377	0.210
	0.078	1.41	0.013	0.007	0.55	0.067	0.490	0.365	0.160
	0.088	1.61	0.020	0.008	0.63	0.173	0.585	0.390	0.260
	0.098	1.65	0.016	0.011	0.630	0.095	0.685	0.427	0.299
	0.088	1.62	0.015	0.010	0.580	0.073	0.663	0.415	0.272
	0.109	1.67	0.017	0.013	0.675	0.118	0.707	0.440	0.326
	0.085	1.59	0.014	0.015	0.520	0.092	0.660	0.420	0.350
	0.070	1.54	0.012	0.014	0.445	0.074	0.600	0.410	0.310
	0.100	1.64	0.017	0.016	0.600	0.110	0.720	0.430	0.390
	0.080	1.45	0.015	0.015	0.480	0.088	0.597	0.385	0.215
	0.070	1.42	0.014	0.013	0.450	0.076	0.585	0.370	0.180
	0.090	1.49	0.017	0.017	0.610	0.100	0.610	0.400	0.250
	0.092	1.63	0.018	0.009	0.540	0.105	0.595	0.400	0.420
	0.075	1.59	0.017	0.009	0.480	0.090	0.580	0.380	0.350
	0.110	1.67	0.020	0.010	0.600	0.120	0.610	0.420	0.490
	0.082	1.44	0.011	0.012	0.500	0.089	0.590	0.390	0.265
	0.070	1.40	0.010	0.012	0.410	0.067	0.580	0.370	0.220
	0.095	1.48	0.013	0.013	0.590	0.110	0.600	0.410	0.310

[a] Top entry is the average value, while numbers shown below each entry indicate the range of composition measurements.

Table 4-4. Parameters in J_D Model

Table 4-5. Parameters in J_M Model

Figure 4-1 K_{IC} Curve

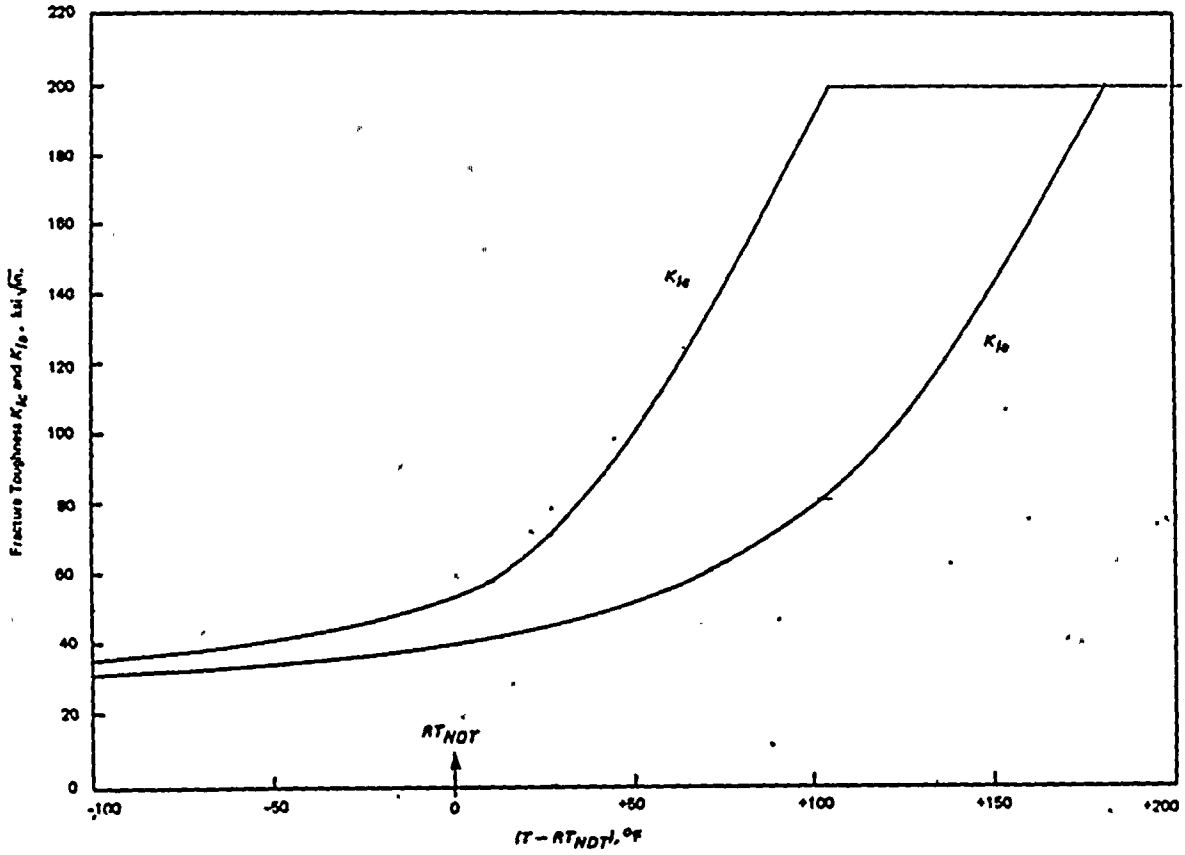

Figure 4-2 J Control Limit Assessment

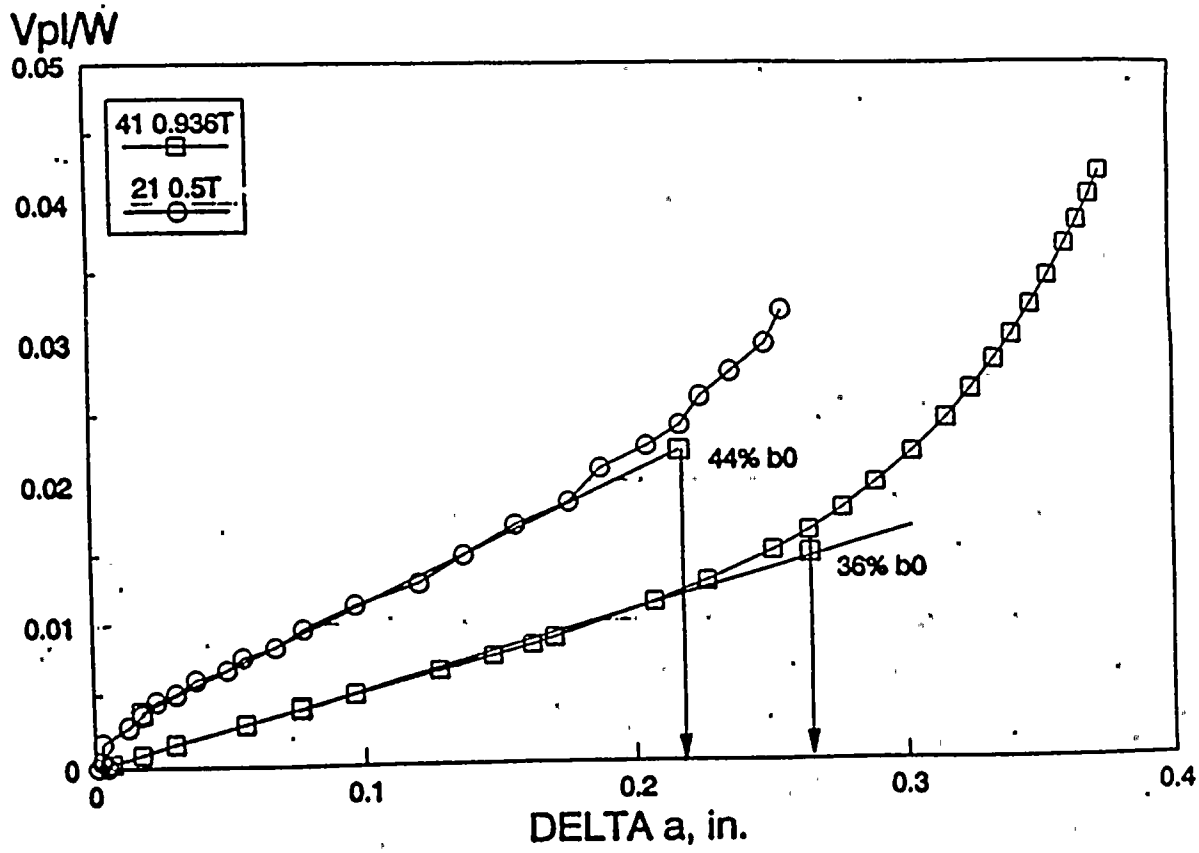

Figure 4-3 B&WOG Data on Log-Log Scale - J_D-Δa

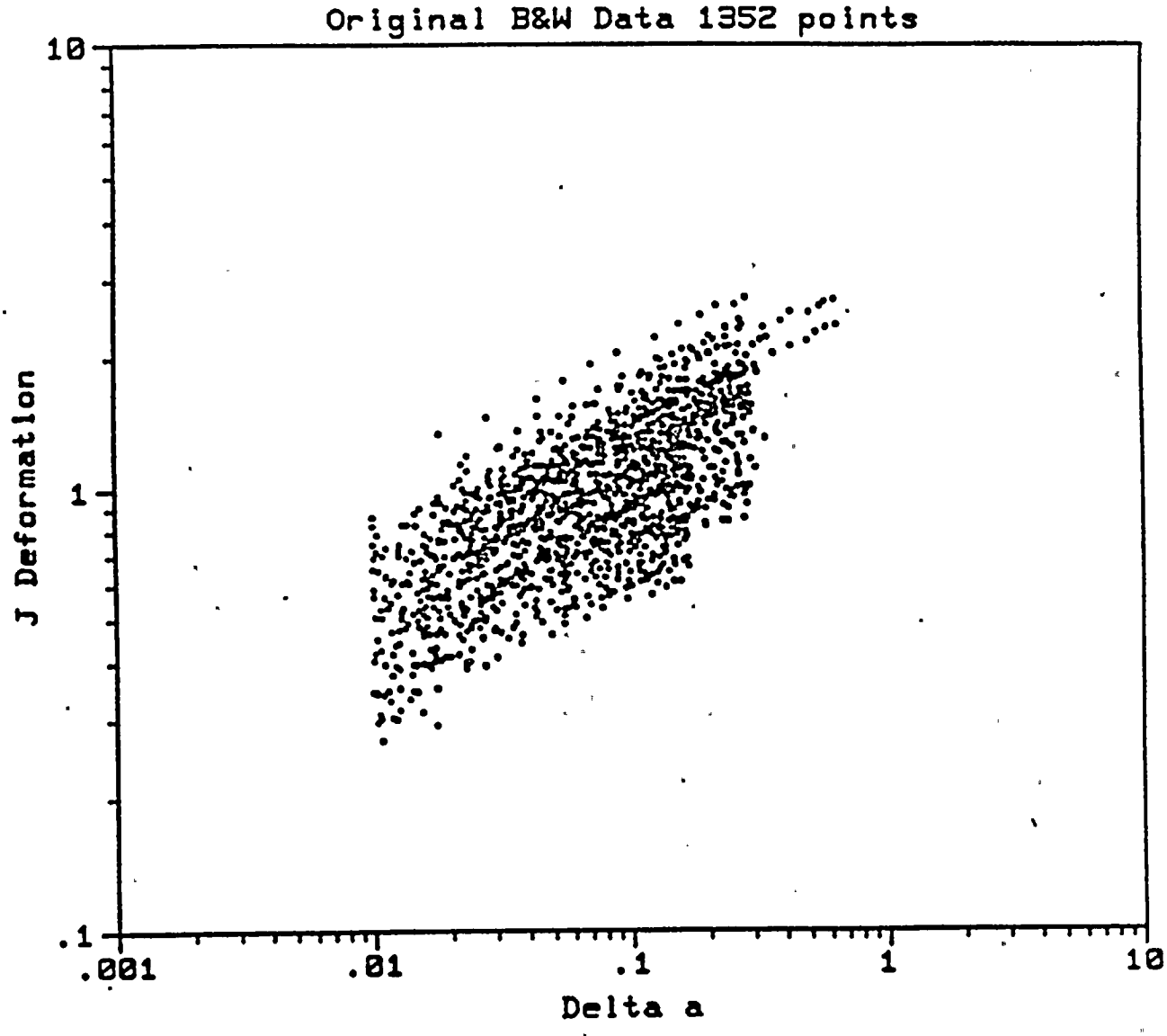

Figure 4-4 B&WOG Data on Log-Log Scale - J_M-Δa

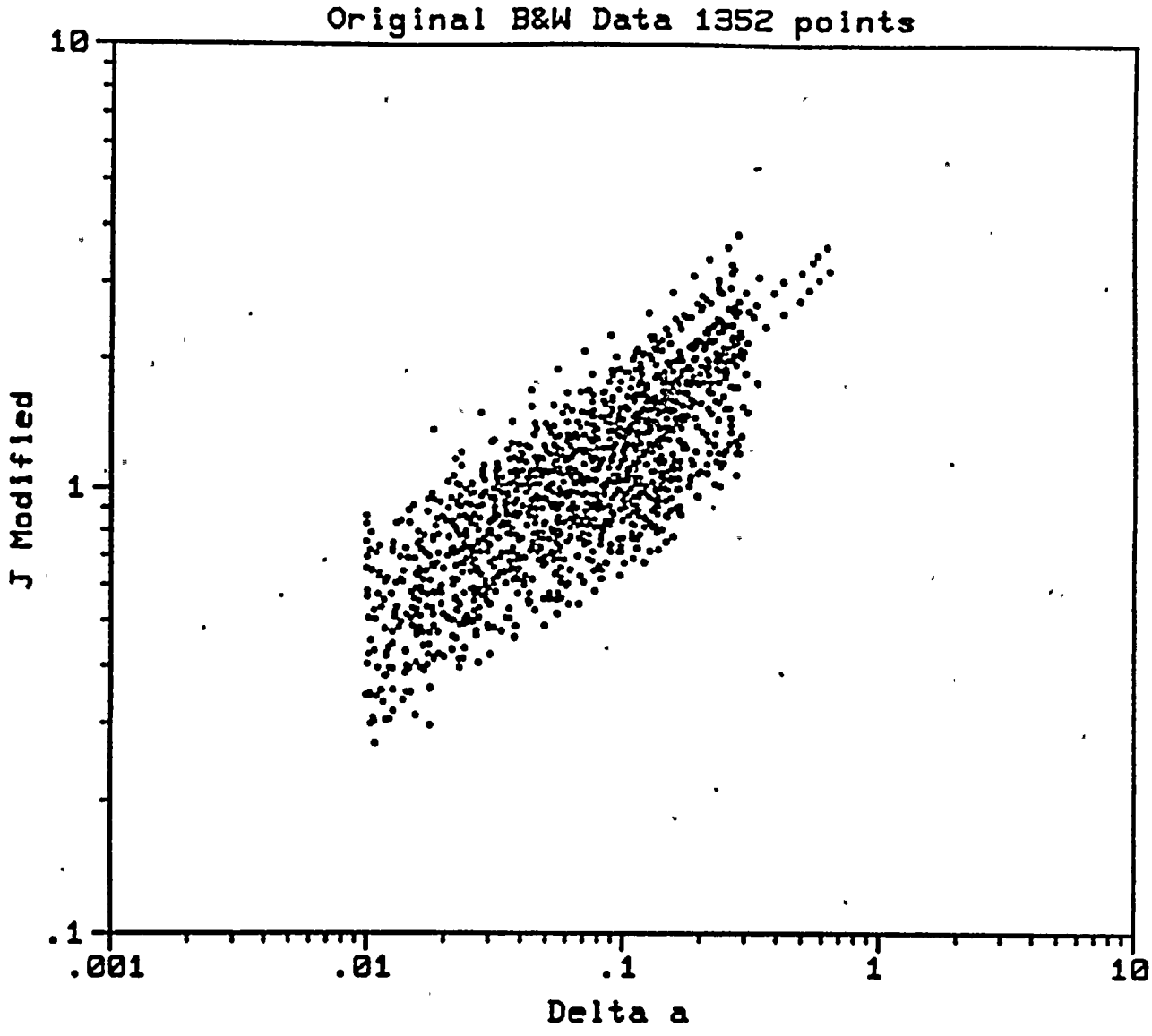

Figure 4-5 Transformation Analysis Plot (TAP) for ln C_1 - J_D

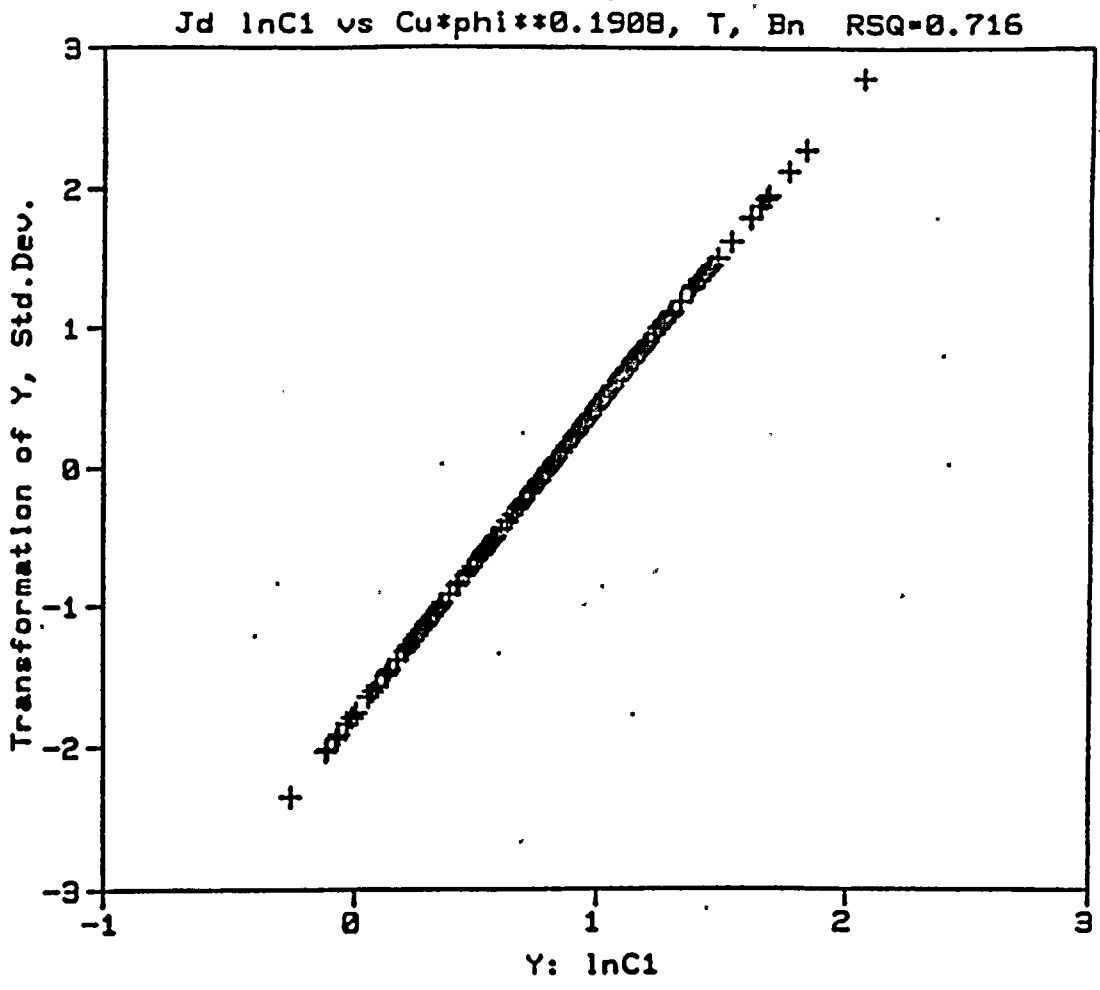

Figure 4-6 Transformation Analysis Plot (TAP) for ln C_1 - J_H

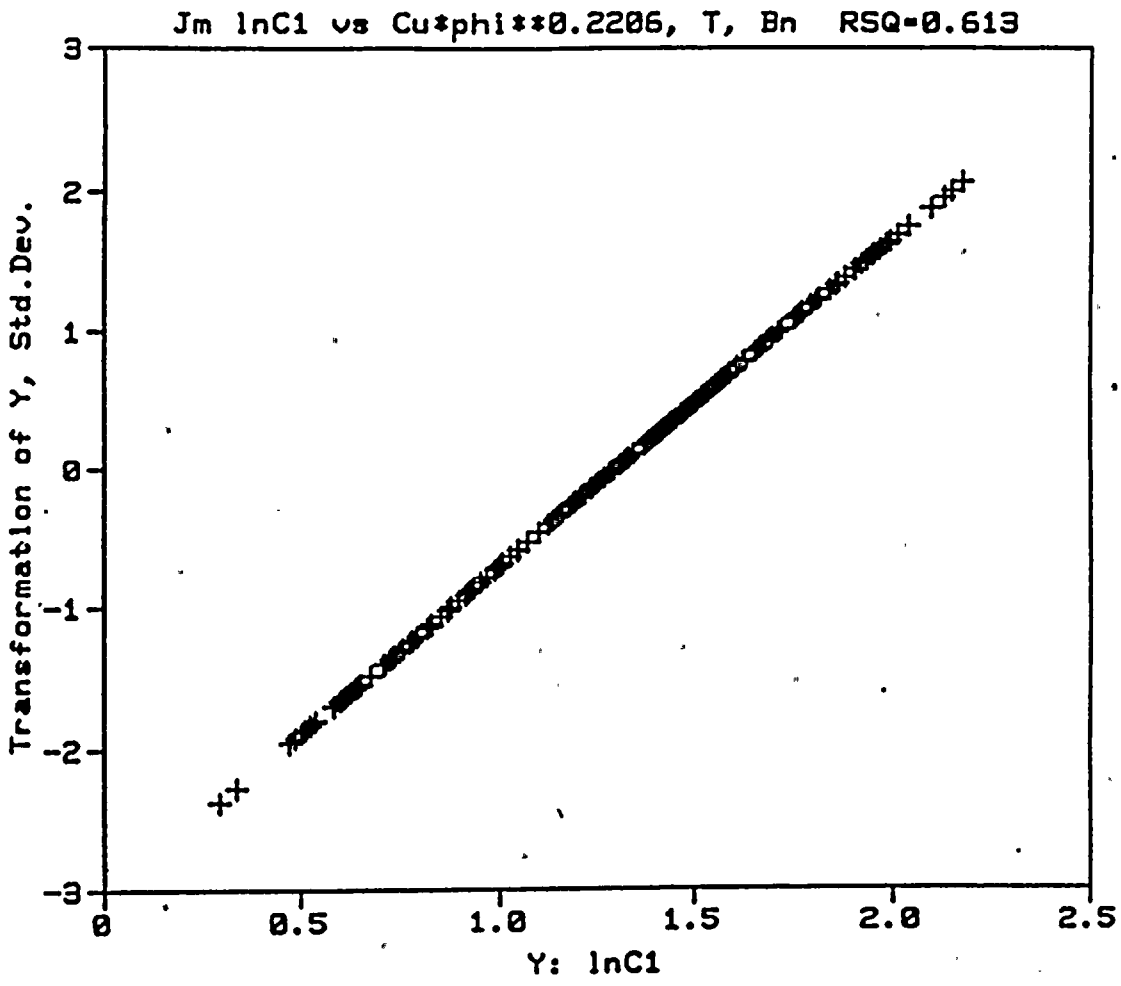

Figure 4-7 TAP for Cu x Fluence$^{0.1908}$ on J_H

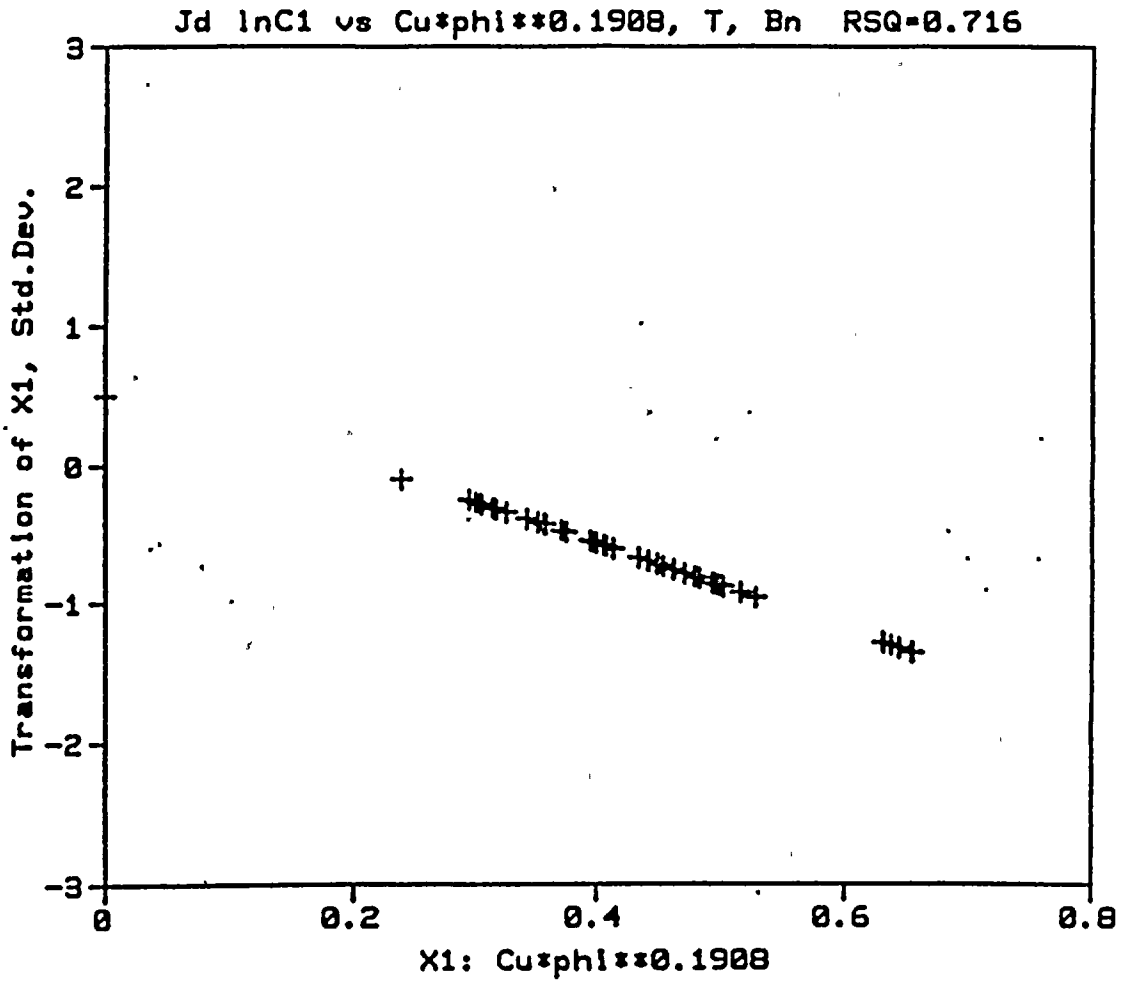

Figure 4-8 TAP for Cu x Fluence$^{0.1908}$ on J_H

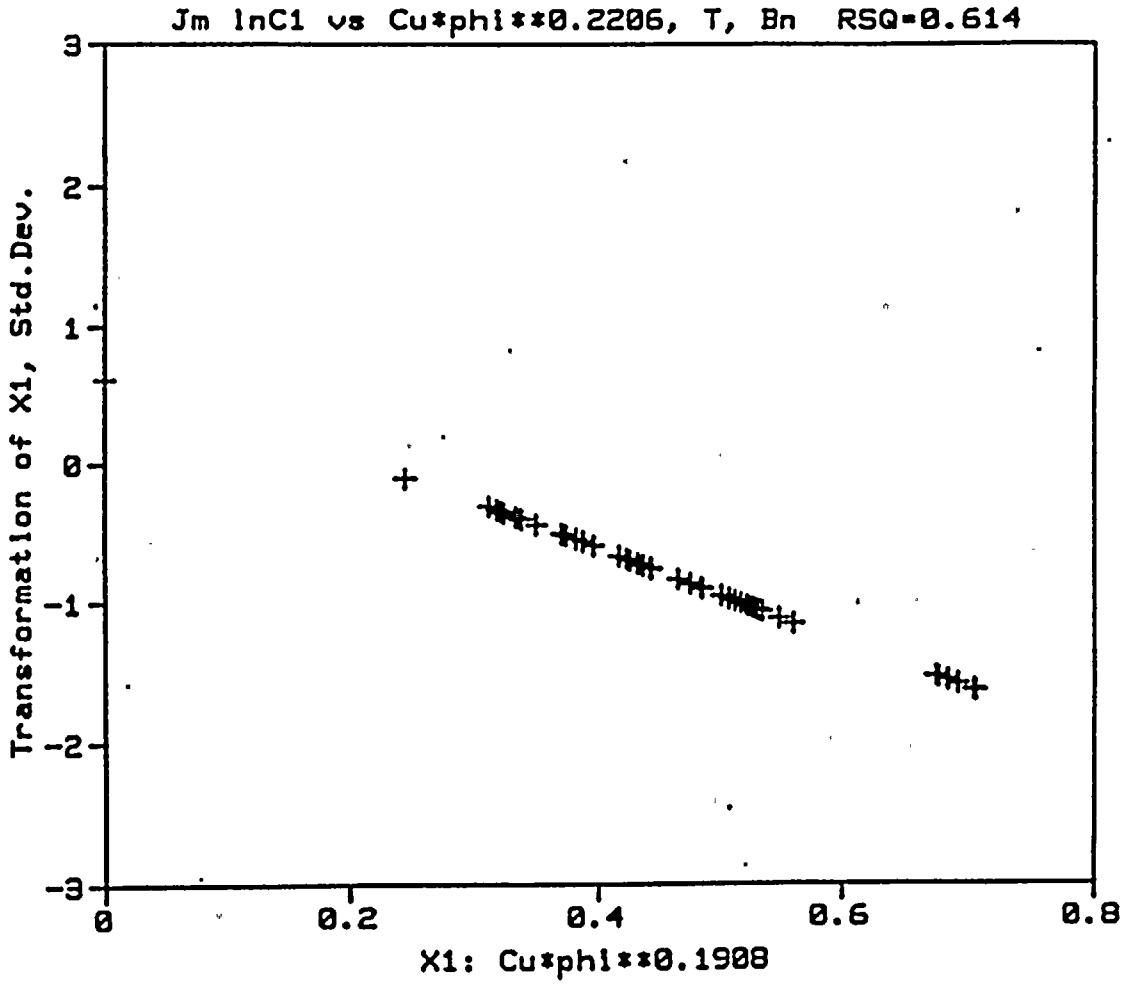

Figure 4-9 TAP for Temperature on J_D

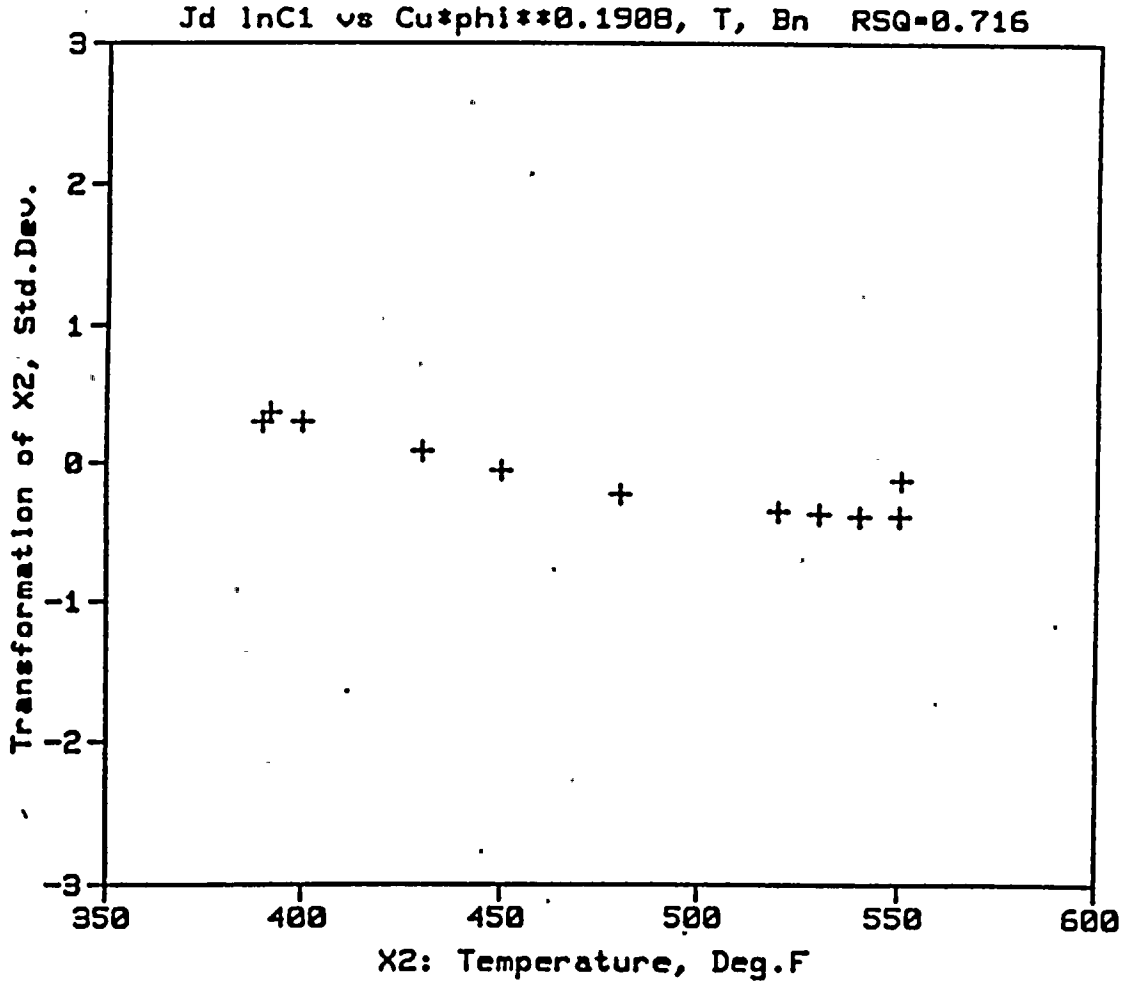

Figure 4-10 TAP for Temperature on J_M

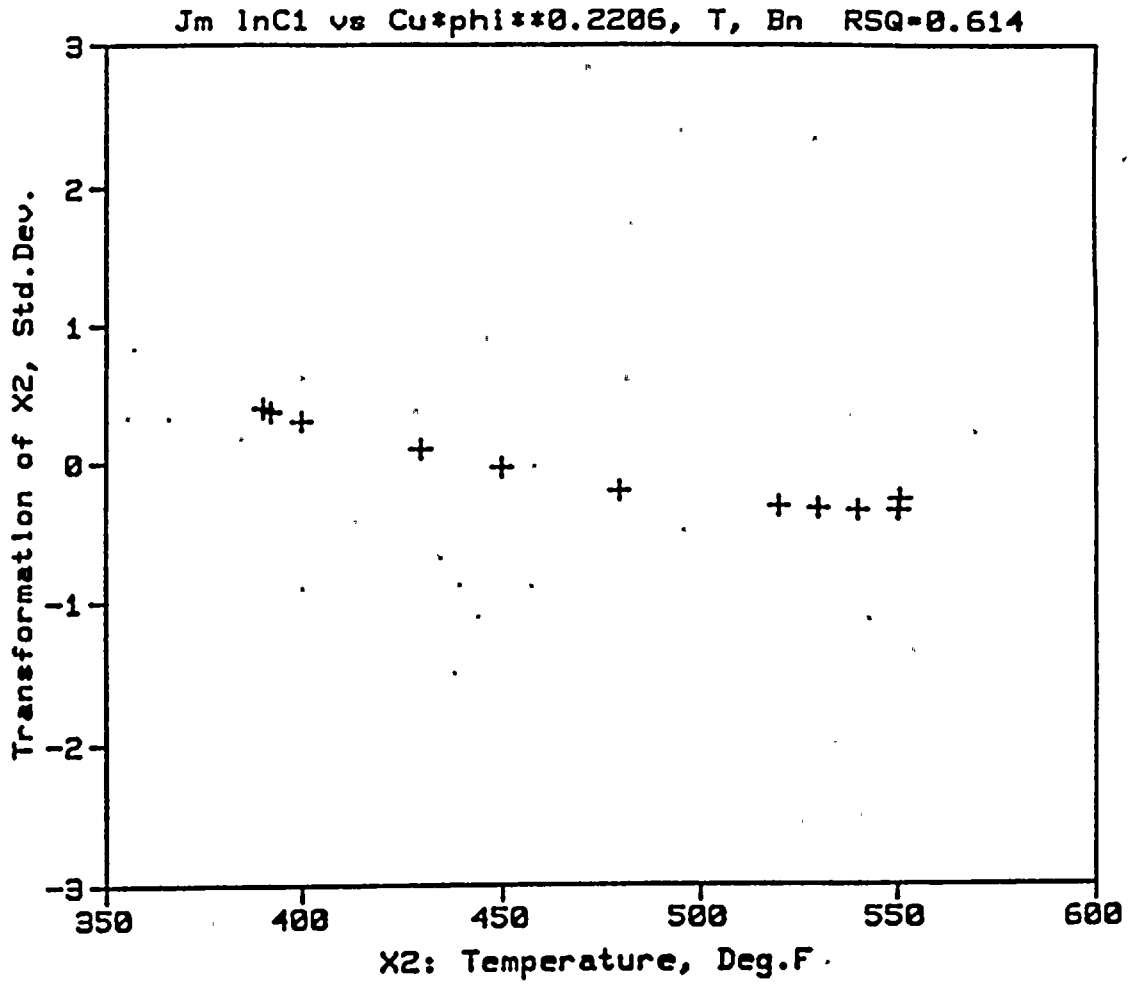

Figure 4-11 TAP for Net Thickness on J_D

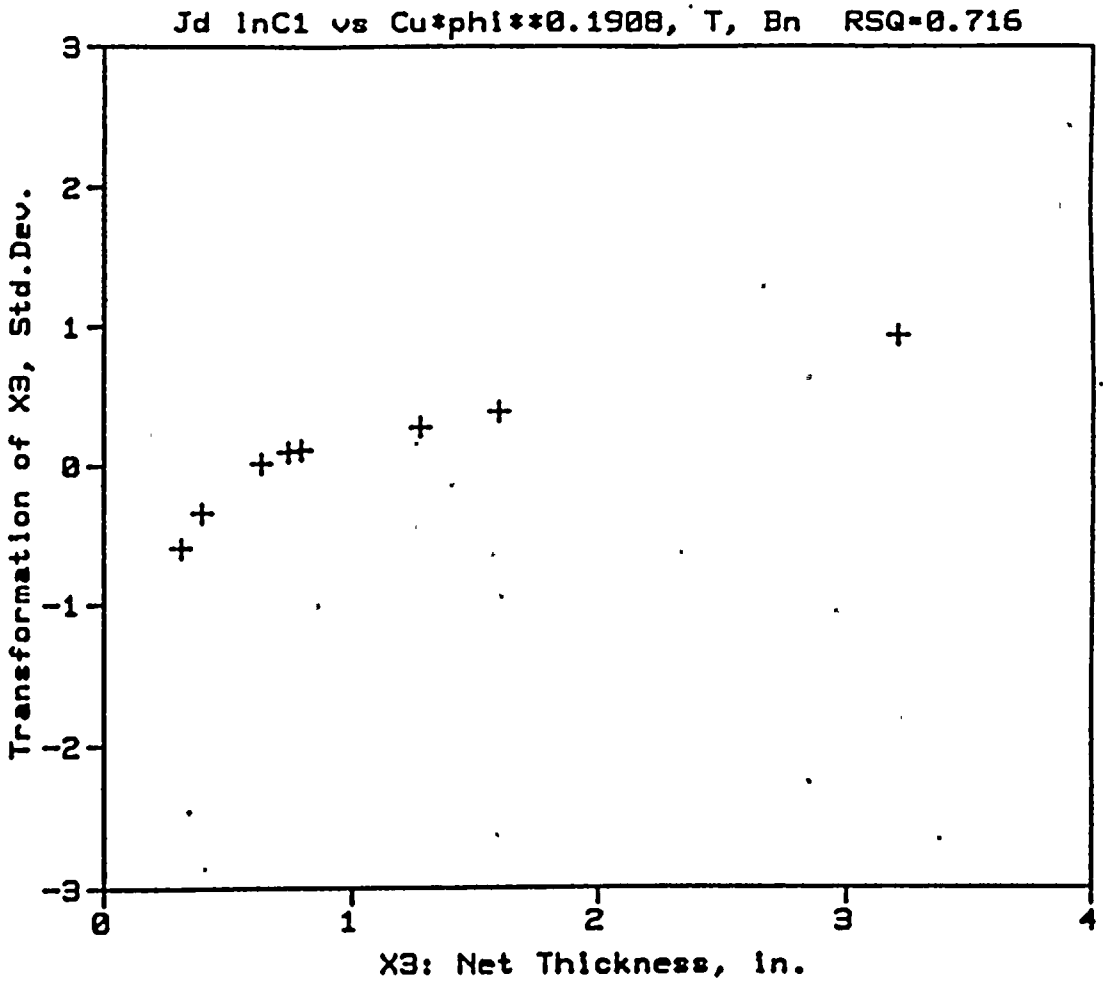

Figure 4-12 TAP for Net Thickness on J_H

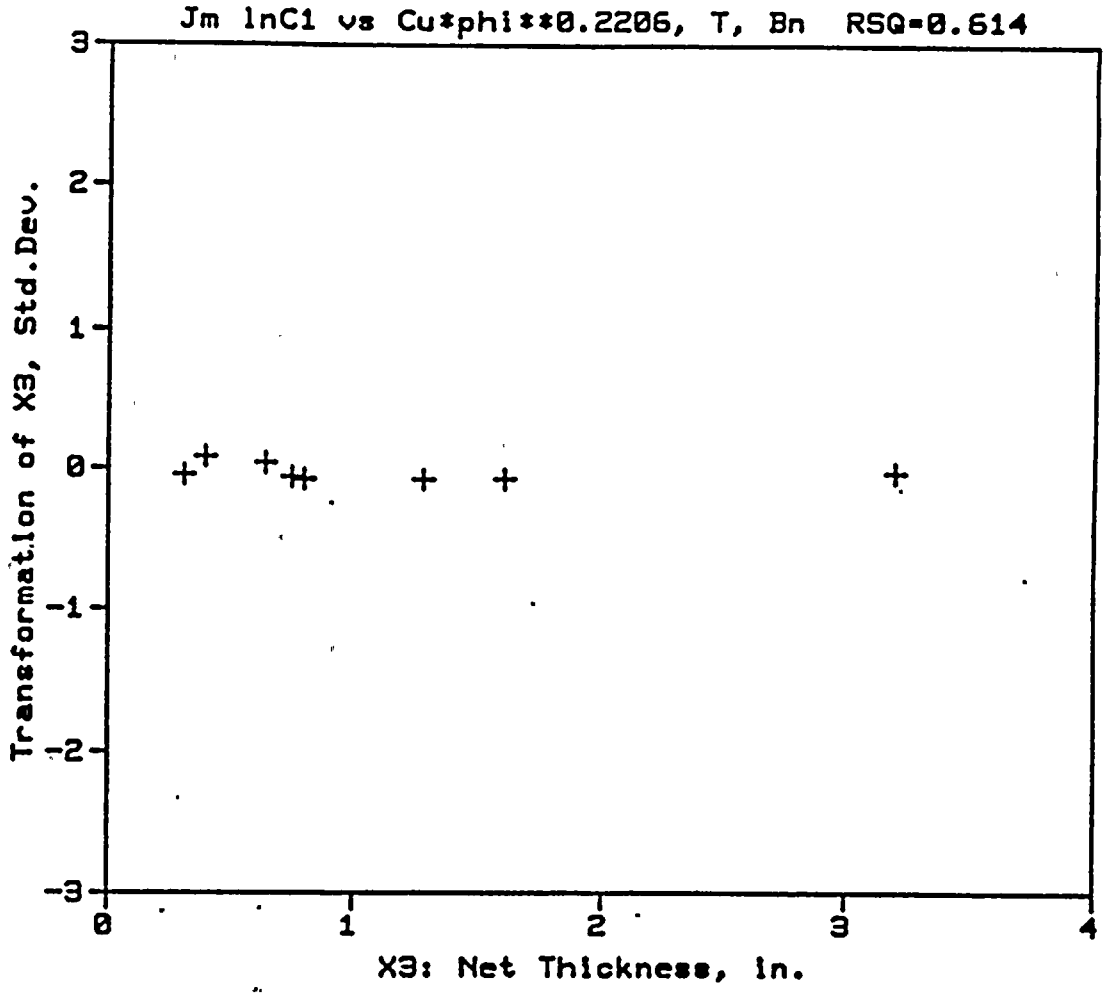

Figure 4-13 Normalized J_D Plot - B&WOG Data

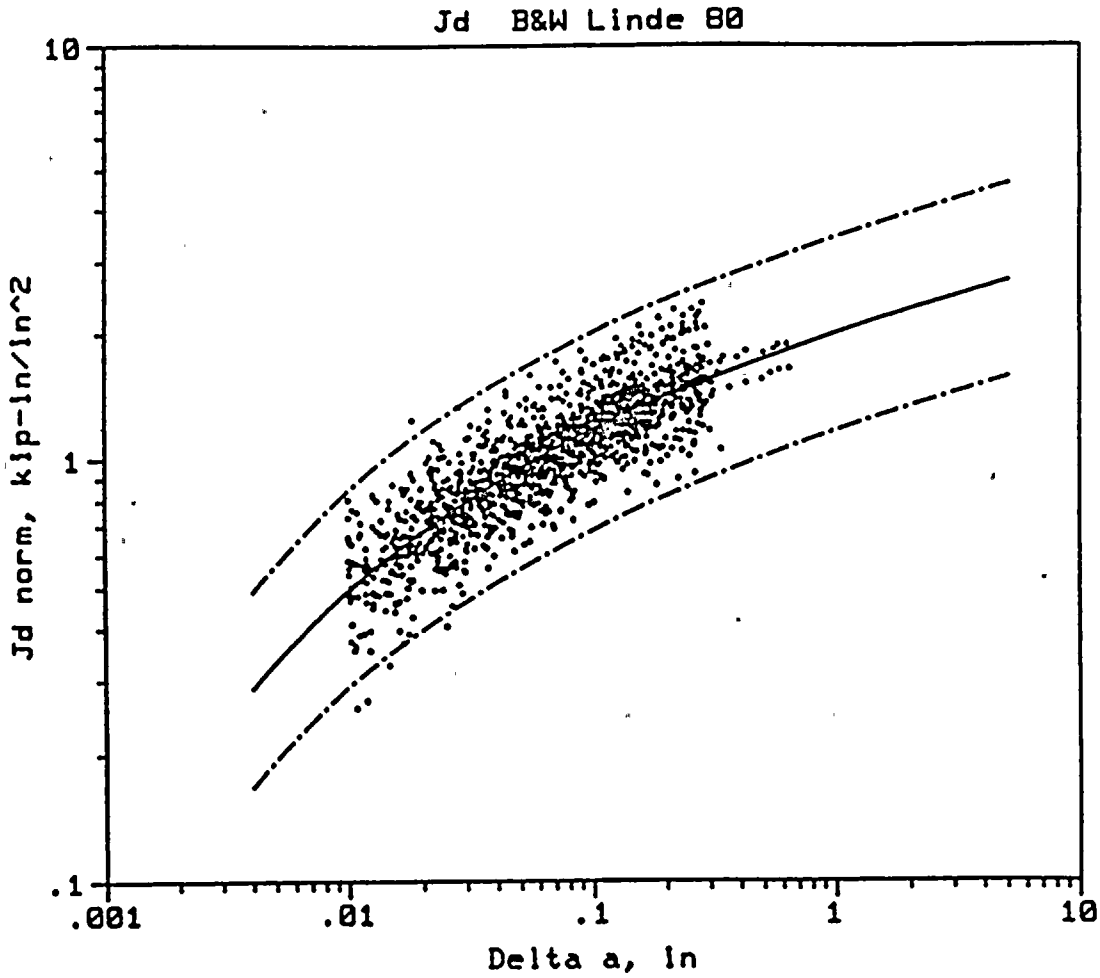

Figure 4-14 Normalized J_R Plot - B&WOG Data

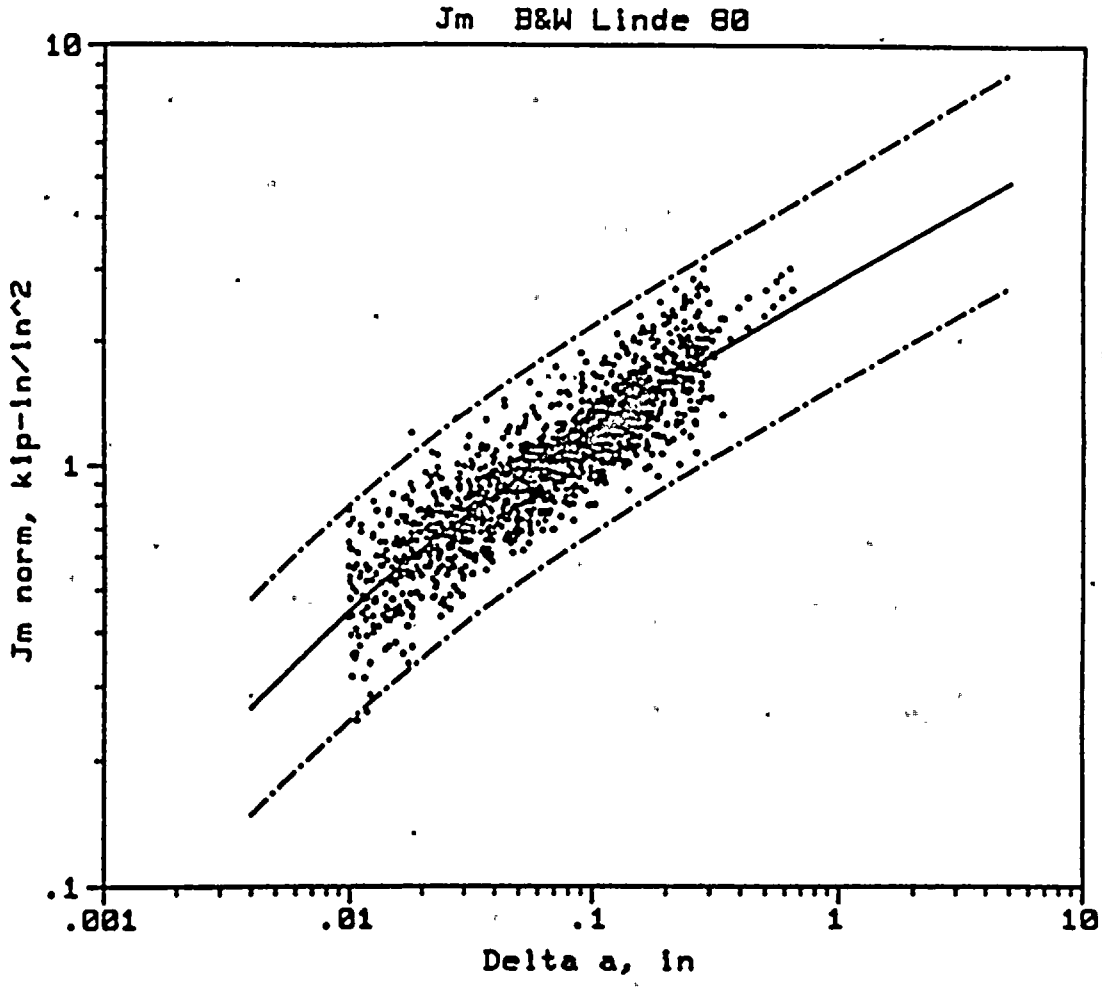

Figure 4-15 Normalized J_D Versus Copper Content

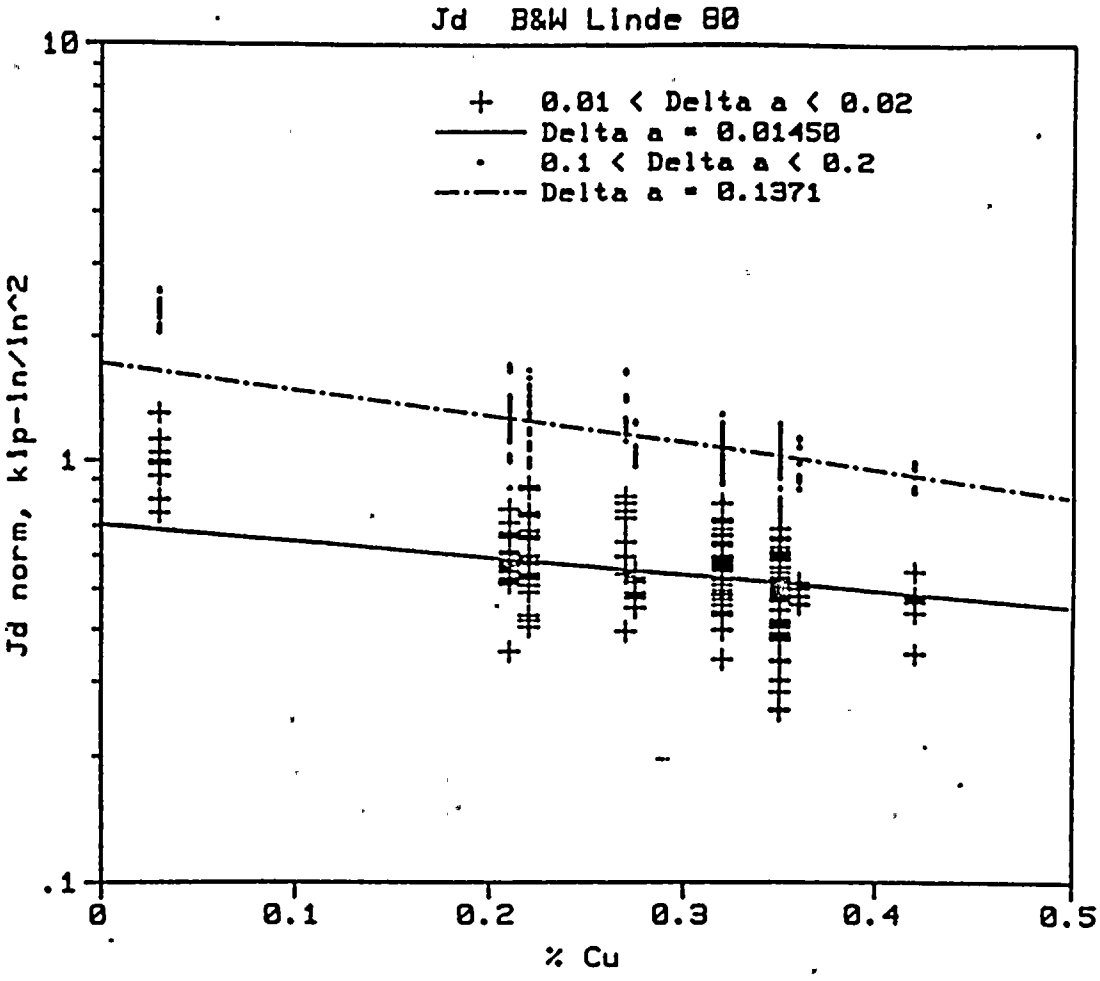

Figure 4-16 Normalized J_D Versus Fluence

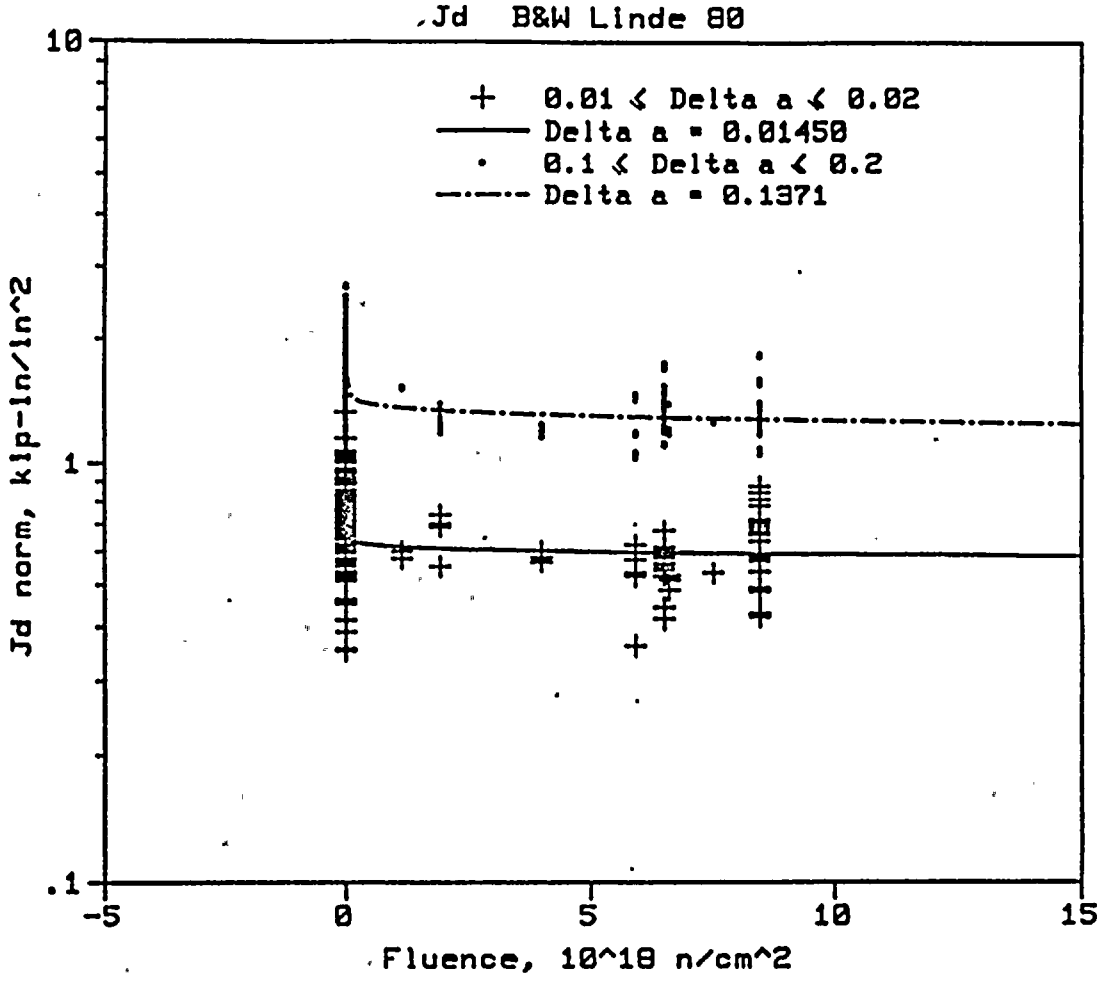

Figure 4-17 Normalized J_D Versus Temperature

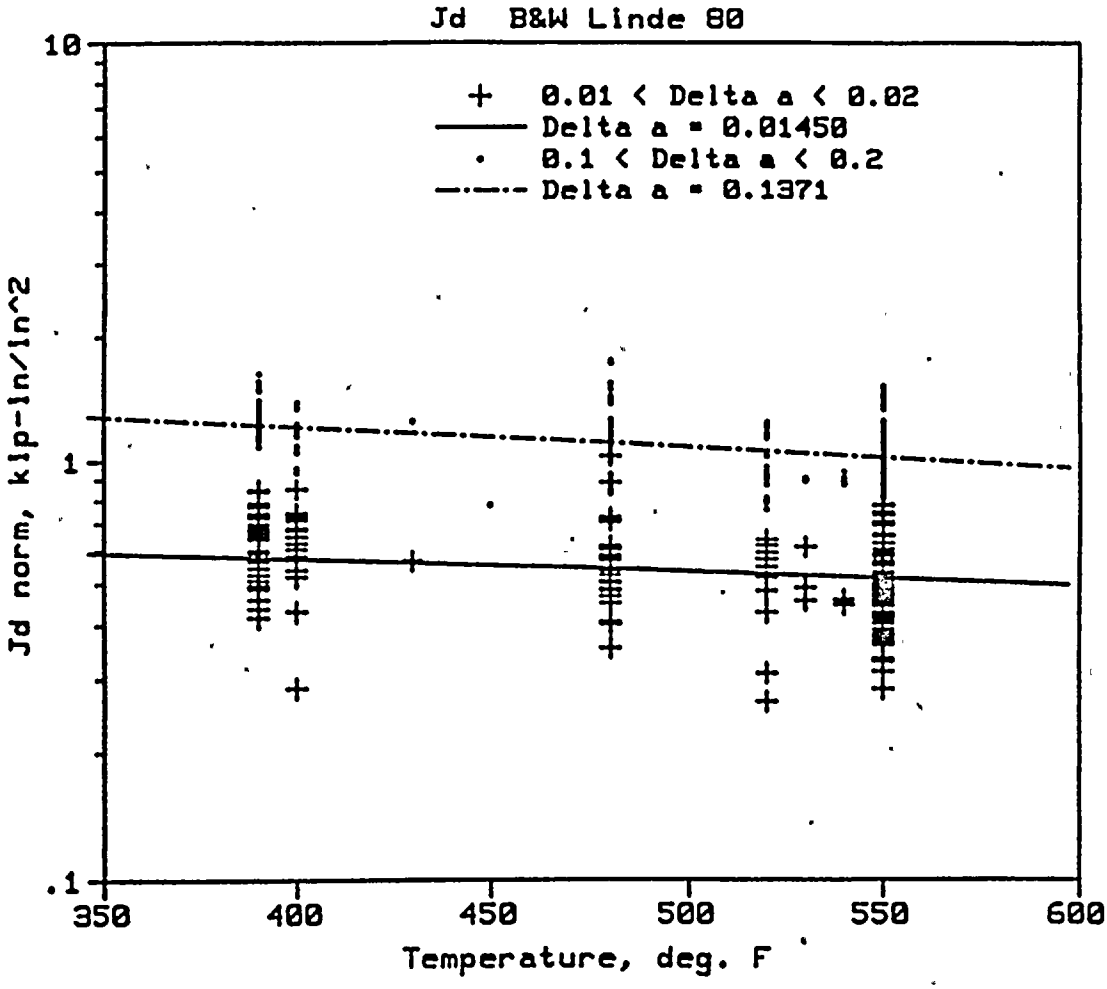

Figure 4-18 Normalized J_D Versus Specimen Thickness

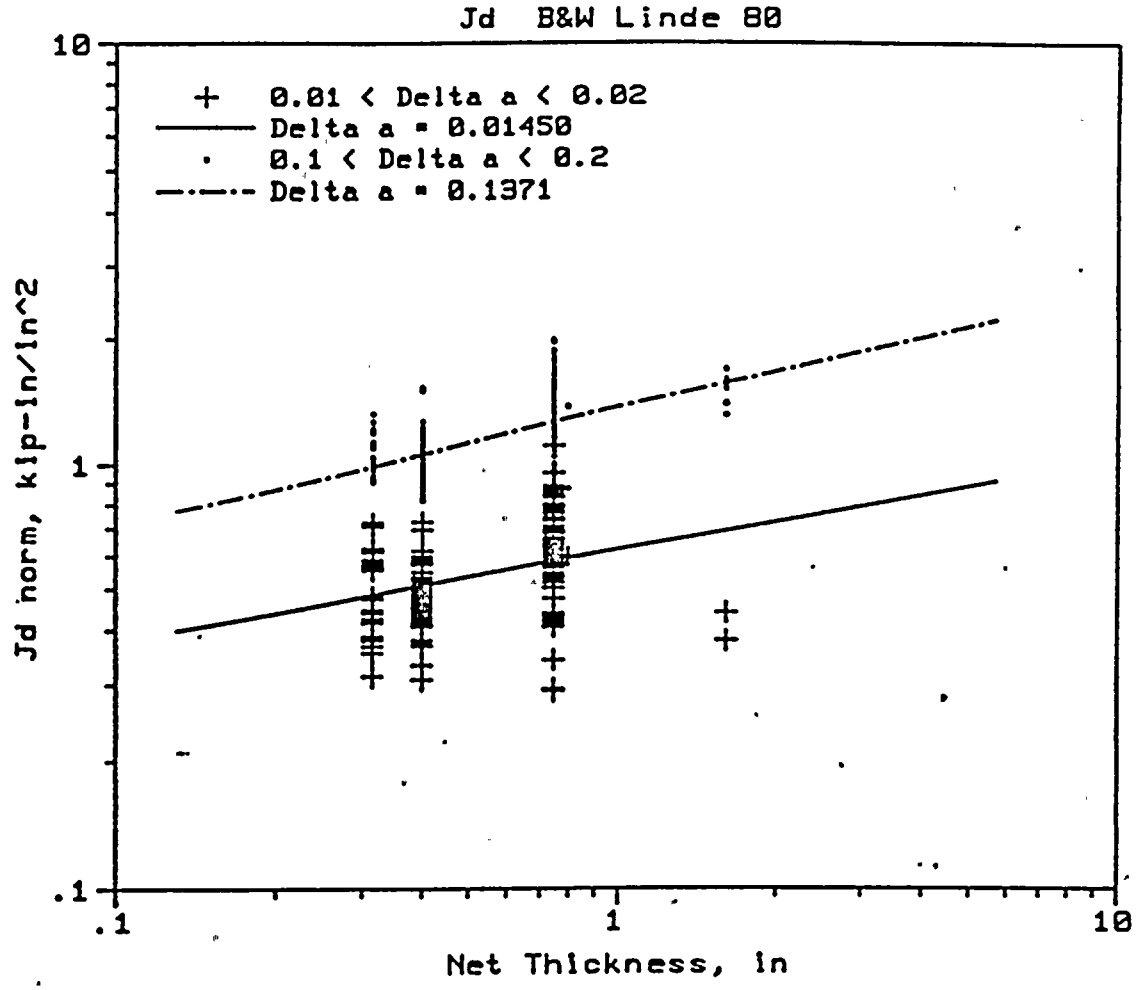

Figure 4-19 Effect of Fluence and Copper Content on J-B&WOG Data

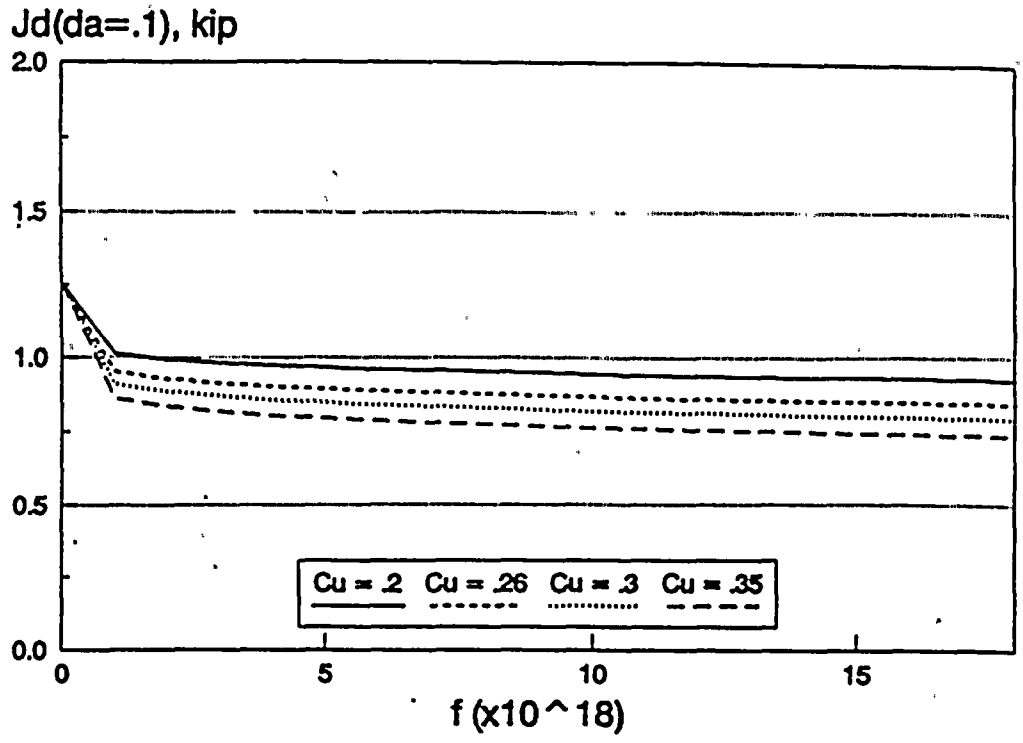

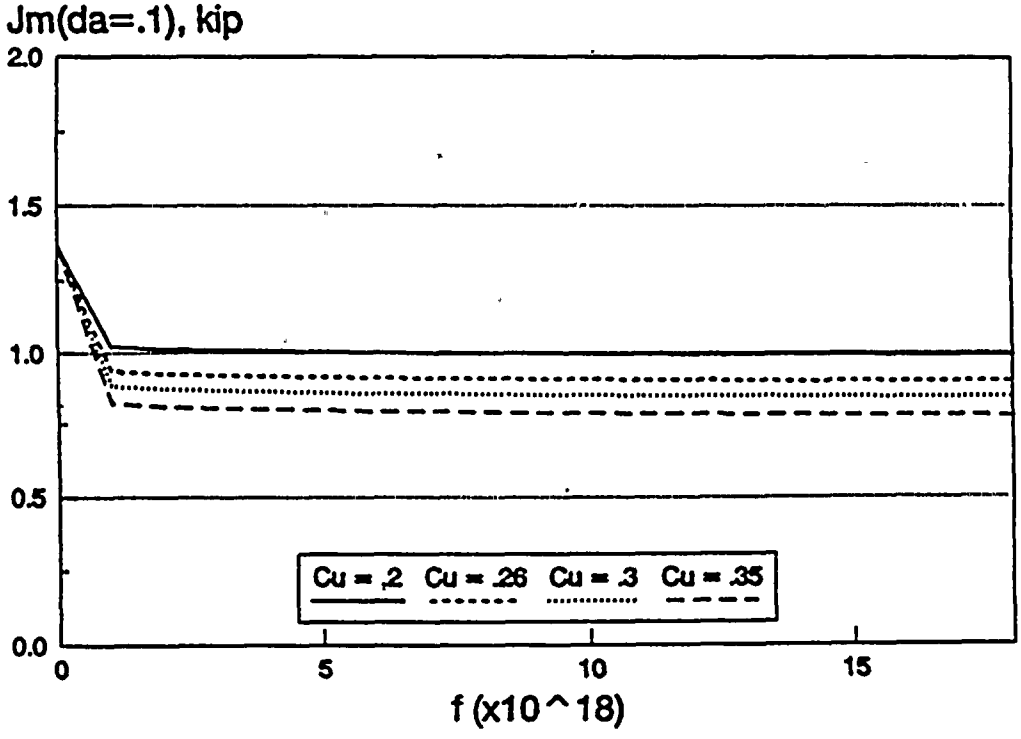

Figure 4-20 Effect of Temperature and Fluence on J

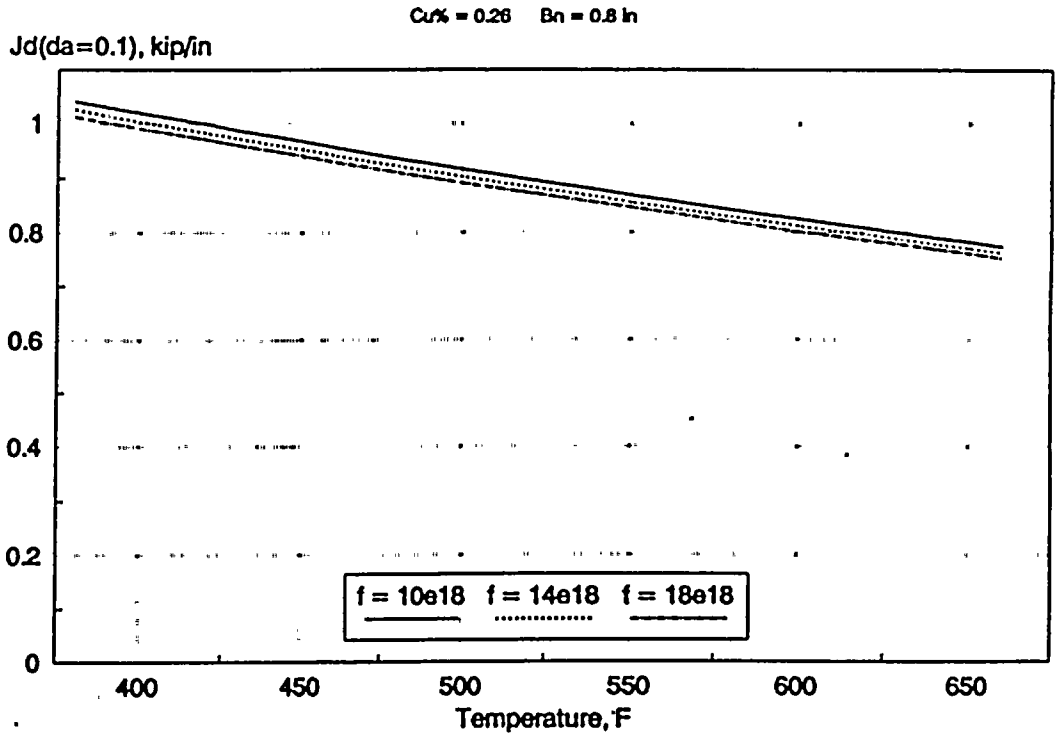

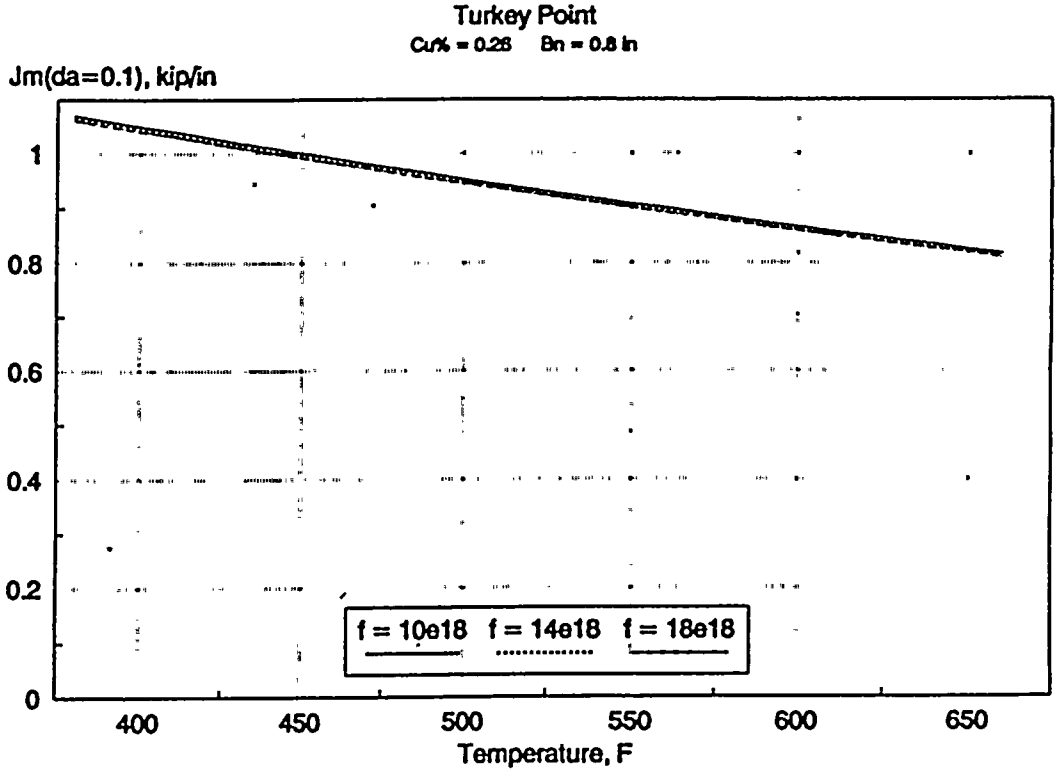

Figure 4-21 Effect of Net Thickness and Copper Content on J

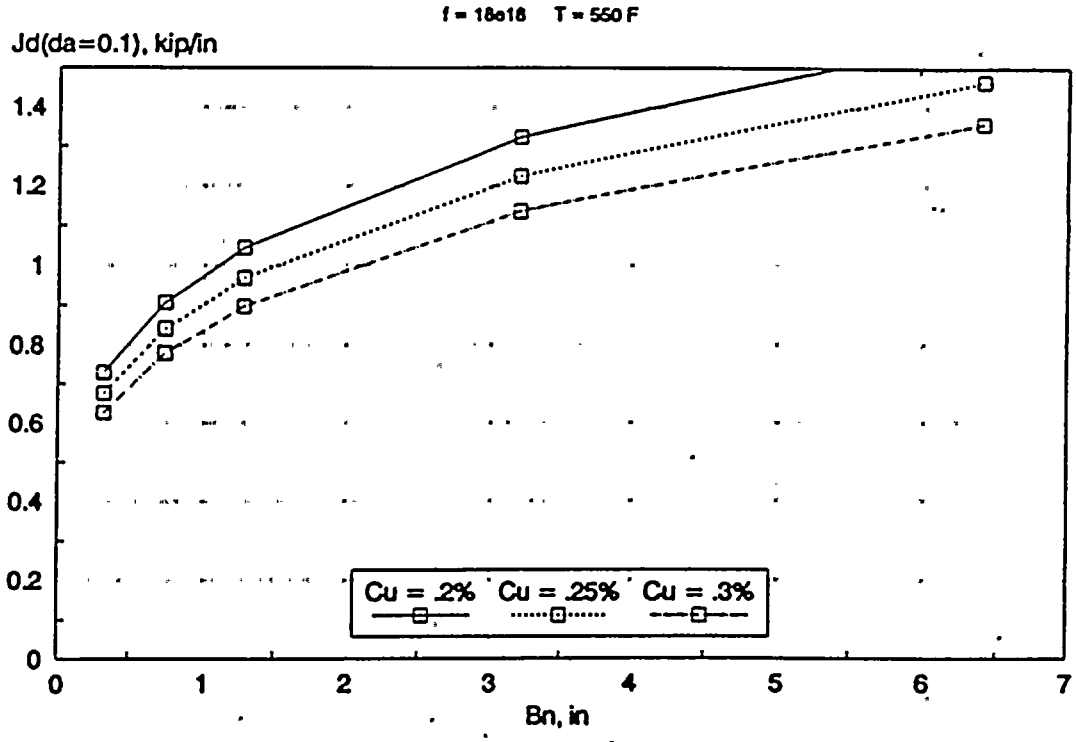

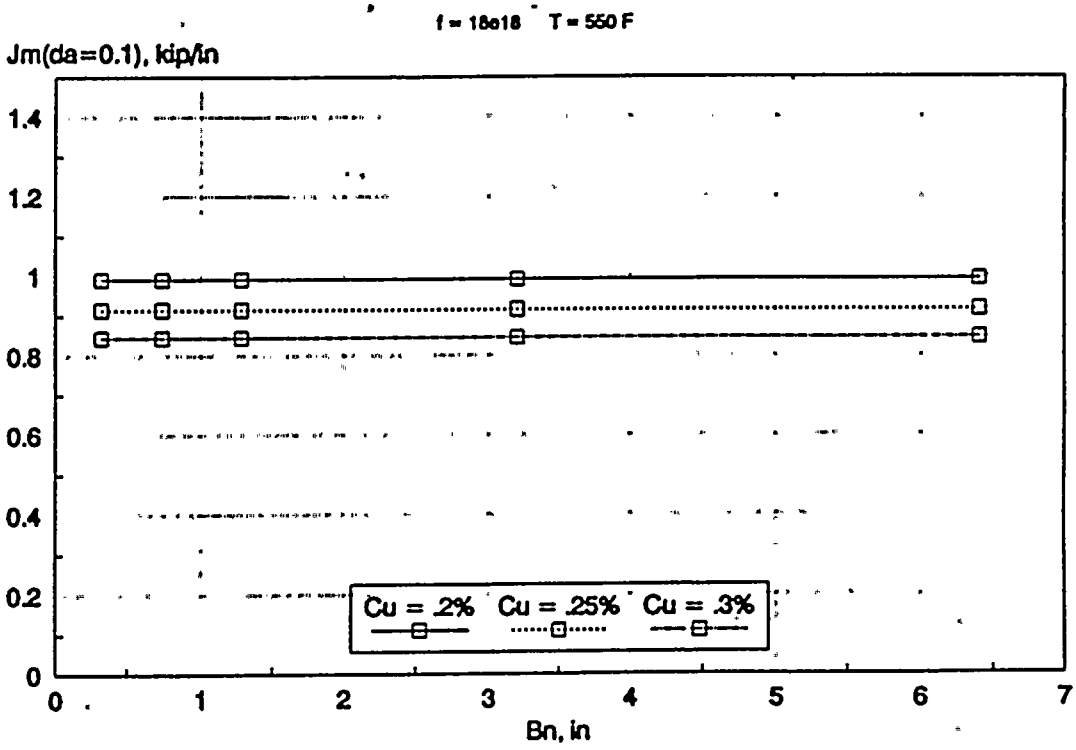

Figure 4-22 J-R Model and HSST Data Comparison - I

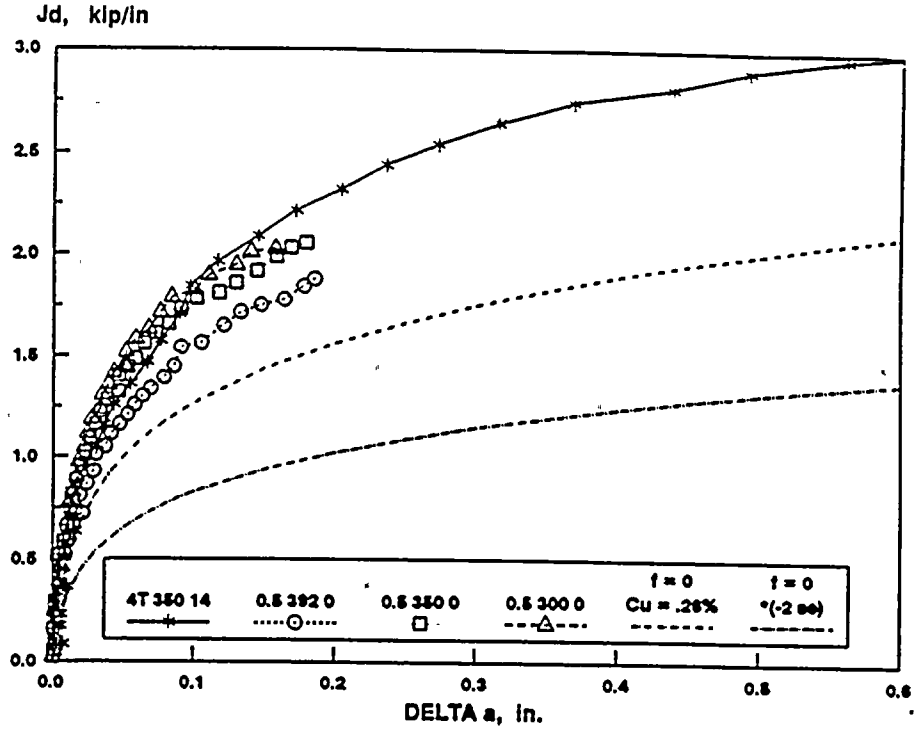

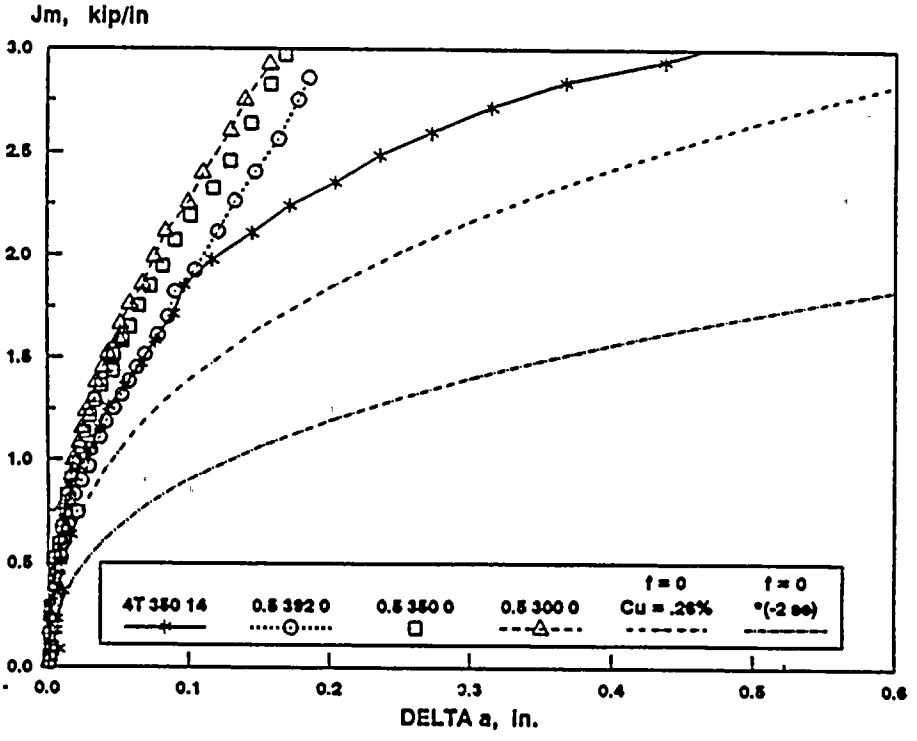

Figure 4-23 J-R Model and HSST Data Comparison - II

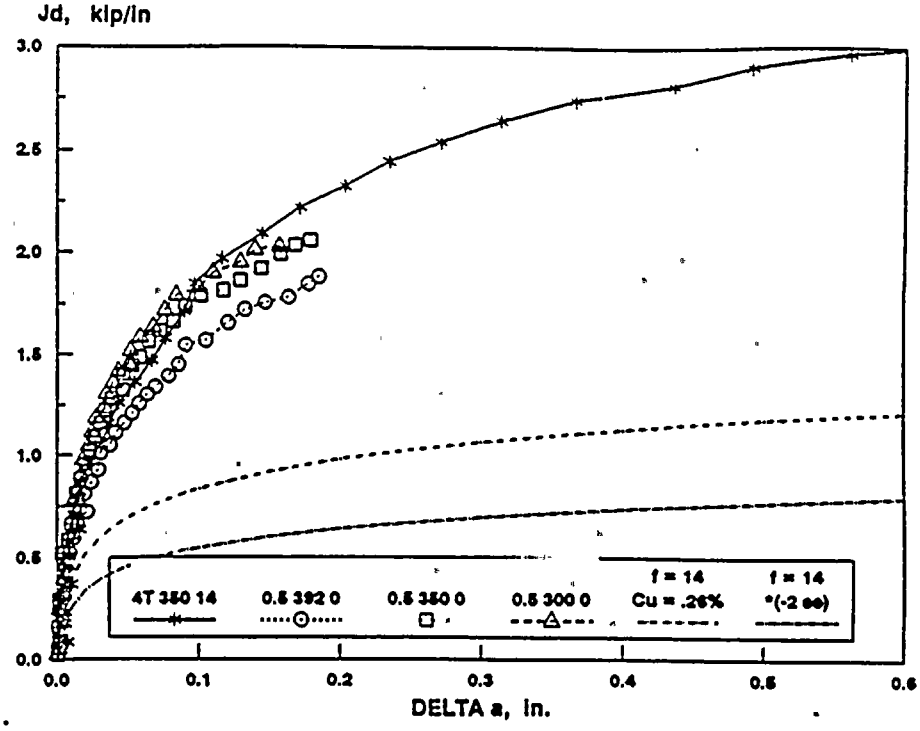

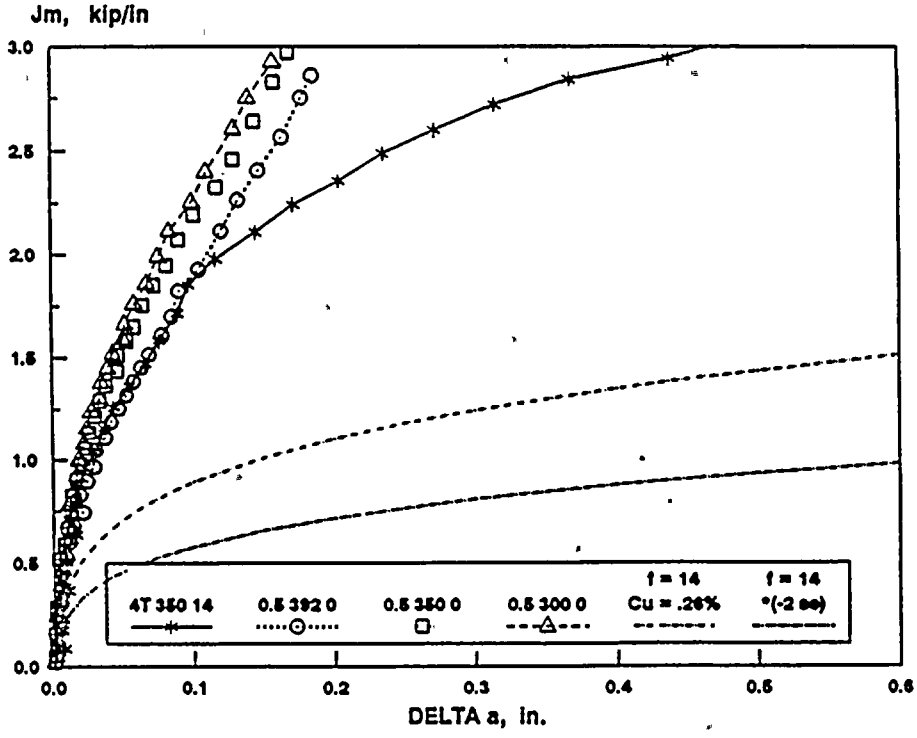

5. FRACTURE MECHANICS ANALYSIS

5.1. Plant Specific Input Data

Turkey Point Units 3 and 4 reactor vessel weld seams are shown in Figure 5-1. The beltline region weld identifications are listed below. These are all circumferential welds.

Turkey Point Unit 3	Turkey Point Unit 4
SA-1484	WF-70/WF-67
SA-1101	SA-1101
SA-1135	SA-1135

End-of-life reactor vessel fracture toughness data are summarized in Tables 2-1. and 2-2. From these tables, it was determined that the controlling welds are SA-1101 and that they are in the area of the highest fluence accumulation. This evaluation will be based on SA-1101 material properties. An input summary including dimensional data for these vessels is provided in Table 5-1.

5.2. Applied Loads for Service Levels A and B Condition

According to the criteria in Section 3.1, loads considered in this evaluation are due to internal pressure and thermal gradients. The accumulation pressure for the Turkey Point Units is taken as a pressure ten percent above the design pressure:

$$P_{acc.} = 1.1 \times 2485 = 2734 \text{ psi}$$

In accordance with Section 3.1 the following pressures are to be applied:

Criterion #1

$P = 1.15\ P_{acc.} = 3144$ psi

Criterion #2

$P = 1.25\ P_{acc.} = 3417$ psi for stability check.

The thermal gradient loading for 100 F/hour cooldown ramp is calculated by B&W computer program PTPC[43]. A time history of stress intensity factor for thermal gradient load, K_{IT}, is presented in Figure 5-2. A round robin computation performed by the ASME Section XI Working Group on Plant Operating Criteria[44] confirmed this K_{IT} value. From Figure 5-2, K_{IT} is 21 ksi $\sqrt{in}$ for the Technical Specification 100 deg F/hour cooldown rate thermal gradient load. As discussed in Section 3.3, the thermal gradient load would be relieved at the onset of ductile tearing. However, in order to be conservative, this fact is ignored and the K_{IT}, as calculated, is included in the evaluation.

5.3. Lower Bounding J-R Equation for Turkey Point Units

The following are plant specific values to be applied to the J-R equation presented in Section 4:

fluence = 1.8×10^{19}

Cu = 0.26

Temperature = 550 F (RC inlet temp. = 546.2 F)

B_N = 0.8

Then, the mean J-R curve is given by

$$J = C1\ (\Delta a)^{C2} \exp(C3\ \Delta a^{C4})$$

where

$$\ell n\ C1 = a1 + a2\ Cu(\phi t)^{a7} + a3\ T + a4\ \ell n\ B_N$$

$$C2 = d1 + d2\ \ell n\ C1 + d3\ \ell n\ B_N$$

$$C3 = d4 + d5\ \ell n\ C1 + d6\ \ell n\ B_N$$

C4 = ~ -0.5 (vary with data set)

The constants derived from the B&W data set from Table 4-6 are applied to this evaluation. The resulting mean J-R curves are

The final mean and lower bound J-R curves are plotted in Figure 5-3. This lower bounding curve is the final resistance curve to be used in this assessment.

The alternate model based on Charpy upper shelf energy value (Model 4A) is not directly utilized in this analysis simply because it would require an estimate of CvUSE at the t/4 location at the end of 32 EFPY design life. In the Charpy based model, CvUSE values are to be obtained for the fluence and temperature conditions of the end of the design life. This is difficult since an extrapolation of CvUSE at a fluence of 18×10^{18} n/cm^2 is required. From the HSST data

base, the 62W series specimens show a CvUSE of 66 ft-lb unirradiated. There is no CvUSE data at a fluence of 18×10^{18} n/cm^2. CvUSE value at the end-of-life was estimated to be approximately 50 ft-lb. It is difficult to assign the characteristics of a J-resistance curve to a single value of absorbed energy which went through a different mode of deformation process. Nevertheless, if one accepts the preceding assumptions, the comparison is as shown in Figure 5-4 where another curve at CvUSE of 44 ft-lb is shown. The J-R curve based on a Cv value of 50 ft-lb agrees very well with that of fluence of 18×10^{18} n/cm^2.

5.4. J Analysis

For criterion 1 in Section 3.1, an applied J needs to be calculated at a flaw size equal to the wall quarter-thickness plus a flaw extension of 0.1 inch:

$$a = a_o + \Delta a$$
$$= t/4 + 0.1$$
$$= 2.0375 \text{ in.}$$

Using J equations given in Section 3, applied J as a function of pressure is presented in Figure 5-5. For pressure loading only, the total J is nearly identical to the elastic part of J, J^E, indicating that the P^P term is very small and negligible. To conservatively combine pressure and thermal gradient stresses, the following approach is proposed:

$$J = J^E + J^P$$
$$= [KI(a_o, p) + K_{IT}]^2/E' \qquad (5\text{-}1)$$

Using this relationship, a second J-pressure curve including the thermal gradient load (K_{IT} = 21 ksi $\sqrt{in}$) is shown in the same figure. The combined loads yields a $J_{app.}$ (a) value of 166.5 lb/in.

The applied J with the above flaw size at 3144 psi and thermal gradient loading is to be compared to material J at Δa equal to 0.1 in. From equation 5-1, the lower bounding J_D is

$J_{m\cdot 2Se}$ (Δa=0.1) = 591 lb/in. > $J_{app}(a)$ = 166.5 lb/in.

Therefore, the first criterion is met with a wide margin as illustrated in Fig. 5-6. Where the J° term is dominant, the applied J is proportional to the square of pressure load. A plot of $\sqrt{J_{appl}}$ versus Δa in Figure 5-7 shows the margin in more realistic term of equivalent pressure load. This is also shown in J-Δa space in Figure 5-7.

5.5. Stability Analysis

The second criterion in Section 3.1 requires that the combined loads of (1) pressure of 1.25 P_{acc} (3417 psi) and (2) thermal gradient should be less than the instability load. Conversely, it can be shown that the combined load is stable.

5.5.1. DPFAD Analysis

Figure 5-8 shows the results of DPFAD analysis using the above combined loads. Since the combined loads include a safety factor, it is obvious that this structure is stable with a margin when all assessment points lie below and left hand side of the FAD curve. Therefore, the second criterion is also met with a wide margin.

5.5.2. J-Δa Method

As described in Section 3.2, it can be shown that the applied J with the combined loads can be compared in a J-Δa plot as shown in Figure 5-6. At the intersection of the applied J and the material resistance J, the slope of the applied J is much smaller than the material J curve and therefore it is demonstrated that the second criterion is met.

Table 5-1. Reactor Vessel Design Data

Design/Operating Pressure, psig	2485/2235
Hydrostatic Test Pressure, psig	3107
Design Temperature, °F	650
Overall Height of Vessel and Closure Head Head, ft-in. (Bottom Head O.D. to Top of Control Rod Mechanism Housing)	42-7
Water Volume, (with core and internals in place), ft^3	3667
Thickness of Insulation, min., in.	3
Number of Reactor Closure Head Studs	58
Diameter of Reactor Closure Head Studs, in.	6
Flange, ID, in.	149.6
Flange, OD, in.	184
ID at Shell, in.	155.5
Vessel Wall Thickness	7.75
OD Across Inlet/Outlet Nozzles, in.	230-5/16/240
Inlet Nozzle ID, in.	Tapered 27-15/32 to 33-13/16
Outlet Nozzle ID, in.	28.97
Clad Thickness, min., in.	0.156
Lower Head Thickness, min., in.	4-3/4 plus cladding
Vessel Belt-Line Thickness, min., in.	9 plus cladding
Closure Head Thickness, in.	6-3/16 plus cladding
Reactor Coolant Inlet Temperature, °F	546.2
Reactor Coolant Outlet Temperature, °F	602.1
Reactor Coolant Flow, lb/hr	101.5×10^6

Table 5-2. Tensile Properties of Irradiated Weld Metal

Specimen No.	Fluence, n/cm^2 (E > 1 MeV)	Test Temp, F	Strength, psi	
			Yield	Ultimate
	8.0E18	79	83,500	98,300
	1.1E19	79	83,400	98,300
	1.4E19	79	87,300	101,100
	1.5E19	79	90,100	102,300
	5.0E18	300	78,200	90,900
	1.5E19	300	83,000	95,000
	5.0E18	550	69,000	87,700
	1.5E19	550	75,400	91,700

Figure 5-1 Reactor Vessels and Weld Metal Orientation

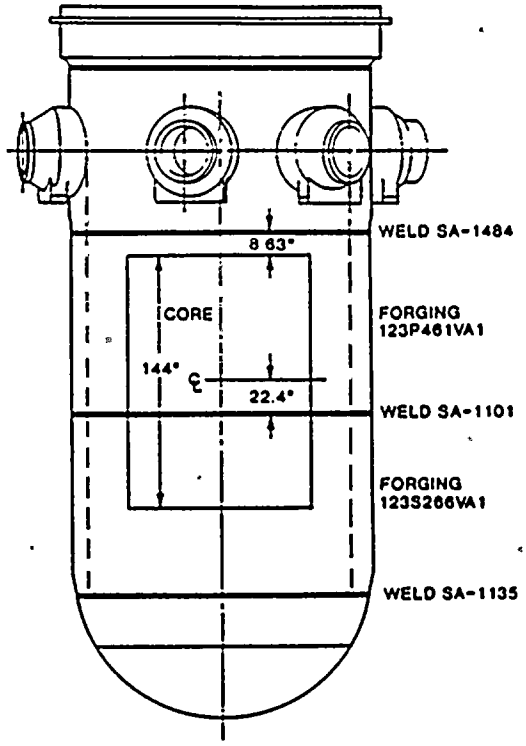

Turkey Point-3 Reactor Vessel

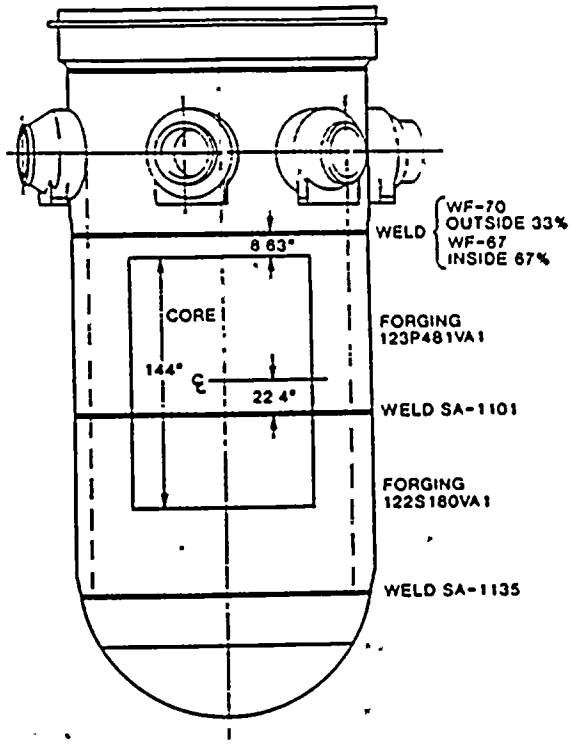

Turkey Point-4 Reactor Vessel

Figure 5-2 Cooldown Ramp and K_{IT}

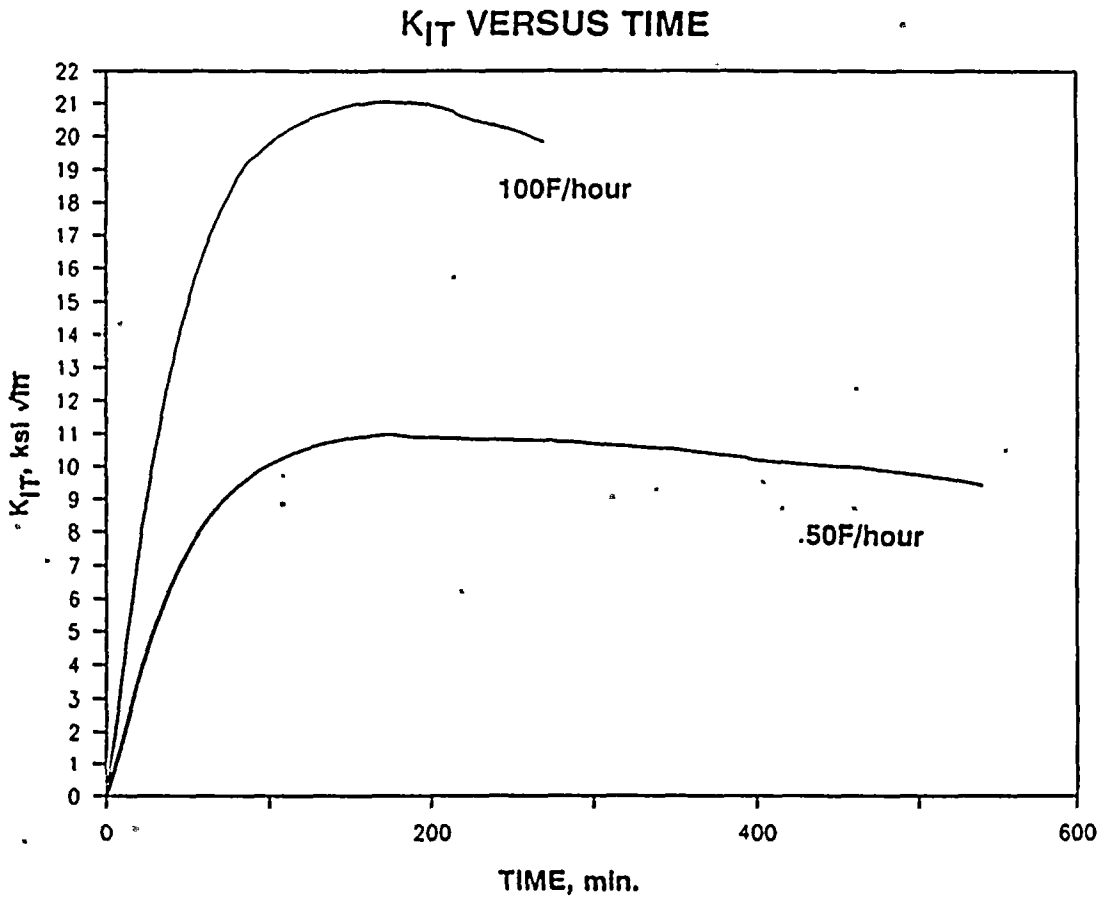

Figure 5-3 Mean and Lower Bound J-R Curves

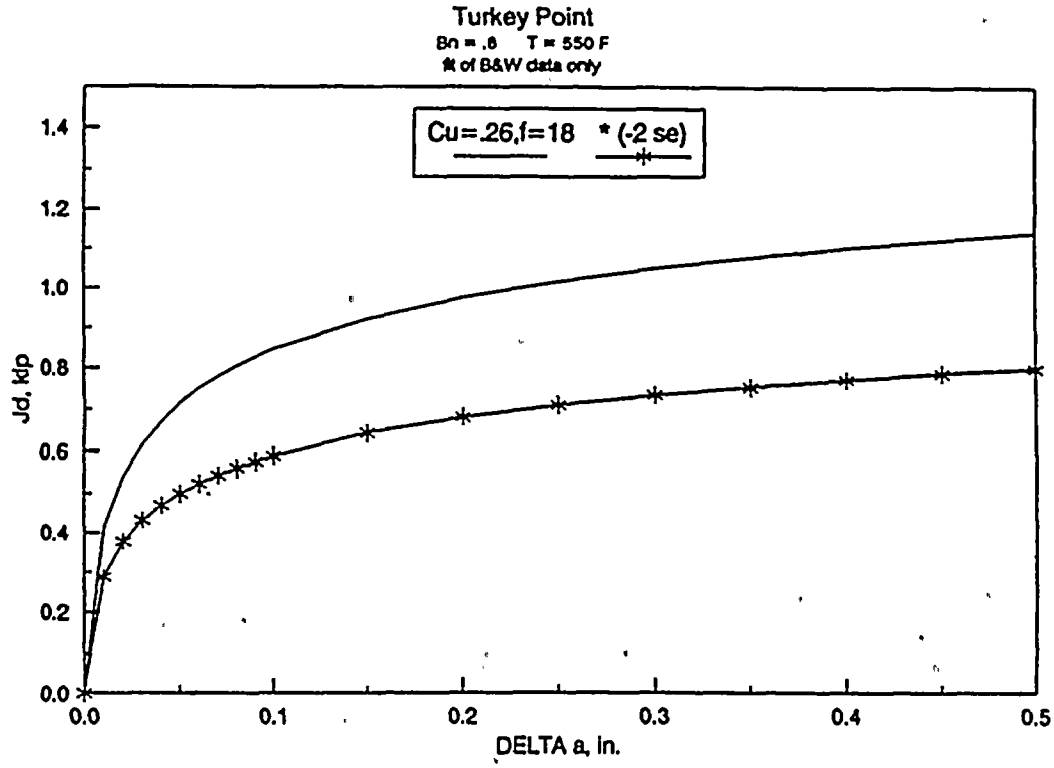

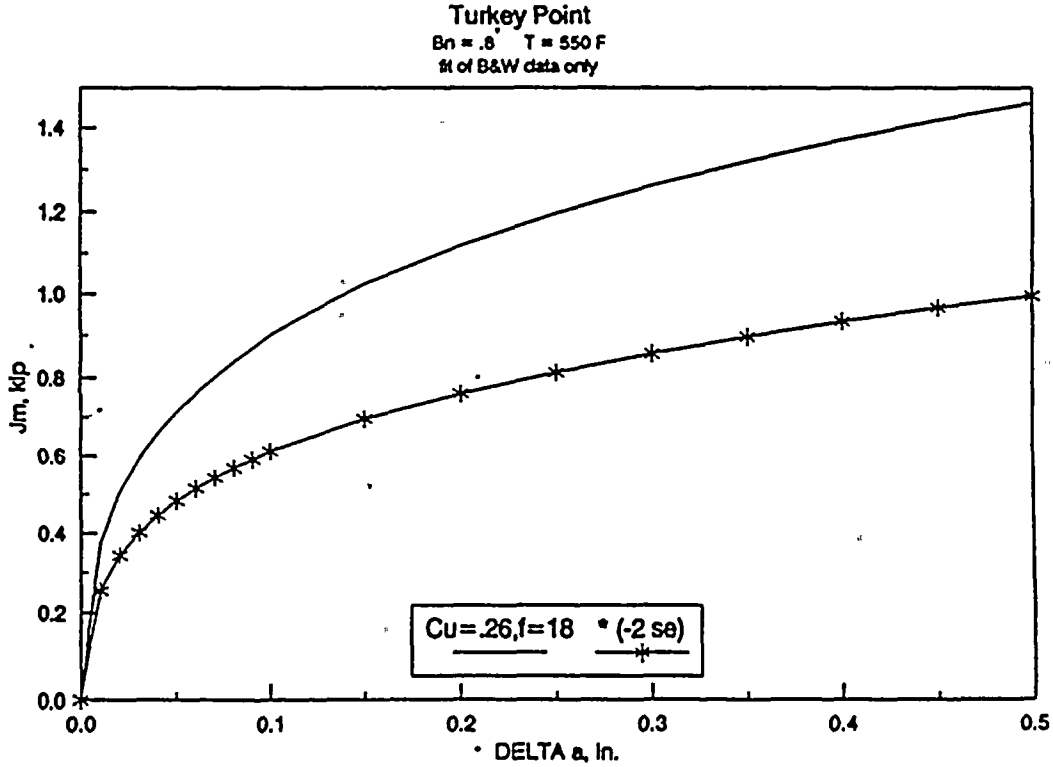

Figure 5-4 Comparison of Two Models

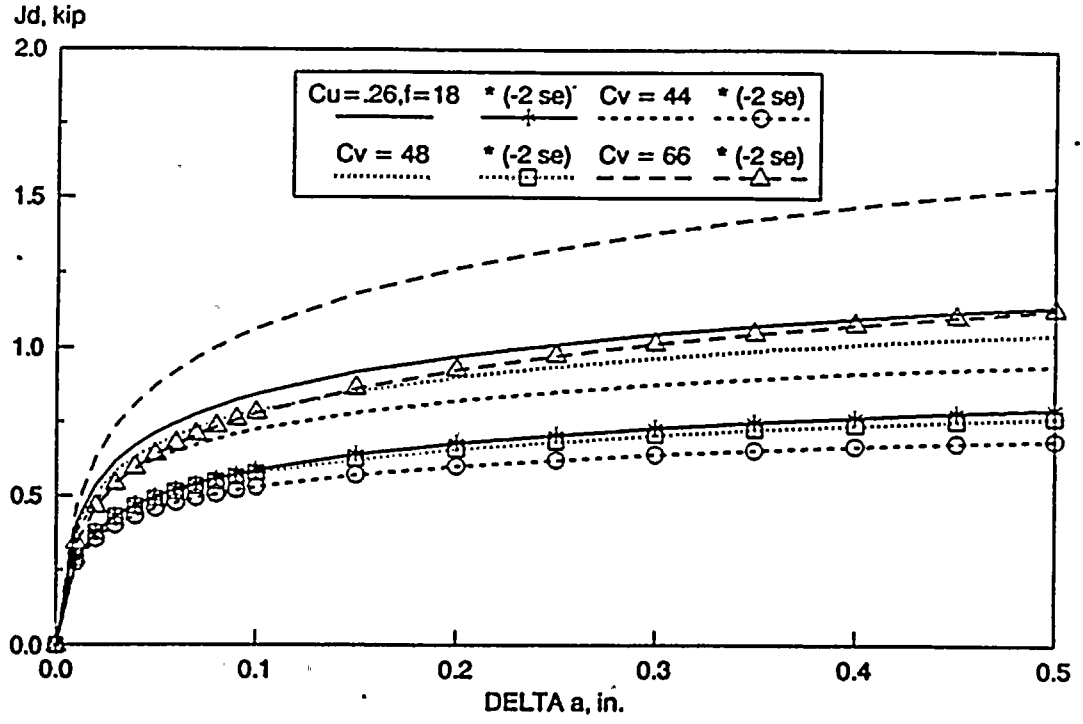

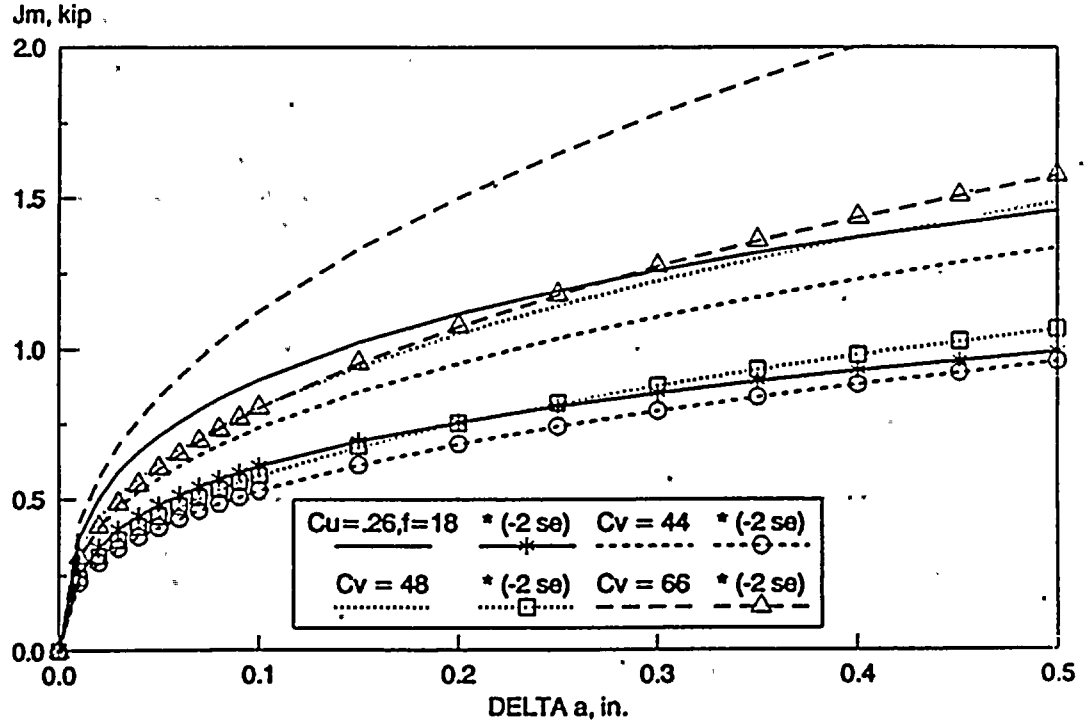

Figure 5-5 Applied J As A Function of Pressure

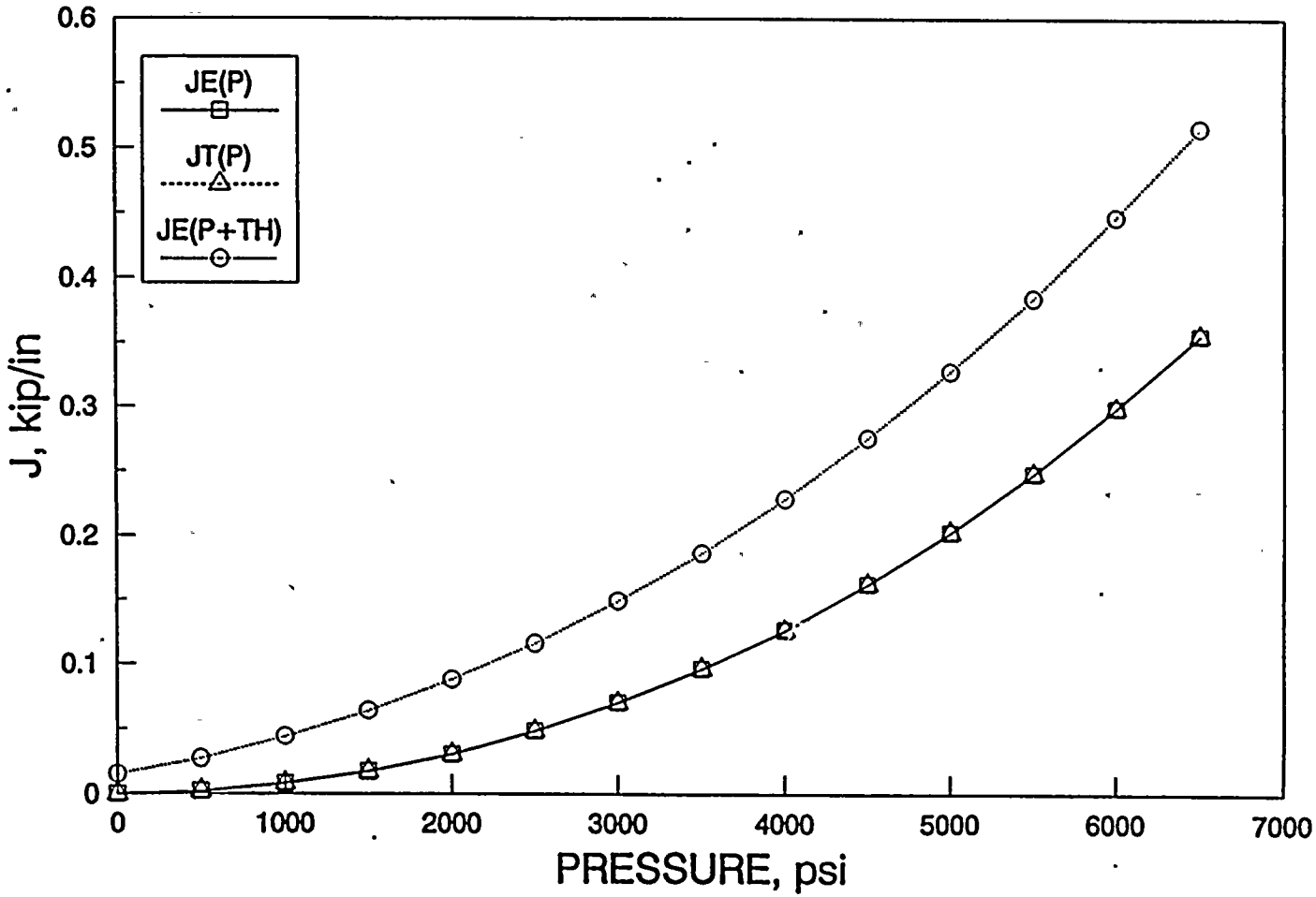

Figure 5-6 Applied J-Δa Against J-R Curve

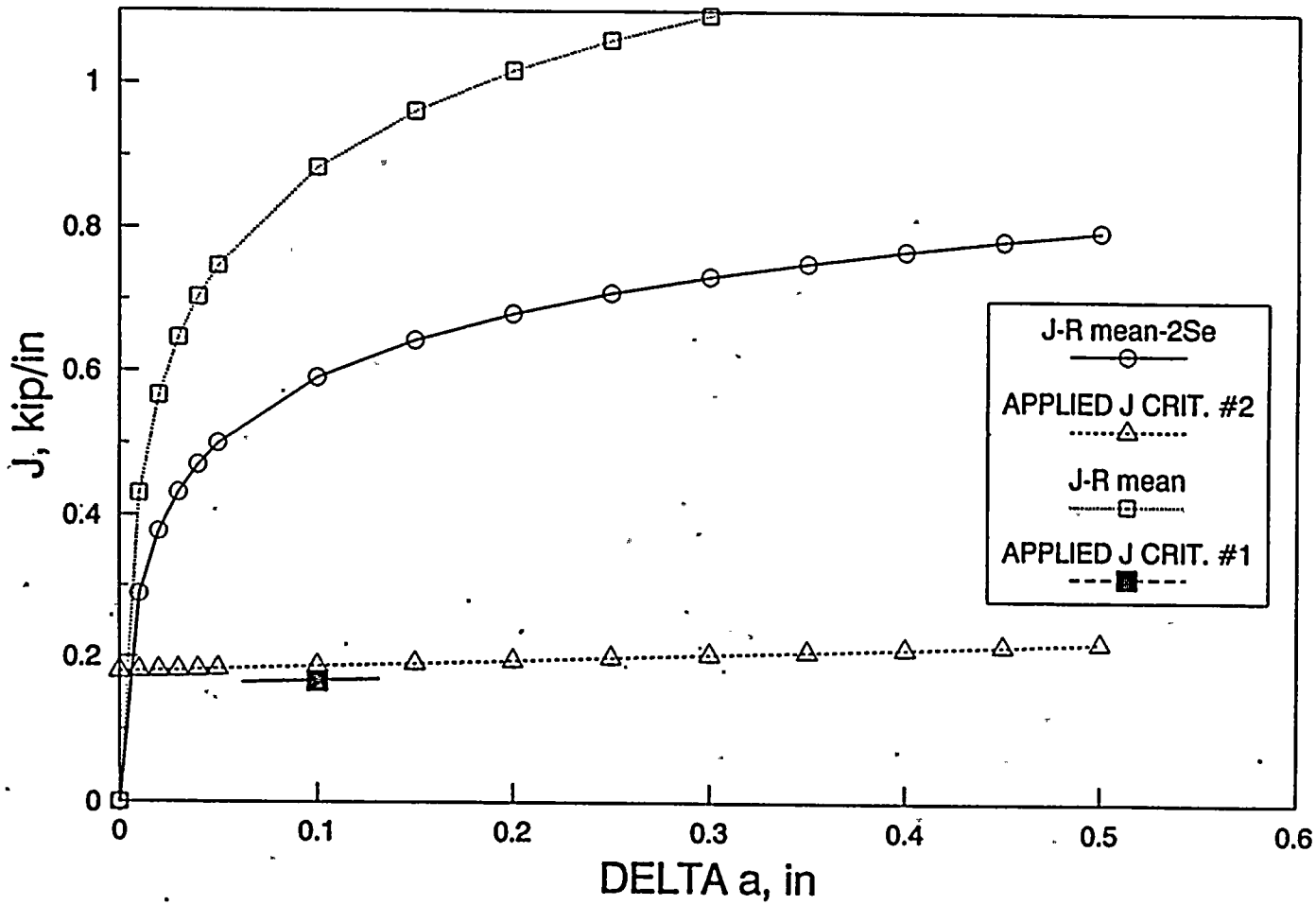

Figure 5-7 DPFAD Analysis

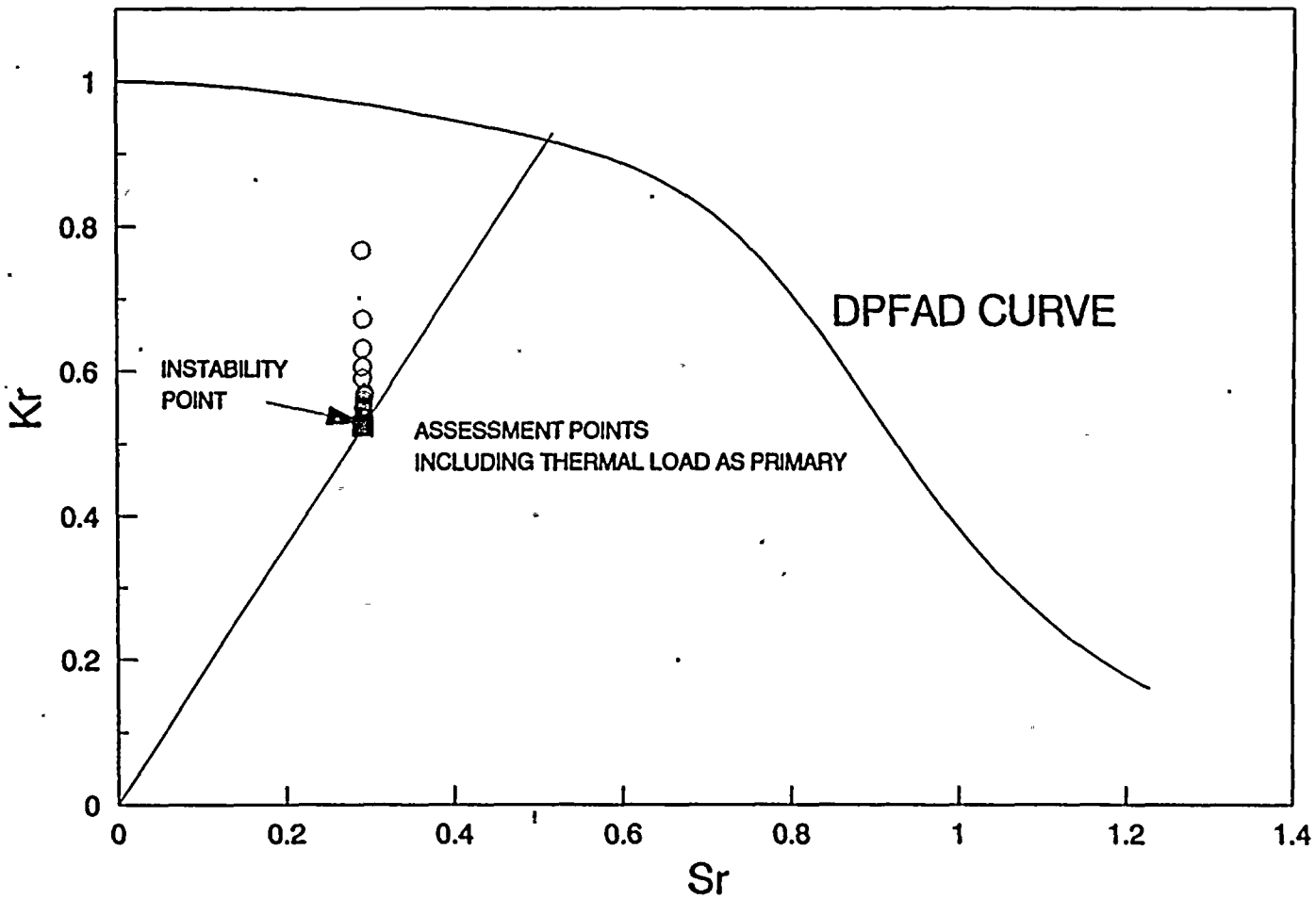

6. CONCLUSION

Through the B&W Owners Group Integrated Surveillance Program, an extensive J-resistance data base was assembled for over more than fifteen years. This was achieved through a carefully planned, long-term cooperative effort by the affected licensees and B&W. A comprehensive mathematical model for J-resistance behavior of Mn-Mo-Ni/Linde 80 weld metals was developed through application of a state-of-the-art pattern recognition method.

While this data collection was in progress, an industry - NRC consensus effort (through the ASME Boiler and Pressure Vessel Code Committee) produced acceptance criteria for low upper shelf fracture toughness under A and B load conditions.

The J-integral based elastic-plastic fracture mechanics methodology developed through NRC regulatory research programs with industry efforts by the B&W Owners Group, EPRI and others, now allows the lower upper-shelf fracture toughness concern to be addressed using the J-resistance model and the acceptance criteria.

The first lead plant analysis for low upper-shelf fracture toughness concern was performed using very conservative material models and load combination, i.e. treating thermal gradient stress as a primary stress.

The results indicate that there is a very large margin of safety to continuously operate Turkey Point Units 3 and 4. This analysis was submitted to the Nuclear Regulatory Commission to demonstrate compliance with 10CFR50, Appendix G.

7. REFERENCES

1. U.S. Code of Federal Regulations, Title 10, Energy, Part 50, "Domestic Licensing of Production and Utilization Facilities, Appendix G, Fracture Toughness Requirements."

2. U.S. Code of Federal Regulations, Title 10, Energy, Part 50, "Domestic Licensing of Production and Utilization Facilities, Appendix H, Reactor Vessel Material Surveillance Program Requirements."

3. BAW-10046A, Rev. 3, "Methods of Compliance with Fracture Toughness and Operational Requirements of 10CFR50, Appendix G," B&W Owners Group submitted to the NRC for approval, April 1990.

4. S. Fyfitch, L. B. Gross and A. L. Lowe, Jr., "Master Integrated Reactor Vessel Program," BAW-1543, Rev. 3, B&W Owners Group, September 1989.

5. ASTM Standard E185-61T, Tentative Recommended Practice for Surveillance Tests on Structural Materials in Nuclear Reactors, American Society for Testing and Materials, Philadelphia, Penn.

6. L. E. Steele, G. W. Knighton, and U. Potapovs, "Radiation Embrittlement of Pressure Vessels and Procedures for Limiting This Effect in Power Reactors," Nuclear Applications, 4 April 1958, p. 230.

7. L. E. Steele and J. R. Hawthorne, New Information on Neutron Embrittlement and Embrittlement Relief of Reactor Pressure Vessel Steels, NRL Rep. 6160, Naval Research Laboratory (October 6, 1964), ASTM STP-380, American Nuclear Society Test Material, Philadelphia, Pennsylvania (1965), p. 283.

8. L. E. Steele, "Radiation Embrittlement of Reactor Pressure Vessels," Nuclear Engineering Des., 3 (1966), p. 287.

9. J. R. Hawthorne, Jr., and L. E. Steele, Initial Evaluation of Metallurgical Variables as Possible Factors Controlling the Radiation Sensitivity of Structural Steels, NRL Rep. 6420, Naval Research Laboratory (September 29, 1966), ASTM STP-426, American Nuclear Society Test Material, Philadelphia, Pennsylvania (1967), p. 534.

10. J. R. Hawthorne, E. Fortner, and S. P. Grant, "Radiation Resistant Experimental Weld Metals for Advanced Reactor Vessel Steels," Weld J. Research Supplement, 49, 10 October 1970, p. 453s.

11. U. Potapovs and J. R. Hawthorne, The Effect of Residual Elements on 550°F Irradiation Response of Selected Pressure Vessel Steels and Weldments, NRL Rep. 6803, Naval Research Laboratory (November 22, 1968), Nuclear Applications, 6, 1 January 1969, p. 27.

12. L. E. Steele, "The Influence of Composition on the Fracture Toughness of Commercial Nuclear Vessel Welds," Proc. 2nd Interamerican Conf. Materials Technology, Mexico City, Mexico, August 1970.

13. C. Z. Serpan, Jr., H. E. Watson, and J. R. Hawthorne, "Interaction of Neutron and Thermal Environment Factors in the Embrittlement of Selected Structural Alloys for Advanced Reactor Applications," Nuclear Engineering Des., 11, April 1970, p. 368.

14. ASTM Standard E185-73, Standard Recommended Practice for Surveillance Tests for Nuclear Reactor Vessels, American Society for Testing and Materials, Philadelphia, Penn.

15. ASTM Standard E185-82, Standard Practice for Conducting Surveillance Tests for Light-Water Cooled Nuclear Power Reactor Vessels, American Society for Testing and Materials, Philadelphia, Penn.

16. Appendix G to Section III, "Nuclear Power Plant Components," of ASME Boiler and Pressure Vessel Code, New York (updated frequently).

17. S. Fyfitch and W. A. McInteer, Requalification of the TMI-2 Reactor Vessel Surveillance Program Capsules, BAW-2042, Babcock & Wilcox, Lynchburg, Virginia, August 1988.

18. ASTM Standard E23-72, Standard Methods for Notch Bar Impact Testing of Metallic Materials, American Society for Testing and Materials, Philadelphia, Penn.

19. ASTM Standard E8-69T, Standard Methods of Tension Testing of Metallic Materials, American Society for Testing and Materials, Philadelphia, Penn.

20. ASTM Standard E399-81, Standard Test Method for Plain-Strain Fracture Toughness of Metallic Materials, American Society for Testing and Materials, Philadelphia, Penn.

21. ASTM Standard E813-81, Standard Test Method for J_{IC}, A Measure of Fracture Toughness, American Society for Testing and Materials, Philadelphia, Penn.

22. K. E. Moore and A. S. Heller, Chemistry of 177-FA B&W Owners Group Reactor Vessel Beltline Welds, BAW-1500P, Babcock & Wilcox, Lynchburg, Virginia, September 1978.

23. S. E. Yanichko, Florida Power and Light Company, Turkey Point Unit No. 3 Reactor Vessel Radiation Surveillance Program, WCAP-7656, Westinghouse Electric Corporation, Pittsburgh, Pennsylvania, May 1971.

24. S. Fyfitch, et al., Master Integrated Reactor Vessel Surveillance Program, BAW-1543, Rev. 3, Babcock & Wilcox, Lynchburg, Virginia, September 1989.

25. S. E. Yanichko, Florida Power and Light Company, Turkey Point Unit No. 4 Reactor Vessel Radiation Surveillance Program, WCAP-7660, Westinghouse Electric Corporation, Pittsburgh, Pennsylvania, May 1971.

26. C. E. Childress, Fabrication History of the First Two 12-in. Thick ASTM A-533, Grade B, Class 1 Steel Plates of the Heavy Section Steel Technology Program: Documentary Report 1, ORNL-4313, Oak Ridge National Laboratory, February 1969.

27. U.S. Nuclear Regulatory Commission, Radiation Damage to Reactor Vessel Material, Regulatory Guide 1.99, Revision 2, May 1988.

28. American Society of Mechanical Engineers, Section XI, "Rules for Inservice Inspection of Nuclear Power Plant Components," of ASME Boiler and Pressure Vessel Code, New York (updated frequently).

29. Letter, Chairman of Subgroup on Evaluation Standards, Section XI, ASME Boiler and Pressure Vessel Code to J. E. Richardson, Director, Division of Engineering Technology, US NRC, "Response to NRC Request, A-11 Issue," dated February 20, 1991.

30. J. C. Newman, Jr. and I. S. Raju, "Stress-Intensity Factors for Internal Surface Cracks in Cylindrical Pressure Vessels," ASME Journal of Pressure Vessel Technology, Vol. 102, November 1980, pp. 342-346.

31. J. M. Bloom, "Extension of the Failure Assessment Diagram Approach - Semi-Elliptical Flaw in Pressurized Cylinder," ASME Journal of Pressure Vessel Technology, Vol. 107, February 1985.

32. V. Kumar, M. D. German and B. I. Schumacher, "Analysis of Elastic Surface Cracks in Cylinders Using the Line-Spring Model and Shell Finite Element Method," J of Pressure Vessel Technology, Vol. 107, November 1985.

33. V. Kumar and M. D. German, "Elastic-Plastic Fracture Analysis of Through-Wall and Surface Flaws in Cylinders," EPRI Report NP-5596, January 1988.

34. J. M. Bloom, "Procedure for the Assessment of the Integrity of Nuclear Pressure Vessels and Piping Containing Defects," EPRI Report NP-2431, June 1982, Appendix B.

35. K. K. Yoon, J. M. Bloom, W. A. Pavinich, and H. W. Slager, "Application of the Failure Assessment Diagram to the Evaluation of Pressure-Temperature Limits for a Pressurized Water Reactor," ASME J of Pressure Vessel Technology, Vol., 107, pp. 192-196, May 1985.

36. E. D. Eason and E. E. Nelson, Improved Model for Predicting J-R Curves from Charpy Data, NUREG/CR 5356, Phase I Final Report, April 1989.

37. E. D. Eason et al., "Multivariable Modeling of Pressure Vessel and Piping J-R Data," SBIR Phase II Final Report," Modeling Computing Services, April 1991.

38. L. Breiman and J. H. Friedman, "Estimating Optimal Transformations for Multiple Regression and Correlation," J. American Statistical Association, Vol. 80, No. 391, September 1985, pp. 580-619.

39. M. J. Powell, "A Method for Minimizing a Sum of Squares of Nonlinear Functions Without Calculating Derivatives," Computer Journal, Vol. 7, p. 303, 1965.

40. U.S. Code of Federal Regulations, Title 10, Energy, Part 50, Section 61, "Fracture Toughness Requirements for Protection Against Pressurized Thermal Shock Events," First Published - Fedral Register, Vol. 50, No. 141, July 23, 1985.

41. ASTM Standard E1152-87, Standard Test Method for Determining J-R Curves, American Society for Testing and Materials, Philadelphia, Penn.

42. J. A. Joyce and E. M. Hackett, "Development of an Engineering Definition of the Extent of J Singularity Controlled Crack Growth," NUREG/CR-5238, U.S. Nuclear Regulatory Commission, May 1989.

43. B&W Nuclear Service Co., "PTPC (PC Based) Pressure-Temperature Limit Analysis Program," Version 3.1, March 1990.

44. Table 4-2, Comparison of Sample Problem Results Working Group Operating Plant Criteria (August 29, 1989), White Paper on Reactor Vessel Integrity Requirements for Level A and B Conditions, Rev. 9, ASME Section XI, Task Group on Reactor Vessel Integrity Requirements, January 1991.

45. A. L. Lowe, Jr. and J. W. Pegram, Correlations for Predicting the Effects of Neutron Radiation on Linde 80 Submerged-Arc Welds, BAW-1803, Revision 1, B&W Nuclear Service Company, Lynchburg, Virginia, May 1991.

46. S. E. Yanichko, et al., Analysis of Capsule T from the Florida Power and Light Company Turkey Point Unit No. 3 Reactor Vessel Radiation Surveillance

Program, WCAP-8631, Westinghouse Electric Corporation, Pittsburgh, Pennsylvania, December 1975.

47. P. K. Nair and E. B. Norris, Reactor Vessel Material Surveillance Program for Turkey Point Unit No. 3: Analysis of Capsule V, Southwest Research Institute, San Antonio, Texas, August 1986.

48. E. B. Norris, Reactor Vessel Material Surveillance Program for Turkey Point Unit No. 4 Analysis of Capsule T, Final Report, Southwest Research Institute, San Antonio, Texas, June 14, 1976.

49. A. L. Lowe, Jr., P.E., The Applicability of the HSST Program Second and Third Irradiation Series Data to the Integrity of Nuclear Reactor Vessels, BAW-1975, Babcock & Wilcox, Lynchburg, Virginia, June 1987.

8. CERTIFICATION

This report is an accurate description of the low upper-shelf toughness fracture analysis of reactor vessels of Turkey Point Units 3 and 4.

For Sections 1 and 2

A. L. Lowe, P.E. 3/10/92

A. L. Lowe, Jr., Advisory Engineer — Date
Materials and Structural Analysis Unit

For Sections 3, 4, 5, and 6

K. K. Yoon 3/10/92

K. K. Yoon, Advisory Engineer — Date
Materials and Structural Analysis Unit

This report has been reviewed and is an accurate description of the low upper-shelf toughness fracture analysis of reactor vessels of Turkey Point Units 3 and 4.

For Sections 1 and 2

M. J. Devan 3/10/92

M. J. Devan, Engineer 2 — Date
Materials and Structural Analysis Unit

For Sections 3, 4, 5, and 6

D. E. Killian, Principal Engineer — Date
Materials and Structural Analysis Unit

Verification of independent review.

K. E. Moore, Manager — Date
Materials and Structural Analysis Unit

This report is approved for release.

D. L. Howell, Project Manager — Date
Reactor Vessel Services